IVW - Schriftenreihe Band 29

Institut für Verbundwerkstoffe GmbH - Kaiserslautern

Barkoula, Nektaria-Marianthi

Solid Particle Erosion Behaviour of Polymers and Polymeric Composites

Die Deutsche Bibliothek – CIP-Einheitsaufnahme

Barkoula, Nektaria-Marianthi:
Solid particle erosion behaviour of polymers and polymeric composites / Nektaria-Marianthi Barkoula. – Kaiserslautern : IVW, 2002
(IVW-Schriftenreihe ; Bd. 29)
Zugl.: Kaiserslautern, Univ., Diss., 2002
ISBN 3-934930-25-5

Herausgeber: Institut für Verbundwerkstoffe GmbH
Erwin-Schrödinger-Straße
Universität Kaiserslautern, Gebäude 58
67663 Kaiserslautern

Verlag: Institut für Verbundwerkstoffe GmbH

Druck: Universität Kaiserslautern
ZBT – Abteilung Foto-Repro-Druck

D-386

Als Manuskript gedruckt. Printed in Germany.

ISSN 1615-021X
ISBN 3-934930-25-5

Solid Particle Erosion Behaviour of Polymers and Polymeric Composites

Vom Fachbereich für Maschinenbau und Verfahrenstechnik
der Universität Kaiserslautern
genehmigte Dissertation
zur Erlangung des akademischen Grades

Doktor-Ingenieurin (Dr.-Ing.)

von

Dipl.-Ing. Nektaria-Marianthi Barkoula

aus Patras, Griechenland

Tag der wissenschaftlichen Aussprache: 07.02.2002

Prüfungsvorsitzender: Prof. Dr.-Ing. R. Renz
1. Berichterstatter: Prof. Dr.-Ing. J. Karger-Kocsis
2. Berichterstatter: Prof. Dr.-Ing. W. Brockmann
3. Berichterstatter: Prof. Dr.-Ing. D.-H. Hellmann

D 386

This work is dedicated to my beloved family

Στην πολυαγαπημένη μου οικογένεια

ACKNOWLEDGEMENTS

The present work was completed between March 1999 and November 2001 at the Institute for Composite Materials Ltd. (IVW GmbH), at the University of Kaiserslautern.

I would like to express my special gratitude to my supervisor, Prof. Dr.-Ing. József Karger-Kocsis for his scientific support, his active participation and his concern about the progress of my study. His diligent example was a real motivation for my work. I would like to thank Prof. Dr.-Ing. Rainer Renz for accepting the presidency of the examination committee as well as Prof. Dr.-Ing. Walter Brockmann and Prof. Dr.-Ing. Dieter-Heinz Hellmann for the co-reference of this thesis.

I am grateful to the IVW for providing me the opportunity of working in an outstanding environment from scientific, technical and human point of view. My special thanks hold for my students, Mrs. Nicole Loriaux, Mr. Jan Niemann and Mr. Marco Klees for their help, hard-working and real interest at the experimental part of this work. Many thanks also to the IVW-staff and especially to my colleges of division II for the perfect and friendly teamwork and the advises they offered during the experiments.

I wish also to thank the German Science Foundation for the financial support of this work (KA 1202/6-1 and 6-3) and DLR (GRI-023-99) for supporting the collaboration with ICE/HT, Greece.

Many thanks also to Dr. Klaus Recker from Bayer AG for the interesting scientific discussion and for the gratuitous supply of the information sheets and the polyurethane materials and to Dr. Tapio Harmia for the preparation of the GF/PP materials.

Last but not least I would like to thank my family in Greece for the encouragement they offered me, their patience and their love.

Table of Contents

ABSTRACT

Solid particle erosion is usually undesirable, as it leads to development of cracks and holes, material removal and other degradation mechanisms that as final consequence reduce the durability of the structure imposed to erosion. The main aim of this study was to characterise the erosion behaviour of polymers and polymer composites, to understand the nature and the mechanisms of the material removal and to suggest modifications and protective strategies for the effective reduction of the material removal due to erosion.

In polymers, the effects of morphology, mechanical-, thermomechanical, and fracture mechanical- properties were discussed. It was established that there is no general rule for high resistance to erosive wear. Because of the different erosive wear mechanisms that can take place, wear resistance can be achieved by more than one type of materials. Difficulties with materials optimisation for wear reduction arise from the fact that a material can show different behaviour depending on the impact angle and the experimental conditions. Effects of polymer modification through mixing or blending with elastomers and inclusion of nanoparticles were also discussed. Toughness modification of epoxy resin with hygrothermally decomposed polyester-urethane can be favourable for the erosion resistance. This type of modification changes also the crosslinking characteristics of the modified EP and it was established the crosslink density along with fracture energy are decisive parameters for the erosion response. Melt blending of thermoplastic polymers with functionalised rubbers on the other hand, can also have a positive influence whereas inclusion of nanoparticles deteriorate the erosion resistance at low oblique impact angles (30°). The effects of fibre length, orientation, fibre/matrix adhesion, stacking sequence, number, position and existence of interleaves were studied in polymer composites. Linear and inverse rules of mixture were applied in order to predict the erosion rate of a composite system as a function of the erosion rate of its constituents and their relative content. Best results were generally delivered with the inverse rule of mixture approach.

A semi-empirical model, proposed to describe the property degradation and damage growth characteristics and to predict residual properties after single impact, was applied for the case of solid particle erosion. Theoretical predictions and experimental results were in very good agreement.

Zusammenfassung

Strahlerosionsverschleiß (Erosion) entsteht beim Auftreffen von festen Partikel auf Oberflächen und zeichnet sich üblicherweise durch einen Materialabtrag aus, der neben der Partikelgeschwindigkeit und dem Auftreffwinkel stark vom jeweiligen Werkstoff abhängt. In den letzten Jahren ist die Anwendung von Polymeren und Verbundwerkstoffen anstelle der traditionellen Materialien stark angestiegen. Polymere und Polymer-Verbundwerkstoffe weisen eine relativ hohe Erosionsrate (ER) auf, was die potenzielle Anwendung dieser Werkstoffe unter erosiven Umgebungsbedingungen erheblich einschränkt.

Untersuchungen des Erosionsverhaltens anhand ausgewählter Polymere und Polymer-Verbundwerkstoffe haben gezeigt, dass diese Systeme unterschiedlichen Verschleißmechnismen folgen, die sehr komplex sind und nicht nur von einer Werkstoffeigenschaft beeinflusst werden. Anhand der ER kann das Erosionsverhalten grob in zwei Kategorien eingeteilt werden: sprödes und duktiles Erosionsverhalten. Das spröde Erosionsverhalten zeigt eine maximale ER bei 90°, während das Maximum bei dem duktilen Verhalten bei 30° liegt. Ob ein Material das eine oder das andere Erosionsverhalten aufweist, ist nicht nur von seinen Eigenschaften, sondern auch von den jeweiligen Prüfparametern abhängig.

Das Ziel dieser Forschungsarbeit war, das grundsätzliche Verhalten von Polymeren und Verbundwerkstoffen unter dem Einfluss von Erosion zu charakterisieren, die verschiedenen Verschleißmechanismen zu erkennen und die maßgeblichen Materialeigenschaften und Kennwerte zu erfassen, um Anwendungen dieser Werkstoffe unter Erosionsbedingungen zu ermöglichen bzw. zu verbessern.

An einer exemplarischen Auswahl von Polymeren, Elastomeren, modifizierten Polymeren und Faserverbundwerkstoffen wurden die wesentlichen Einflussfaktoren für die Erosion experimentell bestimmt.

Thermoplastische Polymere und thermoplastische- und vernetzte- Elastomere

Die Versuche, den Erosionswiderstand ausgewählter Polymere (Polyethylene und Polyurethane) mit verschiedenen Materialeigenschaften zu korrelieren, haben gezeigt, dass es weder eine klare Abhängigkeit von einzelnen Kenngrößen noch von Eigenschaftskombinationen gibt. Möglicherweise führt die Bestimmung der Materialeigenschaften unter den gleichen experimentellen Bedingungen wie bei den

Erosionsversuchen zu einer besseren Korrelation zwischen ER und Materialkenngröße.

Modifiziertes Epoxidharz

Am Beispiel eines modifizierten Epoxidharzes (EP) mit verschiedener Vernetzungsdichte wurde eine Korrelation zwischen Erosionswiderstand und Bruchenergie bzw. Erosionswiderstand und Vernetzungsdichte gefunden. Die Modifizierung erfolgte mit verschiedenen Anteilen von einem hygrothermisch abgebauten Polyurethan (HD-PUR). Der Zusammenhang zwischen ER und Vernetzungsparametern steht im Einklang mit der Theorie der Kautschukelastizität.

Modifizierungseffizienz in Duromeren, Thermoplasten und Elastomeren

Des weiteren wurde der Einfluss von Modifizierungen von Polymeren und Elastomeren untersucht. Mit dem obenerwähnten System (d.h. EP/HD-PUR) läßt sich auch der Einfluss der Zähigkeitsmodifizierung des Epoxidharzes (EP) auf das Erosionsverhalten untersuchen. Es wurde gezeigt, dass für HD-PUR Anteile von mehr als 20 Gew.% diese Modifizierung einen positiven Einfluss auf die Erosionsbeständigkeit hat. Durch Variation der HD-PUR-Anteile können für dieses EP Materialeigenschaften, die zwischen den Eigenschaften eines üblichen Duroplasten und eines weniger elastischen Gummis liegen, erzeugt werden. Deswegen stellt der modifizierte EP-Harz ein sehr gutes Modellmaterial dar, um den Einfluss der experimentellen Bedingungen zu studieren, und zu untersuchen, ob verschiedene Erodenten zu gleichen Erosionsmechanismen führen. Der Übergang vom duroplastischen zum zähen Verhalten wurde anhand von vier Erodenten untersucht. Aus den Versuchen ergab sich, dass ein solcher Übergang auftritt, wenn sehr feine, kantige Partikel (Korund) als Erodenten dienen. Die Partikelgröße und -form ist von entscheidender Bedeutung für die jeweiligen Verschleißmechanismen.

Die Effizienz neuartiger thermoplastischer Elastomere mit einer co-kontinuierlichen Phasenstruktur, bestehend aus thermoplastischem Polyester und Gummi (funktionalisierter NBR und EPDM Kautschuk), wurde in Bezug auf die Erosionsbeständigkeit untersucht. Große Anteile von funktionalisiertem Gummi (mehr als 20 Gew.%) sind vorteilhaft für den Erosionswiderstand. Weiterhin wurde untersucht, ob sich die herausragende Erosionsbeständigkeit von Polyurethan (PUR) durch Zugabe von Nanosilikaten eventuell noch steigern läßt. Das Ergebnis war, dass die Nanopartikel sich vor allem bei einem kleinen Verschleißwinkel (30°) negativ

auswirken. Die schwache Adhäsion zwischen Matrix und Partikeln erleichtert den Beginn und das Wachsen von Rissen. Dies führt zu einem schnelleren Materialabtrag von der Materialoberfläche.

Faserverbundwerkstoffe

Ferner wurden Faserverbundwerkstoffe (FVW) mit thermoplastischer und duromerer Matrix auf ihr Verhalten bei Erosivverschleiß untersucht. Es war von großem Interesse, den Einfluss von Faserlänge und -orientierung zu untersuchen. Kurzfaserverstärkte Systeme haben einen besseren Erosionswiderstand als die unidirektionalen (UD) Systeme. Die Rolle der Faserorientierung kann man nur in Verbindung mit anderen Parametern, wie Matrixzähigkeit, Faseranteil oder Faser-Matrix Haftung, berücksichtigen. Am Beispiel von GF/PP Verbunden weisen die parallel zur Verstreckungsrichtung gestrahlten Systeme den geringsten Widerstand auf. Andererseits findet bei einem GF/EP System die maximale ER in senkrechter Richtung statt. Eine Verbesserung der Grenzflächenscherfestigkeit beeinflusst die Erosionsverschleißrate nachhaltig. Wenn die Haftung der Grenzfläche ausreichend ist, spielt die Erosionsrichtung eine unbedeutende Rolle für die ER. Weiterhin wurde gezeigt, dass die Präsenz von zähen Zwischenschichten zu einer deutlichen Verbesserung des Erosionswiderstands von CF/EP- Verbunden führt.

Eine weitere Aufgabenstellung war es, die Rolle des Faservolumenanteils zu bestimmen. „Lineare, inverse und modifizierte Mischungsregeln“ wurden angewendet, und es wurde festgestellt, dass die inversen Mischungsregeln besser die ER in Abhängigkeit des Faservolumenanteils beschreiben können.

Im Anwendungsbereich von Faserverbundwerkstoffen ist nicht nur die Kenntnis der ER, sondern auch die Kenntnis der Resteigenschaften erforderlich. Ein halbempirisches Modell für die Vorhersage des Schlagenergieschwellwertes (U_o) für den Beginn der Festigkeitsabnahme und der Restzugfestigkeit nach einer Schlagbelastung wurde bei der Untersuchung des Erosionsverschleißes angewendet. Experimentelle Ergebnisse und theoretische Vorhersagen stimmten nicht nur für duromere CF/EP-Verbundwerkstoffe, sondern auch für Verbundwerkstoffe mit einer thermoplastischen Matrix (GF/PP) sehr gut überein.

List of Abbreviations and Symbols

Abbreviation	
CF	Carbon fibre
CT	Compact tension
DDS	Diaminodiphenylsulphone
DIN	Deutsche Industrienormen
DMTA	Dynamic mechanical thermal analysis
DSC	Differential scanning calorimetry
EP	Epoxy resin
EPDM	Ethylene/propylene/diene rubber
EPR	Ethylene/propylene rubber
ER	Erosion rate
ESIS	European structural integrity society
FCP	Fatigue crack propagation
FRPs	Fibre reinforced polymers
GF	Glass fibre
g-GMA	Glycidyle methacrylate
HC	Hot cast
HDPE	High density polyethylene
HD-PUR	Hygrothermally decomposed polyurethane
IROM	Inverse rule of mixture
IT	Infrared thermography
LEFM	Linear elastic fracture mechanics
L,SGF	Long, short glass fibres
LROM	Linear rule of mixture
MA	Maleic anhydride
MDI	Methylene di(phenyl isocyanate)
NBR	Acrylonitrile-co-butadiene rubber
NDI	Naphthalene diisocyanate
Pa	Parallel erosion direction
PA	Polyamide
PBT	Poly(butylene terephthalate)

Pe	Perpendicular erosion direction
PE	Polyethylene
PEEK	Poly(ether-ether-ketone)
PET	Poly(ethylene terephthalate)
phr	Parts per hundred resin (rubber)
PI	Polyimide
PMMA	Poly(methyl-methyl acrylate)
PP	Polypropylene
PU	Thermosetting polyurethane
PUR	Polyurethane
RT	Room temperature
SEM	Scanning electron microscopy
SFRC	Short fibre reinforced composite
TDI	Toluene diisocyanate
TMA	Thermal mechanical analysis
TPE	Thermoplastic elastomer
TPU	Thermoplastic polyurethane
UD	Unidirectional

Symbols

a/W	[1]	Relative notch depth
D	[m]	Fibre diameter
E, E',E*	[MPa]	Young's-, Storage -, Complex- Modulus
E_R	[MPa]	Rubbery plateau modulus (DMTA)
F	[N]	Force
F_{max}	[N]	Maximum force, load
G_c	[kJ/m^2]	Fracture energy
H	[Shore A, D]	Hardness
k	[1]	Empirical constant
K	[1]	Correction factor
K_c	[MPam$^{0.5}$]	Fracture toughness
L	[m]	Distance

L	[m]	Fibre length
d,Δm	[mg]	Mass loss of the worn surface
m	[1]	Mismatching coefficient between adjacent layers
M_c	[g/mol]	Mean molecular weight between crosslinks
n	[1]	Velocity exponent
N_A	[mol^{-1}]	Avogadro's number
R	[J/mol*K]	Universal gas constant
RR	[%]	Rebound resistance
tanδ	[1]	Mechanical loss factor
T_R	[°C]	Rubbery plateau onset temperature
T_g	[°C]	Glass transition temperature
t	[s]	Time
t, B	[m]	Specimen thickness
U	[J]	Impact energy
U_o	[J]	Impact energy thershold
V	[mm^3]	Volume of the specimen
v	[cm^{-3}]	Crosslink density
w	[%]	Weight fraction
W	[m]	Specimen width
α	[°]	Impact Angle
α_{TH}	[10^{-6} K^{-1}]	Thermal expansion coefficient
γ	[1/sec]	Radial frequency, revolution speed
ε_y	[%]	Strain at yielding
ε_u	[%]	Ultimate strain
η	[1]	Erosion efficiency
θ	[°]	Angle in 'double disk method'
λ	[s]	Relaxation time
$\nu_{i,f,m}$	[%]	Volume fraction
ρ	[g/cm^3]	Density
σ_y	[MPa]	Stress at yielding
σ_o	[MPa]	Tensile strength of the non-impacted sample
σ_r	[MPa]	Residual tensile strength after impact

σ_∞	[MPa]	Ultimate tensile strength after impact
σ_∞ / σ_o	[1]	Normalised ultimate tensile strength after impact
σ_u	[MPa]	Ultimate stress
τ_i	[MPa]	Interfacial shear strength
τ_R	[kN/m]	Tear propagation resistance
υ	[m/s]	Speed of the erodent flux, impact velocity
ω	[1/s]	Frequency

1. Introduction

Solid particle erosion describes the local damage and gradual material removal from a surface due to the impingement of many fast-moving solid particles. The first scientific studies on the solid particle erosion behaviour began to appear at the end of the 19th century by Reynolds [1] and Rayleigh [2]. Although the study of erosion has a long history and starts with some famous names, little in the way of a fundamental understanding of the mechanisms by which particles remove material had been developed [3]. Attempts to understand the basic mechanisms involved in erosion started in the last half of the 20th century and have been continued to the present. All these years the interest of the scientists was concentrated on conventional materials and especially metals and only in the last two decades a more intensive study has been made on the erosion behaviour of polymers and related composites.

Nowadays polymers and related composites are extensively used as structural materials in various components and engineering systems due to their excellent specific (i.e. density related) properties. In comparison with metals they offer some extra benefits, like easy processability and forming into the desired shape (especially the thermoplastics). Fibre reinforced polymers (FRPs) possess usually very high specific stiffness and strength when measured in plane. The anisotropic behaviour of the FRPs can lead to beneficial properties in a desired direction but in comparison to metals, composites present different, significant more complex damage- and failure-mechanisms, which affect also the safety hazard.

A successful material substitution with components of reduced weight could have significant effect for the broader use of FRPs instead of traditional materials. Examples of the application of polymer composites are pipelines carrying sand, slurries in petroleum refining, helicopter rotor blades, pump impeller blades, high speed vehicles and aircrafts, water turbines, aircraft engine blades, missile components, canopies, radomes, wind screens and outer space applications. In such applications, one of the most important characteristics is the erosion behaviour as these parts operate very often in dusty environments. Furthermore, solid particle erosion has been considered as a serious problem as it is responsible for failures in the above mentioned applications [4-7] .

Different trends for the erosion behaviour of polymers and polymeric composites have been observed, depending mainly on the experimental conditions and the target properties. However, it is widely recognised that polymers and polymeric composites present a rather poor erosion resistance with erosion rates considerably larger than those obtained in metallic materials. It has been noted that the erosion resistance of polymers is two or three orders of magnitude lower than that of metallic materials. Fibre-reinforced polymers on the same time can indicate a 10 to 30times larger decrease in weight compared with metallic materials. A modification of the composite material enables only gradual improvements, which are not significant enough for some applications. In such cases the development of an effective protective layer against erosion is of great importance [8-10]. Different layers have been proposed for the protection towards erosion. Prerequisites are the minor thickness, the improvement of the erosion resistance and the positive influence of the layers on the overall performance of the structure.

The reported results seem to agree that the elastomers and particular polyurethanes show the best resistance towards solid particle erosion and therefore are suitable as protective films. Despite the serious attempts made in the last years to correlate this extraordinary behaviour of elastomers with their characteristic properties only indications were made and there is still no clear explanation about this behaviour.

It has been stated that none of the models proposed for conventional materials is in state to predict the erosion behaviour with an analytical, practical and usable manner in the case of polymers and polymeric composites. The material removal is dependent on many interrelated factors that include the properties and structures of the target material, the macroexposure and microexposure conditions and the physical and chemical characteristics of the erodent particles. The combination of all these factors, sometimes exceeding 20 in number, results in erosion rates that are peculiar to specific sets of conditions. Additional difficulties arise from the fact that the different processes during erosion occur simultaneously. This complexity in many instances seems to defy simplification on the part of the experimentalist seeking to carefully separate variables and the theorist attempting to accurately model the wearing system.

The main aim of this study was to apply an unified approach in order to characterise the erosion behaviour of polymers and polymeric composites, to understand the nature and the mechanisms of the material removal and to suggest modifications and protective layers for the effective reduction of the material removal due to erosion. In order to overcome the interrelations occurring during solid particle erosion and to find each individual dependence, the experimental conditions were kept at almost all cases constant and the properties of the target materials varied in a wide range. The influence of the characteristic properties of polymers and polymeric composites was examined in details. A model target material facilitated to examine the experimental conditions using a wide range of erodent materials.

In an engineering application, a structural part is not only subjected to solid particle erosion but also to stress- and deformation- profiles, oscillations and impacts. Therefore it should be sufficiently resistant in relation to these demands. Additionally to material removal the FRPs can show strength and stiffness degradation which results to the durability reduction of the construction. Key aspects when selecting a material system is to know how its properties are changing as a function of external (“service”) conditions and in what extent the residual values can be predicted. It was a further aim of this study to investigate the residual properties of the polymeric composites after solid particle erosion, to describe their property degradation and damage growth characteristics, to model their residual properties and finally to propose methods to improve their resistance.

2. State of the Art

2.1 Erosion Modes

Solid particle erosion is a dynamic process that occurs in many different types of equipment due to the impingement of solid particles on exposed components resulting in material removal and surface degradation. Similar to other tribological processes, solid particle erosion is characterised by the fact that the mechanical load can release secondary thermal, tribochemical and physical reactions between the partners involved in the tribological system [11]. Because of the more pronounced viscoelastic character of polymers and related composites in comparison to the conventional materials, a more complicated situation is expected including relaxation and time-dependent responses where the discrete damage modes are not easily identifiable.

The material removal and the involved mechanisms depend on many interrelated factors that include the properties and structures of the target materials, the macro-exposure and micro-exposure conditions, and the physical and chemical characteristics of the erodent particles. In respect to the impact angle (a), solid particle erosion is divided in [12]:

- erosion at normal impact angles ($a \approx 90°$)
- erosion at oblique impact angles ($0° < a < 90°$)

At zero angle of impingement there is negligible wear because the eroding particles do not impact the surface. A low impact angle favours wear processes similar to abrasion because the particles tend to track across the worn surface after impact. A high impact angle causes wear mechanisms which are typical of solid particle erosion.

A great difference in the classification of various materials in respect to their erosive wear response exists, when the impact- angle and –time variation is regarded. Figure 2.1 shows typical erosion diagrams as a function of impact -time and -angle, respectively. The erosion mechanisms can be categorised as ductile and brittle, which do not directly follow the traditional categories of materials [4]. It can be seen in figure 2.1 that in ductile mode of erosion the maximum material removal prevails at

low impingement angles whereas if the maximum is found at high impingement angles then the brittle mode is assumed. Regarding the variation of the material removal with the impact time, it is seen that in the ductile mode of erosion, there may be an incubation period whereby the weight of the target increases during the initial part of the test before settling down to a steady state. For normal impacts, this is due to the initial inclusion of particles in the target surface. After the subsequent removal of these particles, steady state erosion is established [4,5,13,14]. As far as the glancing impacts are concerned, during the incubation period of a ductile polymer, energy is dissipated in roughening the target surface [5,15-17]. The roughening process includes a high degree of plastic deformation of the polymer under compressive and tensile stresses, mainly resulting in little surface bumps of material being pushed away from the individual impact locations.

Elastomers may show maximum erosion at oblique impact angles similar to the ductile response, but they present a much lower weight loss compared to that observed at typical ductile responses. At normal impacts there are cases that the material does not reach a steady state. Failure can however happen even if no reduction in mass of the polymer has taken place, simply by pushing of the deformed material away from the point of erosion [17].

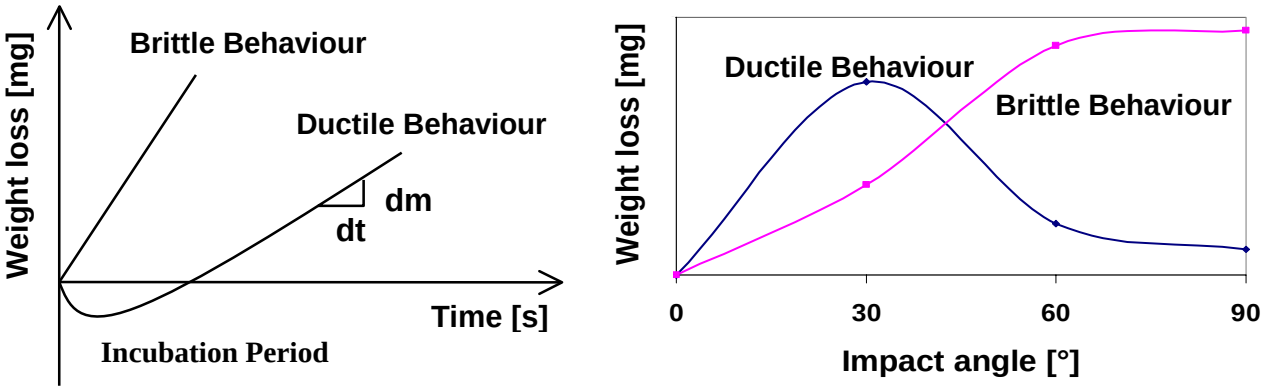

Figure 2.1: Typical behaviours in erosion

The differences in the erosion behaviour can be connected with the mechanisms of particle detachment, which can range from tearing and fatigue for rubbers, through

cutting and chip formation for ductile -metals and -polymers, to crack formation and brittle fracture for ceramics, glasses and brittle polymers [18].

A remarkable feature of the ductile behaviour is that the variation of the weight loss with angle of impingement is very similar for materials with widely different thermal- and physical- properties [3]. On the contrary, a relatively small change in the applied experimental conditions can lead to transitions in the wear mechanism of materials which show traditionally brittle response [19]. The occurrence of transitions between plasticity-dominated and fracture dominated behaviour is a widespread phenomenon in materials science. Such transitions often represent a change in the extent or nature of fracture, leading to a concomitant change in the rate of material removal. The simplest explanation for this behaviour is in terms of the energy stored in an elastic stress field on the one hand, and the work required to produce new crack surface on the other [19].

2.2 Processes during solid particle erosion

Solid particle erosion includes cutting, impact and fatigue processes. The local energy concentration of the erodent on the impacting surface is crucial for the erosive wear [8,11,14,19-22]. This depends practically on the characteristics of the erodent particles (size, shape, hardness, mass) and on those of the target material. Apart from these factors, are impact -angle, -velocity and other sizes of crucial influence [8]. The hitting of a particle corresponds to a certain impact force on the material surface. During impact, the initial energy of the particle is converted into different energy terms. The following cases present a simplification of the expected phenomena [22]:

Normal Elastic Impact

The initial energy of the particle is reconverted into elastic energy and during the rebound phase again into kinetic energy of the particle. Some rubbers show such behaviour, where no erosive wear is observed, in case of normal impact. Erosive wear occurs only after longer erosion duration due to thermal decomposition. Tearing or separation of the macromolecules is the result when the impact comes from sharp edged particles. Almost elastic impacts result also in case of high-strength, hard

materials, which are impacted with particles of small initial energy, this means small velocity and/or small mass.

Normal Plastic Impact

This case is not very common in practice, since the entire energy is not so easily converted into plastic deformation energy without initiation of fracture.

Normal, elastic/plastic impact

This type of impact is occurring most frequently. A certain amount of the initial energy remains to one or both impact partners in the form of plastic energy, whereas the largest section of it is converted due to internal friction into heat. The kinetic rebound energy of the particle is accordingly reduced. A unique impact does not cause generally fracture. Only frequent impacts of many particles on the same surface area can cause shifts of individual material areas against each other with the consequence of further dislocations and increase of the transfer density of the impacting particle. After a certain number of deformations the material is not any longer able to follow these displacements. The strength is exceeded and small micro-fractures are developed inside the material, which entail material removal.

The amount of the plastic energy is determined from the properties of the target material and the erosive particle. The smaller the ductility of the impact partners, the smaller generally the number of stress cycles up to failure, and the greater the amount of energy converted to fracture energy and therefore to erosive wear. This is obvious from the comparison of materials that show ductile and brittle behaviour, respectively. The latter ones display a greater erosive wear once the initial energy of the impacting particle is enough to create stresses that exceed the strength of the material. The larger the ductility, the smaller the impact -force and -stresses.

When the erosive wear of elastomers is regarded a much lower amount of kinetic energy will be absorbed on impact, depending on the rebound resilience of the elastomer. It is clear that the impact stresses will play a large part in determining the erosive wear of elastomers, although the nature of the deformation induced in a roughened surface by an irregular particle is likely to be complicated. At normal

incidence, as Poisson' s ratio for rubber is approximately 0.5, the surface tensile stresses due to an impacting particle will be predominantly frictional in nature. The tensile stresses in the surface arising from the frictional forces due to particle impact cause fine cracks to grow progressively into the surface; where these cracks intersect, material loss occurs. A reduction in friction due to lubrication would cause the surface tensile stresses to be lowered, leading to the observed reduction in erosion rate (ER) [20].

Another process proposed for the case of elastomers involves a build-up of strain on the surface due to incomplete strain relaxation between impacts. Following this concept, it is supposed that the strains produced by a single impact are insufficient to cause material removal, and that several successive impacts are necessary to raise the strain to a sufficient level to cause material removal. This mechanism would explain the greater erosion resistance observed for more resilient elastomers [23,24].

Oblique, elastic/plastic impact

This case is the most general type of the impact. It differs from the normal impact, because of the mechanisms of micro-cutting and micro-ploughing where the material is deformed similar to normal impact but is additionally cut and ploughed, in particular by sharp edged particles. The micro-cutting and micro-ploughing phenomena are mainly connected with the hardness of the particles, which can penetrate into the target surfaces. The softer erodent material leads to micro-cracking at higher impact angles, while the harder mainly to plastic deformation.

The particles deform ductile materials due to their arranged movement perpendicularly and parallel to the surface, this means that both velocity components transfer accordingly the initial energy in deformation energy. This is one of the reasons for the increased erosive wear of materials following the 'ductile mode', found by low-middle angles. Because of the friction, the particles are shifted in the contact area in rotation. The amount of energy initiated due to this process is however of subordinated importance.

Brittle materials are not so easily cut by the particles. The energy transfer parallel to the surface direction can take place contrary to the ductile materials only by means of friction forces and is therefore accordingly small. Only the perpendicular component of the velocity or the respective part of the initial energy determines the energy that goes into the material. The mechanism of the erosion is the same as in the case of 90°-impact therefore the well-known constant reduction of the erosive wear in small impact angles. Deviations from this erosive wear behaviour are to be expected if the coefficient of friction of the impact partners is high so that also the horizontal part of the initial energy can be transferred to the material. The consequence is an increase of the internal stresses, which by middle-high angles of impingement leads to erosive wear maximum.

Elastomers eroded at glancing incidence show transverse features that suggest the formation of tears and cracks perpendicular to the erosion direction. A series of ridges, running transversely to the impact direction, is produced during the initial stage of erosion. Impacting particles slide over the surface and deform the ridges, causing the growth of fatigue cracks from the base of each ridge. It can be assumed that the growth of these fatigue cracks is the rate-determining step in the erosion wear process driven by tensile stresses [25].

Figure 2.2 summarises schematically the known mechanisms of the erosive wear [16]. This short description of the processes in the micro area shows that both the experimental conditions and the material properties determine the type of the predominated mechanisms, the energy conversion as well as the height of the occurring forces and stresses.

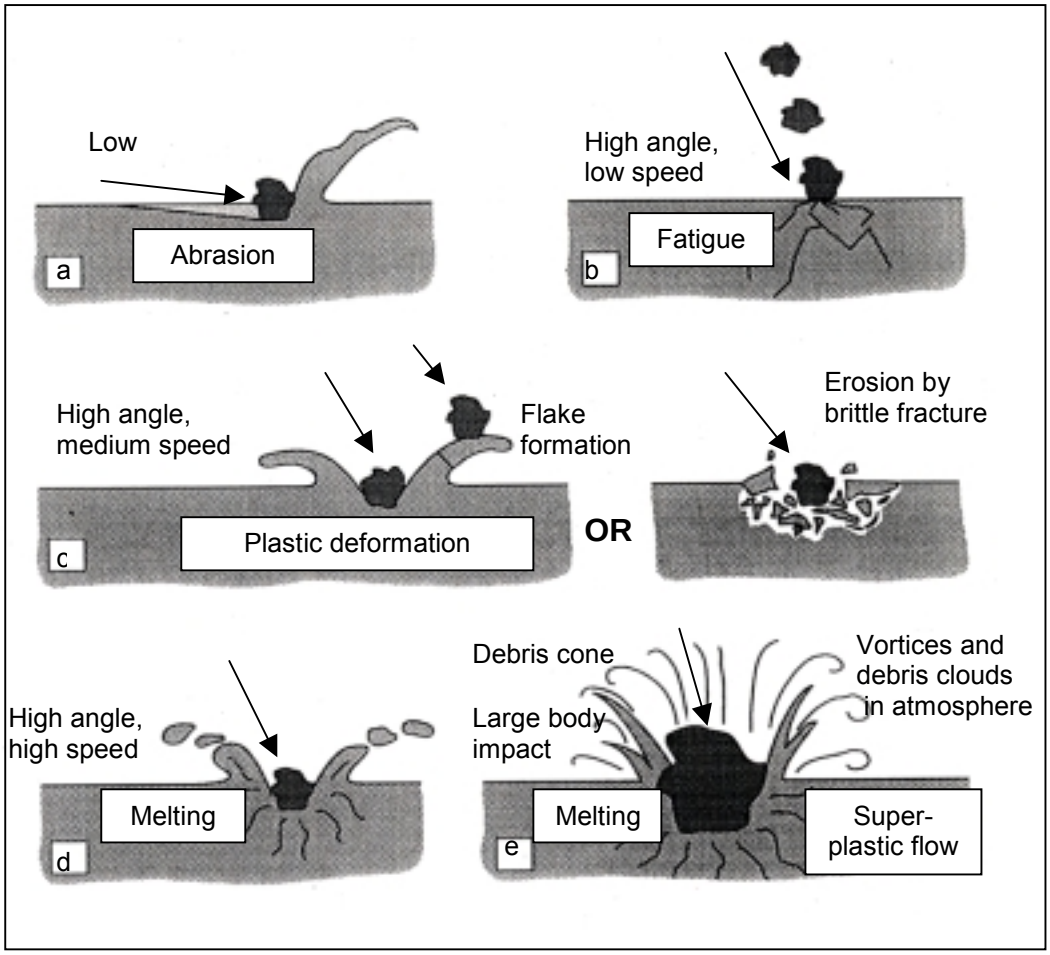

Figure 2.2 Possible mechanisms of solid particle erosion; a) abrasion at low impact angles, b) surface fatigue during low speed, high impingement angle impact, c) brittle fracture or multiple plastic deformation during medium speed, large impingement angel impact, d) surface melting at high impact speeds, e) macroscopic erosion with secondary effects (from [16])

2.3 Influencing parameters

Although some of the influencing parameters on solid particle erosion are already mentioned, figure 2.3 summarises the most important and discussed ones.

It has been stated that the effects of the various parameters on the solid particle erosion behaviour are interrelated therefore, it is not easy to distinguish the individual influencing parameters. Nevertheless, in the next paragraphs some obvious trends will be reviewed based on literature data.

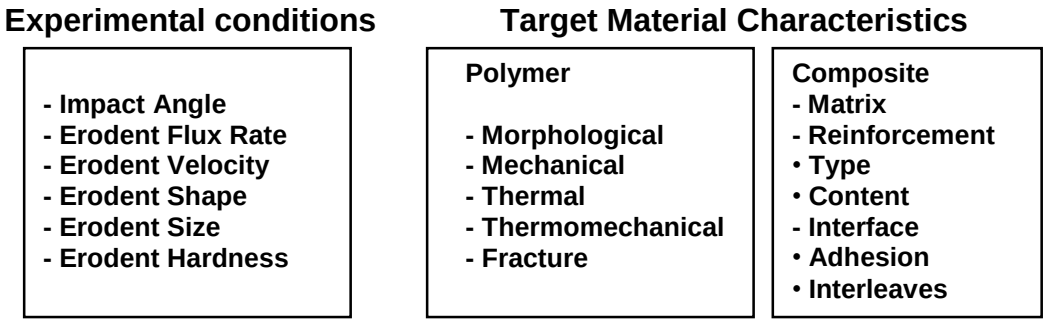

Figure 2.3: Parameters influencing the solid particle erosion

2.3.1 Experimental conditions

2.3.1.1 Effect of erodent velocity

The velocity (υ) of the erosive particle has a very strong effect on the wear process. If the velocity is very low then stresses at impact are insufficient for plastic deformation to occur and wear proceeds by surface fatigue [16]. When the velocity increases, it is possible for the eroded material to deform plastically on particle impact. In this regime, wear may occur by repetitive plastic deformation. At brittle wear response wear proceeds by subsurface cracking. At very high particle velocities melting of the impacted surface might even occur.

From medium to high velocities, a power law [16], can describe the relationship between wear rate and impact velocity:

$$-\frac{dm}{dt} = k\upsilon^n$$

where:

m is the mass of the worn specimen

t is the duration of the process

k is an empirical constant

n is a velocity exponent.

The characteristics of the erodent and that of the target material determine the value of the exponent ‘n’. It has been stated that ‘n’ varies in the range 2-3 for polymeric materials behaving in a ductile manner, while for polymer composites behaving in brittle fashion the value of ‘n’ should be in the range 3-5 [6,26].

2.3.1.2 Effect of erodent characteristics

A major aspect of the erosion problem are the erodent characteristics. Variations in particle size and shape in the range of engineering applications can cause fundamental changes in the erosion response [16]. Transitions in wear mechanism have been associated with a change in the shape, hardness or size of the erodent [16,19]. If the eroding particles are blunt or spherical then plastic deformation exists, if the particles are sharp then cutting and brittle fragmentation is more likely. A blunt particle has a mostly curved surface approximating to a spherical shape while a sharp particle consists of flat areas joined by corners with small radii which are critical to the process of wear [16].

It is assumed that the ER is independent of particle size above a critical value [17,27,28]. This critical value has been observed between 100-200 µm, however it is dependent on the exposure conditions and the particle-target interaction [17,28]. Up to this critical value, experimental results showed that as the size of the erodent increases, the ER also increases. This has been attributed to a range of factors [28], i.e.

(i) Strain rate effects, where for small particles, it has been shown that strain rates are higher than for larger particles, resulting in an increase in flow stress of the target material for erosion with smaller particles.

(ii) Differential work hardening effects for erosion with various particle sizes. It has been suggested that a surface layer of 50-100µm hardens more than the bulk material. Hence, small particles will encounter a layer with a significantly higher flow stress than the bulk material whereas large particles should penetrate this layer. Above the critical size, the influence of this layer will be negligible.

The opposite trend has been observed after this threshold size, because of the increased possibility of particle collisions as the erodent size increases. Another possible reason is that less number of particles will reach the sample per unit weight of erodent when the particles impacting the sample have larger sizes and mass. In that case the larger particles become less effective and that results in a lower ER [29].

The erodent fracture toughness may influence the erosive procedure if fragmentation of the erodent occurs during impact. When a particle breaks to several fragments, the initial energy and therefore the stresses on the surface are distributed over a larger area. Additionally these break processes reduce the part of the energy getting into the material. From energetic view the fracture of the particle has a wear-reducing effect. If the developed fragments are sharper edged compared to the original particle, the wear can also increase [22].

The effect of erodent hardness depends mainly on the particular mode of erosive wear taking place, e.g. ductile or brittle. In the brittle mode the effect of particle hardness is much more pronounced than in the ductile mode. Generally it is believed that hard particles cause higher wear rates than soft particles, but it is impossible to isolate hardness completely from other features of the particle such as its shape. Even if the particle is hard but relatively blunt then it is unlikely to cause severe erosive wear [16].

With respect to the size and type of the erodent material, two trends can be considered to be valid for harder and/or more brittle material. The erosive wear increases the higher the hardness of the erodent and the larger the erosive particle size (until a level of saturation is reached in both cases) [17].

In ductile polymers, however, the situation may be quite different. Due to the relatively low hardness no pronounced effects of changes in the hardness of the usually much harder erodent materials should be expected [17].

2.3.1.3 Effect of erodent flux rate

The particle flux rate, or the mass of impacting material per unit area and time is another controlling parameter of erosive wear rates. Theoretically, the ER should be independent of the flux of particles striking a target since it is assumed that all the particles strike the target with the same velocity and angle of impact, and that the properties of the target pertinent to erosion are independent of particle flux. In practice, however, significant effects of particle flux on measured ER are observed [30].

It has been reported that erosive wear rate is proportional to the flux rate up to a certain limiting value of the flux rate. This limit is believed to be the result of interference between rebounding- and arriving- particles [16]. This effect can be rationalised in terms of a first-order particle collision model where the collisions remove incident particles from the erosion process [31] and can be significant, even for relatively low values of flux. The limiting particle flux rate is highly variable, ranging from as low as 100 kg/m^2s for elastomers to as high as 10000 kg/m^2s for erosion against metals by large and fast particles. It is also possible for wear rates to decrease marginally when the limiting flux is exceeded [16,24].

Although the effect of erodent flux has been mainly attributed to the above mentioned interaction, there are other mechanisms that can take place owing to this parameter and can have a serious effect on the erosive wear. Darkened areas have been observed on the surface of eroded sample creating a debate about the reason of their origination. Some studies state that this is due to a chemical change on the surface possibly associated with localised heating, which further leads to mechanical softening or surface melting. This heating allows the embedding of particles on the material surface. It has been suggested that erosion exceeds the deposition period and net weight loss occurs once the surface is saturated with particles and degraded [5].

Although this could be a good explanation of above phenomenon, it was observed that the darkened areas were not affected by ultrasonic cleaning of the sample in acetone, implying that other reasons should hind behind this phenomenon [24].

Environmental degradation is one rational proposal. Environmental conditions are known to affect the abrasion and fatigue of rubber and as a fatigue mechanism has been proposed for the erosion of elastomers, the influence of environmental conditions could be of importance. Silica and glass, with a large amount of adsorbed water, cause extensive degradation; alumina, with a smaller amount of adsorbed water, causes less degradation, and silicon carbide, which is virtually free from adsorbed water, has a negligible effect. The process can be regarded as a series of transient reactions occurring after each impact. As the flux increases, the time between impacts on one particular surface site decreases. The degradation reaction will then have less time to occur before the next impact, and so the degree of degradation and hence the amount of erosion will be reduced [24].

From the above analysis it is clear that a specific flux should be adjusted in order to avoid simultaneously significant effects of particle interaction and environmental degradation [30].

2.3.2 Target Characteristics

The effect of the experimental conditions was briefly discussed. In the next paragraphs the effects of the target characteristics will be reviewed and different trends will be discussed.

2.3.2.1 Polymers

Material characteristics exert a strong effect on erosive wear and have been extensively studied. It has been found that there is no general recipe for high resistance to erosive wear. Because of the different erosive wear mechanisms that can take place, wear resistance can be theoretically achieved by more than one type of materials. In some cases the material can be extremely hard and tough so that the impacting particle is unable to make any impression on the surface. Alternatively, the material can be highly elastic so that the kinetic energy of the particle is harmlessly dissipated. However, difficulties with materials optimisation for wear reduction arise from the fact that a material can show different behaviour depending on the impact angle and the experimental conditions. The choice of the ideal properties may also

be compromised by other considerations such as operating temperature or material transparency [16].

Attempts have been made in the past to correlate the erosion resistance with morphological-, mechanical-, thermomechanical- and fracture- characteristics.
In the area of polymer morphology the physical and chemical network characteristics of the polymers and the crystallinity have been suggested as controlling parameters. A general evaluation of the influence of physical and chemical network characteristics on the wear behaviour of elastomers has been adopted more intensively in the last decade. The nature of the base components and their content ratio [32-34], the molecular weight of the elastomer [35,36], the presence of crosslinks [32,37], the molecular weight between the crosslinks [38], the degree of phase separation between soft and hard segments [39-42] and the effect of annealing on this degree [39,41-42] are the most discussed characteristics.

In these attempts it was found that the presence of crosslinking improves the wear behaviour. It was suggested that the crosslinked material requires a higher strain energy density to initiate crack growth while the uncrosslinked material gives crack growth at quite low strain energy densities. It would be expected that this increase in the fracture toughness would translate into better wear resistance in those conditions where the wear mechanism was one of fatigue crack growth.

Many studies are concentrated on the effect of morphology on the wear response of polyurethanes. The special interest arises from the fact that even within a particular group such as polyurethane elastomers which have relatively outstanding wear properties, there exists a range of performance in which some materials behave much better than others. In polyurethanes, structures capable of producing the network required for rubbery behaviour can be either chemical, in the form of crosslinks, or physical, in the form of hard domains. The governing parameters are the ratio of the starting components in synthesis and the rigid block concentration.

The polymer molecular weight is also an important parameter for the TPUs (thermoplastic polyurethanes). The effectiveness of the rigid blocks as physical

crosslinks will also depend on phase separation in the polymer and the structure of the rigid blocks, such as their level of crystallinity and hydrogen bonding. Preliminary studies of similar TPUs with varying percent hard segments indicate that the lowest hard segment content gives the lowest ER; however, the mechanical integrity becomes a problem with decreasing hard segment content. Hence a combination of chemistry and morphology should be used to optimise TPU properties for a given loading environment.

General conclusions about the correlation of the polymer physical and chemical structure with erosion response can not yet be obtained, as the related study is in progress and the existing results refer more to other wear processes (i.e. abrasion) than that of erosion.

Concerning the effect of crystallinity, it has been stated that amorphous polymers show more brittle features, while semicrystalline have a more pronounced viscoelastic character, therefore the first erode usually faster than the latter ones [17, 43].

From the thermal and thermomechanical point of view, the thermal conductivity and the glass transition temperature (T_g) seem to have an important effect on solid particle erosion. The localised deformation caused by the erosive impact of a particle on a target material and the possibility of adiabatic conditions associated with high strain rates in a material of low thermal conductivity may cause the generation of high temperatures. The maximum temperature will be determined by the amount of work that is done on the target material and the specific heat and density of the material. The work done is a function of the maximum pressure during impact and this in turn is determined by the target- and particle- hardness. The temperature will be moderated if heat can flow away from the impact site faster than it is being generated [44,45]. High temperatures may briefly soften the material [43-44,46], and may result in a thermal stress field being superimposed upon the mechanical field of the deformation. This will have important repercussions since it is acknowledged that the development and relaxation of the plastic zone at an impact site is associated with

viscoelastic extrusion and fracture in polymers. These damage modes ultimately account for degradation and material loss [44].

Nevertheless, the assumption of perfectly adiabatic conditions needs to be carefully examined. An indication of the adiabatic situation existing in polymers will be the deformed region after relaxation. If this region is larger than the indentation crater depth then a more adiabatic situation should exist. In praxis, a small value of the hardness ensures that only small temperature rises may be expected and thermal degradation of the surface of a plastic material will not be expected to affect erosion radically [44].

In refer to the influence of T_g on the erosion resistance of polymers the following trends have been observed:

a) Erosion is higher for polymers with a glass transition temperature T_g above room temperature (RT) relative to those with T_g below RT [17].
b) For T_g below RT, the wear rate decreases the greater the difference between the experimental temperature and T_g [17, 23].

A demand for a designer with polymers and composites is usually to improve the mechanical properties of the engineering component. Similar to other tribological procedures, improvements in mechanical properties do not always coincide with superior erosive resistance. A great number of studies [13,16,17,37,39,46-57] are concentrated on the possible relations between mechanical properties and ERs but no single property dependence is clearly dominant.

The following mechanical properties are the most discussed for their correlation with the erosive wear response:
Hardness, tensile -strength and -modulus of elasticity, fracture toughness, stress yield σ_y and (after σ_y is exceeded) yield strain ε_y, rebound resilience, friction coefficient, ultimate –strength (σ_u) and –elongation (ε_u) etc. Tearing energy is also a decisive parameter for the erosion resistance of elastomers. This parameter can change the erosion mechanism from progressive fatigue crack growth to single-cycle tensile failure of the rubber. It is well known that the crack growth rate in fatigue is

dependent on tearing energy. The critical frictional input work in erosion is similar to the critical tearing energy in fatigue. Both of them are in good agreement with the fracture energy. It is therefore suggested that the erosion mechanism is mechanical fatigue below the critical frictional input work, i.e. the erosion mechanism changes from mechanical fatigue to direct tearing above the critical frictional input work [38, 49].

Although generally impact wear is not related to the work of the friction forces, if we assume the above mentioned process of wear, i.e. that of fatigue, the relationship between impact wear and the coefficient of friction under impact, should be determined. There are three types of external friction, namely static friction at rest, kinetic friction (in motion) and dynamic friction (under impact). In dynamic friction dissipation of energy is usually characterised by the portion of energy lost at impact. Thus under a permanent contact the value of the friction coefficient should be known for the calculation of the friction force (moment) [58].

Various trends have been observed in the erosion behaviour in respect to the above parameters not only between the different categories of materials (thermosets, thermoplastics, elastomers), but also within the same category. This can be due to the following reasons:

- The strain rates in the impact of erosive particles are very high, whereas the mechanical properties used in the correlation are measured at much lower rates, and in some cases under rather different stress distributions [37,39,46,59].
- The properties of worn surface layers can be very different from those of the bulk material because of thermal-, mechanical- and chemical- degradations during erosion [16,18,24,30,44,46,50,60].
- Some properties are related to the experimental conditions and furthermore are not independent of each other [59].

Friction coefficient and hardness, for example, seem to change dramatically during solid particle erosion. The friction coefficient depends significantly on the impact angle. For elastomers, it decreases with increasing angle of attack while for plastics at small and medium angles of attack usually increases insignificantly and then, as in

the case of elastomers, decreases to zero as normal impact is approached. A variation in the friction coefficient within the smaller angle range is probably caused by a change in load. Indeed, with an increase in the angle of attack equivalent to a load increase, the friction coefficient for elastomers is lowered as it is in normal sliding while the coefficient of friction for plastics increases slightly as is usually observed for a plastic contact under increasing load. From this standpoint, the friction coefficient of plastics should steadily increase with the attack angle; however, above 40°-60° the friction coefficient begins to decrease. It may be assumed that the reason for this phenomenon is a shortened path of movement of a particle over the surface. When this path becomes smaller than the value of the preliminary displacement a reduced friction force occurs, this is manifested in a reduced coefficient of friction [58].

An increased value of hardness seems to be important for the erosion resistance when the erosion process takes place at oblique angles and a brittle erosion mode privileges. Conversely, elastomeric materials show generally better erosion resistance with lower values of hardness. However, a better correlation of the ER with hardness has been experimentally found when the surface hardness was considered. This hardness is not the initial hardness of an non-eroded surface but the one during the course of erosion, which can be obtained by estimating the degree of work hardening and softening by heat generation [46].

The influence of the other mechanical properties on erosion was also confusing owing to the literature data. The estimation of the mechanical properties under specific experimental conditions is complicated and does not assure better correlation, because of the interrelated mechanisms in erosion. This led the scientists to introduce empirical relationships in order to distinguish the possible modes of erosion and to propose combination of material characteristics appropriate to prevent or to minimise the erosion effects.

It is suggested [26,61] that the parameter $\eta = \frac{2 \times ER \times H}{\rho \times \upsilon^2}$ (ER: erosion rate, H: Hardness, ρ: density, υ: impact velocity), known as erosion efficiency, is of

considerable interest since it can be used to identify the brittle and ductile erosion response of various materials. Ideal micro-ploughing involving just the displacement of material from the crater without any fracture (and hence no erosion) will have zero erosion efficiency. Alternatively, in the case of ideal micro-cutting, η will be unity. In case erosion occurs by the formation of a lip and its subsequent fracture, erosion efficiency will be in the range 0-1. In contrast, as happens with brittle material, if the erosion takes place by spalling and removal of large chunks of material by interlinking of lateral or radial cracks, then the erosion efficiency is expected to be even greater than 100%.

The “brittleness index” of the form (hardness H/fracture toughness K_c) is proposed as an indicator for the erosion resistance of materials of different fracture energy classes [62]. A modified correlation of the form of $H^{0.5}/K_c^2$ has been found to work well in describing the erosion resistance of brittle target materials [63]. For polymers, better correlations have been found on combined term of hardness and fracture energy (G_{Ic}). For polymer composites under severe abrasive wear conditions, an expression of the form ($H^{1/2}/G_{Ic}$) has been proposed to correlate quite well with the wear rate [64], whereas a modified one (i.e. H/G_{Ic}) seems to hold for the erosive wear of polymers [17].

According to the Ratner-Lancaster equations [65,66], the wear rate is proposed to be proportional to $1/\sigma_u\varepsilon_u$ where σ_u and ε_u are the ultimate tensile stress and elongation of the polymer, respectively. The term $\sigma_u\varepsilon_u$ is a rough measure of the area under the stress-strain curve to fracture and therefore gives an estimate of the energy to fracture. Similar to this correlation, the combination of high yield stress and strain, has also been used to assess a high fracture energy or in general a high resistance against crack initiation and propagation under very complex (fatigue and/or impact) loading conditions.

Finally, good correlation of the erosion resistance has been found with rebound resilience (RR) within the elastomer group of materials. The ER is found empirically to be proportional to the quantity $(1\text{-}RR)^{1.4}$. This quantity represents the fraction of the initial energy of the impacting particle which is absorbed by the rubbers and is

therefore available, at least in principle, to cause permanent deformation or fracture, and hence erosion [47].

The empirical relationships proposed above may give satisfactory results within a group of materials, but they have limited applicability in a wide range of materials as they are not always in the position to comprise a range or a transition of the erosion mechanisms.

2.3.2.2 Polymeric Composites

Polymer composites are often used as structural components where erosive wear occurs. Differences in the erosion behaviour of various types of composite materials are caused by the amount, type, orientation and properties of the reinforcement on the one hand and by the type and properties of the matrix and its adhesion to the fibres/fillers on the other.

Studies made on the erosive wear of composites refer more on fibre-reinforced polymer (FRP) and less on filler-reinforced-systems. The effect of fillers is considered more as modification of the matrix and less as reinforcement, possibly because of the low percentage of fillers. As in case of polymers, the interrelated phenomena occurring during erosion do not allow to derive general conclusions about the influence of various parameters. The situation becomes more complicated if the geometrical aspects of the microstructure are considered.

It appears that the factors governing ERs in FRPs are mainly influenced by (a) whether the matrix is thermosetting or thermoplastic, (b) the brittleness of the fibres and (c) the interfacial bond strength between the fibres and the matrix [6]. The following sequence in the erosion process of fibre reinforced composites is usually observed [67]:

(1) erosion and local removal of material in the resin zones
(2) erosion in the fibre zones associated with breakage of fibres
(3) erosion of the interface zones between the fibres and the adjacent matrix

Since the resin matrix is removed first, the erosion characteristics of resin materials could be the prime factor for the resistance of composites. During the erosion process the fibres are exposed to the erosion environment subsequent to the removal of matrix. Thus the toughness of exposed fibres directly affect the erosion mechanisms of composites. The effect of fibre reinforcement can be classified in importance as fibre material, fibre content, reinforcement type and fibre orientation. Further continuation of the erosion results in damage to the interface between the fibres and the matrix. This damage is characterised by the separation and detachment of broken fibres from the matrix. The material with the strongest interface strength should show the best erosion resistance [68].

Generally composites with thermosetting matrix erode in a brittle manner. A totally different morphology is observed in the thermoplastic matrix composites. The matrix is uniformly grooved and cratered with local material removal showing a clear tendency to a ductile mode of erosion [4,6,21,26,68,69].

It is also stated, that short fibre reinforced composites show a better resistance to erosion in comparison to the unidirectional ones (UD). In a randomly oriented short fibre composite a reasonable proportion of the fibres will be oriented such that they are nearly aligned with the direction of the impinging particles. The fibres that are not favourably oriented will still derive support from the underlying fibres [6]. On the contrary, in UD composites, as the resin is removed essentially nothing remains to support the exposed fibres, which are more easily removed.

Many studies report on the role of fibre orientation on the solid particle erosion of UD composites [6,29,67-75]. Different trends have been reviewed for the role of this parameter. It is claimed that the fibre removal is due to bending of the unsupported fibres when the surrounding matrix is removed. Additionally, it is shown that as the fibre orientation angle changes, the exposed fibre shape also changes. The exposed shape is a geometrical aspect that depends mainly on the impact angle, while the bending resistance of the fibres depends on the art of the fibre- and matrix- material and on their bonding. Therefore, it would be sounder to consider the role of the fibre

orientation in a group of other parameters such as the angle of impingement and the constituent properties of the composite and not as an individual parameter.

One of the crucial questions in the design with composites is the following:
Given the ERs of the individual constituent, what will be the overall ER in the combined multiphase material, i.e. is the erosion process in a composite controlled by the erosion properties of the individual constituents and what is the 'averaging law' imposed by the microstructure? The linear (LROM) and inverse (IROM) rule of mixture have been proposed for the prediction of the ER. Equations 2.1 and 2.2 describe the LROM and the IROM, respectively:

$$ER_c = w_f \times ER_f + w_m \times ER_m \tag{2.1}$$

$$\frac{1}{ER_c} = \frac{w_f}{ER_f} + \frac{w_m}{ER_m} \tag{2.2}$$

where subscripts c, f and m mean composite, fibre and matrix respectively, whereas ER and w denote the erosion rate and the weight fraction of the related material.

The key aspect in the problem of the 'averaging law', is the size of the impact site in comparison to the size of the microstructural phase [76].

- When the size of erosion impact events is comparable with the microstructural size scale, the analysis of microstructure-related effects requires consideration of the specific erosion mechanisms operative for each particular system.

- In contrast, when the impact events are small relative to the microstructural scale, the averaging effect of the microstructure should depend primarily on geometric considerations. In this case, a mechanism-independent averaging law can be derived which depends only on the intrinsic ERs for each constituent together with appropriate geometric parameters. It can be assumed that the ERs of the two phases in the combined microstructure are the same as the intrinsic rates that would be measured separately on bulk samples. This is physically reasonable because the scale of the microstructure imposes no constraint on the individual

mechanisms. The inverse rule of mixtures (IROM) is proposed to govern the above-mentioned case. Experimental results are in good agreement with the IROM when the prerequisite of the microscructural size is fulfilled.

- Significant deviations can occur for larger particle sizes. For larger particle sizes the IROM underpredicts the measured values by a significant amount. Generally, the linear rule of mixture (LROM) greatly overestimates the measured rates and an LROM is clearly not applicable to the experimental data.

- In the case that the two constituents are continuous and linearly aligned along the incident erodent particle beam direction, the IROM will not apply. The LROM is applicable for this special case because the material removal processes for each constituent occur in parallel; in fact, this in one of the only cases found where the LROM might apply. Even for this case, there are difficulties with the LROM because of the fact that the slower eroding phase will gradually project outward from the surface without limit in steady state. Another difficulty can arise in composites because of internal stresses that can be generated during fabrication.

- Another microstructural effect is the following case: The discrete second-phase particles that form the minor constituent have a lower ER than the surrounding matrix. If the microstructural scale is large relative to the impact event size, the IROM should apply here. In fact, the inverse law suggests that erosion resistance can be significantly improved by adding a relatively small mass fraction of large very erosion-resistant particles to a less erosion-resistant matrix.

- Complications can occur if the second-phase particles are not strongly bonded into the surrounding matrix. In this case a small impact event on a large second-phase particle may cause failure along the interfaces and the entire particle can be ejected. Clearly, the intrinsic ER of the bulk second-phase particle would not apply for this situation.

The above analysis showed that generally an increase of the fibre/filler content leads to an increase to the ER. This is due to the fact that usually the erosion resistance of

the fibres is lower than that of the matrix. A further reason is the quality of the bonding of the reinforcement with the matrix [67,69,70,74,75,77]. In case of particulate composites interfaces of matrix and filler are not only weak to keep the filler bonded on the composite but also can be good promoters of subsurface crack propagation. This will accelerate further the ER. Such phenomena have been reported in case of rubbers reinforced with fillers [23,78].

However, it is possible a composite material to show better resistance to erosion with increasing reinforcement content. This has been observed for instance in an Aramid fibre reinforced epoxy [29]. A plausible reason for this behaviour lies in the behaviour of the Aramid fibre, which fibrillates during failure, thereby absorbing significantly more energy than the brittle matrix. In case of particulate systems, when the amount of filler is enough to modify the properties of the composite then a positive influence of the filler content on the ER of the composite can be observed.

3. Objectives of the Study

As it was stated in chapters 1 and 2 of the study, solid particle erosion is a widespread phenomenon in applications where polymers and composites are used. Solid particle erosion is usually undesirable, as it leads to development of cracks and holes, material removal and other degradation mechanisms that can have as final consequence the durability reduction of the structure imposed to erosion.

Chapter 2 reviewed the processes occurred during solid particle erosion as well as its influencing parameters. It was shown, that the interrelation of experimental conditions and target material characteristics makes the study of erosion a great challenge that demands simplifications in order to understand the individual mechanisms and to propose afterwards a unified approach.

Table 2.3 summarised the most significant influencing parameters in solid particle erosion. Following the literature survey presented in paragraph 2.3, it was concluded that many studies have been devoted on the problem of erosion nevertheless a lot of questions are still open. The basic aim of this study was to investigate the influence of selected target material characteristics and experimental conditions that are of high interest for the case of erosion. The study tried to shed light in areas that are:

a) Less discussed, b) already discussed but not well understood.

Following this analysis, the scope of this work was to study:

In Polymers

- The effect of crystallinity, content of crosslinking agent, mean molecular weight between crosslinks, crosslink density
- The effect of mechanical properties, fracture -toughness and –energy
- The effect of T_g and loss factor (tanδ)
- The effect of polymer modification, through:

a) Mixing or blending with elastomers

b) Inclusion of nanoparticles

- The effect of erodent size, shape and hardness

In Polymer Composites

- The effect of fibre length, orientation
- The effect of fibre content
- The effect of fibre/matrix adhesion
- The effect of stacking sequence, number, position and existence of interleaves

A crucial parameter for the design with composites is the fibre content. In order to obtain the favoured material properties for a particular application, it is important to know how the material performance changes with the fibre content under given loading conditions. The literature survey showed that information on the effects of fibre content on the erosive wear behaviour is scarce and its modelling is also limited.

A further aim was therefore:

- to evaluate the existing models and
- to propose possible equations that could predict the ER of a composite system as a function of the ER of its constituents and their relative content.

Solid particle erosion is in analogy with repeated impact. In case of erosion, the impact process is caused by many fast moving small particles whereas low-energy repeated impact (also called impact fatigue) is usually generated by a large mass of low velocity. Until now the research interest was concentrated on tests performed by instrumented falling weight or Charpy impact devices [79-97].

It was the final target of this work to:

- describe the property degradation and damage growth characteristics and finally
- to model the residual properties of advanced composites.

The study is divided in five units; the three first units are aimed to discover the solid particle erosion behaviour of polymers, modified polymers and polymer composites, in terms of the characteristics mentioned above. The forth part of the study evaluates the existing averaging rules of mixture for the prediction of the ER of a composite as a function of its constituents ERs and their relative content. Modified rules of mixture proposed for the case of abrasion are adopted for the case of oblique (30°) erosion.

The fifth part of the work uses a model obtained to predict the residual strength after single impact for the case of solid particle erosion. The model is evaluated for both thermosetting- and thermoplastic- systems.

The materials selected to illustrate the role of the above mentioned characteristics are these that are widely used in applications and that are not yet cited in the literature.

4. Experimental

4.1. Materials selection and preparation

4.1.1. Polymers

4.1.1.1. Thermoplastic Polyethylene

Four different grades of polyethylene (PE1,PE2, PE3 and PE4) were selected. PE1-3 were made from a monomodal grade produced with a Ziegler catalyst. In these samples, different crosslinking rates achieved by varying the amount of crosslinking agent during the composition (0%, 50%, 70% respectively). In addition a monomodal grade with a chromium catalyst was tested (PE4). All samples contained antioxidant additives.

4.1.1.2. Thermoplastic and the Thermosetting Polyurethanes

Six thermoplastic (TPU) and twelve thermosetting (PU) commercial polyurethanes with a wide range of mechanical, thermomechanical and chemical network

Table 4.1: Designation and product details of the tested polyurethanes

Designation	**Brand Name**	**Grade**	**Chemical Basis /crosslink agent**	**Producer**
TPU-1	Elastollan	1190A	Polyether	Elastogran
TPU-2,TPU-3	Elastollan	C90A, B90A	Polyester	Elastogran
TPU-4,TUP-5	Estane	58109, GP9078	Polyester	BFGoodrich
TPU-6	Desmopan	KU 2-8791	Polyester	Bayer AG
PU-1,PU-2,PU-3	Vulkollan	30, 18, 18/40	Polyester/NDI	Bayer AG
PU-4	Baytec HC	PU 0352/B/PC	Polyester/MDI	Bayer AG
PU-5	Baytec HC	PU 20EL08/B	Polyester/MDI	Bayer AG
PU-6	Baytec HC	PU 0383/1604	Polyester/TDI	Bayer AG
PU-7	Vulkollan	18W	Polyester/NDI	Bayer AG
PU-8	Baytec	PU 0310/PU 0140	Polyether/TDI	Bayer AG
PU-9	Baytec	PU 0357/PU 0140	Polyether/TDI	Bayer AG
PU-10	Baytec	PU 0384/PU 0140	Polyether/TDI	Bayer AG
PU-11	Baytec	Tec 41/PU 0353	Polyester/TDI	Bayer AG
PU-12	Baytec	RC 1705/PU 0356	Polyester/MDI	Bayer AG

characteristics were chosen to represent the typical characteristics of this group of materials. Table 4.1 provides details about the designation, the producer as well as a compound guide of the tested materials.

4.1.2. Modified Polymers

4.1.2.1. Thermosetting Epoxy Resin modified with Hygrothermally Decomposed Polyurethane

The hygrothermal decomposition of polyurethane (HD-PUR) along with its characteristics and the way of EP modification are analytically described elsewhere [98-100]. Briefly, polyester-based PUR processing waste was ground to a particle size of 1-3mm. To these PUR particles 10 wt. % of water was added and fed in the hopper of a laboratory-scale twin screw extruder in which the hygrothermal decomposition of PUR was performed. The HD-PUR produced for this study was decomposed at 230°C and its acetone insoluble fraction was 14 wt %.

A trifunctional EP resin (MY 0500, Ciba) was mixed with 20 to 80 wt. % HD-PUR. The EP/HD-PUR mixtures were homogenised by careful stirring before the hardener, diaminodiphenylsulphone (DDS; HT 976, Ciba) was introduced in 33 wt. % and mixed again. The crosslink density of the material was characterised through the mean molecular weight between crosslinks (M_c) which was computed from the rubbery plateau modulus (E_R) determined by dynamic-mechanical thermoanalysis (DMTA). Table 4.2 lists the composition and designation of the modified EP resins tested.

Table 4.2: Designation and composition of the modified EP resins studied

Designation	**HD-PUR (wt. %)**	**Hardener (DDS: 33 wt. %)**
EP	0	+
EP/HD-PUR	20, 40, 60, 80	+

4.1.2.2. Polymer Blends with Thermoplastic Elastomers (PET, PBT)

Thermoplastic elastomers (TPE) were developed with co-continuous phase structures based on polyesterelastomer blends in the framework of a previous project [101]. Table 4.3 presents the composition and designation of the specimens tested.

Table 4.3: Designation and composition of the thermoplastic elastomers (TPE) with graft rubber blends

Designation	Composition
PET	PET
PET5NBR	PET+5 wt. % NBR-g-GMA
PET10NBR	PET+10 wt. % NBR-g-GMA
PET50NBR	PET+50 wt. % NBR-g-GMA
PET50R	PET+50 wt. % Rubber
	Rubber : 35% EPDM-g-GMA+15% PE
PBT	PBT
PBT5EPDM	PBT+5 wt. % EPDM-g-GMA
PBT10EPDM	PBT+10 wt. % EPDM-g-GMA
PBT50EPDM	PBT+50 wt. % EPDM-g-GMA
PBT50NBR	PBT+50 wt. % NBR-g-GMA

The employed elastomers were chemically functionalised by free-radical initiated grafting of glycidyl methacrylate (g-GMA), in order to improve the compatibility with the polyesters. An optimised grafting method developed for the case ethylene-propylene rubber (EPR) [101,102] was transferred to ethylene/propylene/diene (EPDM) (Buna AP 447, Bayer AG) and to nitrile (NBR) (Perbunan NT 3946, Bayer AG) rubbers. Additionally, an elastomer component consisted of cryogenically shredded EPDM(-g-GMA) (35 wt. %) and PE (Affinity KC 8852, Dow Plastics) (15 wt. %) was dryblended prior feeding. The functionalised elastomers were melt blended with a virgin poly(ethylene terephthalate) (PET) of bottle grade (KODAPAK 9921W, Eastman) and poly(butylene terephthalate) (PBT) (ULTRADUR B 4520, BASF AG). The reactive compounding of the blends and the elastomers(-g-GMA) was conducted both discontinuously using a Brabender® batch mixer and continuously in a twin-screw extruder (Werner & Pfleiderer ZSK 25). Dumbbell specimens for tensile tests and rectangular plates for the erosion tests were injection moulded on an Arburg Allrounder 500-150 type injection moulding machine. Parameters used for the composition and the moulding of the specimens are elsewhere specified [101].

4.1.2.3. TPU Elastomers filled with Nanoparticles

Two commercial available organophil nanosilicates, Cloisite 30B (Southern Clay) and Nanomer I.30P (Nanocor), recommended for compounding with thermoplastic polyurethanes were added in 5 phr (parts per hundred) to a less crystalline polyether type TPU (TPUa) and highly crystalline polyester type (TPUb). Compounding occurred in a Brabender co-rotating twin-screw laboratory extruder (DSE 25). Prior to compounding with nanosilicates the TPUs were dried (in an air-circulating oven at 105°C over one day). The TPU grades were dry-blended with the nanosilicates and extrusion compounded (screw rotation: 90 rpm, feeding screw rotation: 30rpm) at the following temperature profile (from feeding to die): TPUa: 150, 175, 178 and 167°C and TPUb: 231, 241, 235 and 243°C. Dumbbells specimens and thick sheets (2mm) were injection-moulded from the neat and nanoreinforced TPUs on an Arburg Allrounder 500-150 type injection moulding machine. The injection- pressure and speed, the dwell pressure and time as well as the temperature profile varied depending on the TPU grade (nanoreinforced or not) and target injection moulded part (dumbbell or sheet). Table 4.4 gives a list of the materials tested along with their designation.

Table 4.4: TPU elastomers filled with nanoparticles

Designation	**Chemical Basis of TPU**	**Nanoreinforcement (5phr)**
TPUa-0/TPUa-1/TPUa-2	Polyether	none / Southern Clay / Nanocore
TPUb-0/TPUb-1/TPUb-2	Polyester	none / Southern Clay / Nanocore

4.1.3. Composites

4.1.3.1. Glass Fibre Reinforced Polypropylene

Table 4.5 lists the composition and designation of the glass fibre reinforced polypropylene (GF/PP) samples. In the present study, the PP matrix (homo-PP) was reinforced with continuous unidirectional (UD) E-glass (ϕ17µm) and processed into parts via hot pressing. Fibre matrix adhesion was promoted using a polymeric coupling agent. Coupling was achieved by adding 5 wt. % of a maleic-anhydride grafted PP (maleic anhydride content ca. 2 wt. %) to the PP during the melt impregnation of GF tows. The fibre weight fraction (wt. %) of the UD composition

varied from 40 to 60 wt. % following a proprietary impregnation technique of FACT GmbH (Kaiserslautern Germany).The relative densities of GF and PP do not allow to produce composites of higher fibre content within a specific volume of the sample. In order to investigate the role of fibre length on the erosive wear behaviour of GF/PP composites, GF/PP compositions with 40 wt. % discontinuous short (S) and long (L) GF reinforcement were also produced. For this purpose the impregnated tows were cut in different lengths (discontinuous short (~ 2 mm) and long (~ 10 mm) respectively). From these, granules plaques were injection moulded. The erosive wear behaviour of both pure PP and glass (window grade) was additionally examined.

Table 4.5: Designation and composition of the GF/PP studied

	GF			
	W_f	V_f	Fibre	
Designation	**(weight fraction %)**	**(volume fraction %)**	**type**	**Coupling**
PP	0	0	-	+
SGF/PP	40	20	short	+
LGF/PP	40	20	long	+
UD-GF/PP	40, 48, 55, 60	20, 26, 32, 38	UD	+

4.1.3.2. Glass and Carbon Fibre reinforced Epoxy Resin

Glass Fibre Reinforced Epoxy Resin (GF/EP)

Three glass fibre reinforced epoxy resin systems (GF/EP), viz. two composites reinforced by differently sized GF, in addition to the pure EP resin were investigated (cf. Table 4.6).

A hot-curing epoxy system (bisphenol-A-based resin Araldit LY 556; anhydride hardener HY 917, 90phr; heterocyclic amine catalyst DY 070, 1 phr; all from Ciba, Basel, Switzerland) was selected. The E-GF (diameter: 17μm) provided by PPG Industry Fiber Glass (Hoogezand, The Netherlands) varied only in their sizing. Either an EP-compatible sizing, or an -incompatible (having a polypropylene compatible sizing) one was applied on GF. UD laminates were produced by wet filament winding of the GF rovings on a flat aluminum plate. Their consolidation occurred in an

autoclave curing cycle: 4h/80°C + 8h/120°C with subsequent cooling. The mean fiber volume fraction (V_f) of the GF/EP composites was of about 0.68±0.02 established by ashing the material.

Table 4.6: Composition and designation of the GF/EP materials tested

Designation	V_f (Volume fraction %)	Compatible Sizing
UD-GF/EP	68	-
UD-GF/EPM	68	+

Carbon Fibre Reinforced Epoxy with and without Interleaves

UD carbon fibre reinforced epoxy prepregs (CF/EP) with thickness 0.125mm (AS4/3501-6; BASF) were stacked in different lay-ups (cf. Table 4.7) and cured by the usual autoclave bagging according to the producer recommendation. As adhesive interlayer (I) a modified EP (FM300, American Cyanamid) with a thickness of 0.125mm served. The consolidation quality of all laminates was checked by Ultrasonic C-scanning.

Table 4.7: Designation and stacking sequence of the CF/EP composite systems

Designation	Stacking sequence	Interleaf
CF/EP1a	$[0_5 / 90_5 / 0_5]$	-
CF/EP1I	$[0_5 / I / 90_5 / I / 0_5]$	FM300
CF/EP2a	$[0_2 / 90_2 / 45_2 / -45_2]_S$	-
CF/EP2I	$[0_2 / 90_2 / I / 45_2 / -45_2]_S$	FM300
CF/EP3a	$[45_2 / 0_2 / -45_2 / 90_2]_S$	-
CF/EP3I	$[45_2 / I / 0_2 / I / -45_2 / 90_2]_S$	FM300

4.2. Mechanical characterisation

4.2.1. Tensile tests

Tensile properties were measured either on a Zwick™ 1485 or 1445 (Ulm, Germany) universal testing machines equipped with mechanical extensometres. The extensometers provided very accurate measurements of the specimen strain in the loading direction. Different load cells (50N-250kN) and crosshead speeds (1-500mm/min) were applied depending on the material properties. All tests were

performed at controlled conditions, i.e. ambient temperature 25±2°C with relative humidity 45%. A data link to an IBM compatible PC featuring Zwick^{TM} specialized software was used in order to transmit on line the data to force-displacement or stress-strain curves.

4.2.2. Fracture-mechanical characterisation

The determination of the fracture toughness (K_c) and fracture energy (G_c) was done in accordance with a testing protocol in a recent ESIS book [103]. Depending on the material properties either the high-speed three-point impact bending or the compact tension (CT) configuration were used. The notch of compact tension (CT) specimens (dimensions: 35x35x4 mm^3), sawn from the cured plates was sharpened by a razor-blade prior to their tensile loading. For the K_c determination the maximum load (F_{max}) of the CT specimens was always considered.

In case of high speed three point impact bending specimens rectangular specimens (dimensions: 50x10x4) were cut and notched by a Ceast Notchvis® device. The relative notch depth (a/W) was varied between 0.2 and 0.6. The specimens were impacted by 1.5m/s at room temperature. The specimens were subjected to instrumented impact bending at span length of L=40mm without cushioning the striker. The instrumented impact pendulum (AFS-MK3 fractoscope of Ceast) recorded the force during impact as a function of time (F-t). The primary data stored were converted into force-deflection, energy-time and energy-deflection traces as well using a suitable data evaluation program. This program computed all necessary data by cursors movement at any displaying mode. From the registered and computed data the fracture energy (G_c) was determined by two methods: linear regression applied for the point pairs and the best linear fit which is passing obligatory the origin of the coordinate system.

4.2.3 Microdroplet pulloff test

The single fibre microdroplet pulloff technique was used to characterise the bonding between matrix and fibres in a composite material. The interfacial shear strength was determined by this test. The samples for the microdroplet pulloff test were prepared by hanging up microtomed matrix chips onto the fibres. Droplets were formed by

pulling the fibre through the polymer melt. Consolidation of the single fibre microcomposites was always realised by air-cooling.

The microdroplet pulloff test was performed on the specimens using a specially-designed and tailor-made micro-tensile testing machine equipped with highly precise Hottinger-Baldwin load (Q11, full range: 1N) and displacement (W10, full range: 10mm) transducers [104]. This device allows the tests to be visually monitored by stereoscope light microscopy. Pull-out speed (0.5 mm/min) and fibre free lengths (7-8 mm) were kept constant in order to achieve similar conditions in terms of stored elastic energy (mainly in the fibre free length) for interface failure initiation and propagation. The embedded fibre lengths varied in a range from 60 to 160 μm, according to the specific sample preparation techniques. Load-displacement curves were monitored on a x-y plotter. Interfacial failure occurred when the applied force reached the maximum value F_{max} and dropped subsequently.

The calculation of the interfacial shear strength (τ_i) values was obtained by the following expression:

$$\tau_i = \frac{F_{\max}}{\pi \times D \times L}$$

F_{max}: maximum tensile load

D: fibre diameter

L: embedded fibre length (determined by SEM)

4.2.4. Hardness tests

A Zwick 3114 hardness tester was used for the rapid determination of hardness to Shore (DIN 53505 [105]) on elastomers and relative soft plastics. The test method was based on the penetration of a specific indentor forced into the material under specified conditions. The Shore A hardness testers was used in the range of 10 to 90 Shore A, and the Shore D hardness testers in the range of 30 to 90 Shore D. The Shore A was suitable for relatively soft material and the Shore D for slightly harder material. Hardness test is however complicated since the phenomenon of elastic recovery and that of creep are usually involved. Therefore it is not valid to compare the hardness of various plastics entirely on the basis of one type test.

4.3. Thermal Characterisation

4.3.1. Differential Scanning Calorimetry, Thermomechanical Analysis

Melting behaviour of the materials tested was studied by differential scanning calorimetry (DSC) in a DSC 821^e apparatus (Mettler Toledo, Germany). DSC traces were registered as a heating rate of 5-10 °C/min on samples weighing ca. 10-20 mg. Determination of the linear expansion coefficient of the materials tested was studied by thermomechanical analysis (TMA) in a TMA40 apparatus (Mettler Toledo, Germany). Heating rate was 5 °C/min in 30 ml/min N_2 environment. Both apparatus were connected on-line with an IBM compatible PC which enabled the recording of thermal traces.

4.3.2. Dynamic Mechanical Thermal Analysis

The viscoelastic response of the polymers and composites tested was studied by dynamic mechanical thermal analysis (DMTA). An Eplexor^{TM} 150N (Gabo Qualimeter, Ahlden, Germany) DMTA machine was employed to carry out the tests. The measurement principle is based on forced oscillations below the resonant frequency of the samples. The specimens were subjected to oscillating dynamic loading consisting of a static preload of 10-20 N on which a sinusoidal wave of 5-10 N at a constant frequency was superimposed. Viscoelastic material parameters such as mechanical loss factor and complex Young's modulus ($\tan\delta$ and E^*, respectively) were measured. The measurements were made, mainly, under 3 point bending loading according to the ISO 6721 standard [106]. For soft polymers and elastomers a tensile mode was selected [107]. Heating occurred at a rate of 1 °C/min and in a temperature range between –150...300°C depending on the material tested. The testing frequency varied from 0.001-100Hz.

4.4. Erosion test

4.4.1. Erosion chamber

All the erosion tests were performed in a commercial sand-blasting chamber (ST 800, Paul Auer GmbH, Mannheim, Germany). The equipment was modified in order to carry out measurements according to standards (ASTM G76 83; DIN 50 332) [108, 109]. The sand-blasting chamber (cf. Figure 4.1) enclosed the sample holder (a) and the nozzle (b). The nozzle consisted of two parts, a boron carbide jet nozzle and an

air nozzle with internal diameters of 10mm and 4mm, respectively. The sample was covered by a steel cover frame with different circular openings (ϕ10, 20 and 30mm), depending on the testing procedure after erosion. Working distance and impact angle was adjusted by moving the nozzle holder (g) and turning the sample holder(a). The speed of the erodent particles was set by modifying the air pressure of the nozzle (h).

Figure 4.1: The sandblasting chamber and its parts

The erodent material was collected at the bottom of the chamber (e) and transferred to a cyclone that removes the solid particles from the air stream generated by the suction-fan of the air filter. The air filter collected the light-weight dust. The erodent material from the bottom of the cyclone was recycled to the nozzle in order to maintain the equipment's continuous work. Positions (b) and (c) show the particles- and the air stream- hoses, respectively. The mass flow was regulated from the hose in the position (f) in order to avoid collision of the particles. The working distance and the air pressure were kept constant during the experiments at 16cm and 6bars, respectively.

4.4.2. Erodent Materials

Table 4.8 lists the erodent materials used during this study along with their characteristics. Corundum 1 was used as standard erodent during the study. Figure 4.2 presents a scanning electron microscopy observation (SEM) of this erodent.

Table 4.8: List of the erodent systems used in this study

Designation	**Size [µm]**	**Shape**	**Density ρ [g/cm^3]**	**Hardness Mohs scale**
Corundum1	60-120	Angular	4	9
Corundum2	120-240	Angular		
Steel Grit	120-300	Angular	7	8-9
Glass Beads	150-300	Round	2.6	6-7

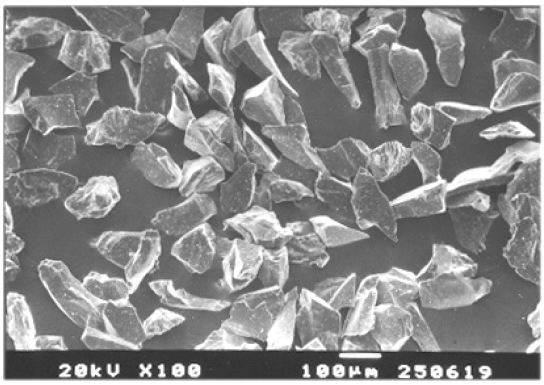

Figure 4.2: SEM observation of corundum1 particles

4.4.3. Erodent Velocity Measurement

The most commonly used method for measuring the velocity υ (m/sec) of the erodent particles is the double-disc method [110], in which two circular discs with a known spacing are fixed on the same rotating shaft. By measuring the angle θ (°) through which the discs rotated while the particles passed from the first to the second disc, the time of flight t (sec) through a known distance l (m) and consequently the velocity are found using equation 4.1 [111].

$$\upsilon = \frac{l}{t} = l \times 360° \times \frac{\gamma}{\theta} \qquad [4.1]$$

where γ the revolution speed (1/sec).

A mask having a 6 mm diameter hole was used in the present work for determining the particle velocity (cf. Table 4.9). While useful, this method has several shortcomings [112] which should be taken into account: i) the determination of the position of the centre is subjective, ii) the velocity measurements can not be made during the erosion test, iii) the velocity distribution is not determined, iv) the gas stream in disturbed by the rotation of the disks, v) the velocity distribution at low velocity may be twisted by particles losing energy as they strike the edges of the slit, vi) Using erodent material of small particle size, the air stream that makes the material recirculate can drag the particles and transfer them to the air filter. This leads to a continuous removal of erodent from the reicirculation cycle.

A comparison, however, of the values measured with this method with that measured with the Laser-Doppler Anemomerty [113] shows a deviation of 5% which is acceptable as the cost of the Laser-Doppler Anemomerty is prohibitive.

4.4.4. Erodent Mass Flow Measurement

An other mask having a hole of 30 mm diameter was employed to measure directly the mass flow of all the erodent material that touches the sample surface. In this way the mass flow perpendicular to the flow axis is measured (cf. Table 4.9). At an angle of impingement different from 90°, the projection of the specimen surface on the plane perpendicular to the flow axis is smaller. Therefore, a lower amount of erodent reaches the surface in the unit time. For flat surfaces, the factor K (K=sinα) can be used in the calculation of mass of erodent. At low angles of impingement a shadow effect due to the finite thickness of cover plate influence further the mass flow of the erodent. This effect is significant for angles lower than 20° for the test geometry used, therefore it was not taken under consideration.

Table 4.9: Mass flow rate and mean velocity of the applied erodents

	Corundum1	**Corundum2**	**Steel Grit**	**Glass Beads**
Mass Flow [kg/s]	0.015	0.032	0.039	0.036
Velocity [m/s]	70	102	60	75

4.4.5. Calculation of the Erosive Wear

The weight loss of a test specimen due to erosion was recorded as a function of erosion time by a precision balance (AT261 Mettler Toledo; sensibility 50µg). The erosive wear rate (ER) is calculated according to the method of the least squares by the slope of the line in a steady state, that is, weight loss per impact time and indicated in mg/s. The determination of the erosive wear rate contains an measuring error of 3%. Figure 4.3 presents the change of mass of an eroded target and the variation of 'erosion rate' with the duration of the erosion test. After an initial incubation period t_i a linearly increasing is established. The plateau region is an indication that a constant rate has been established. If the weight loss increase linearly from t=0 the ER graph would become a straight line parallel to the time axis.

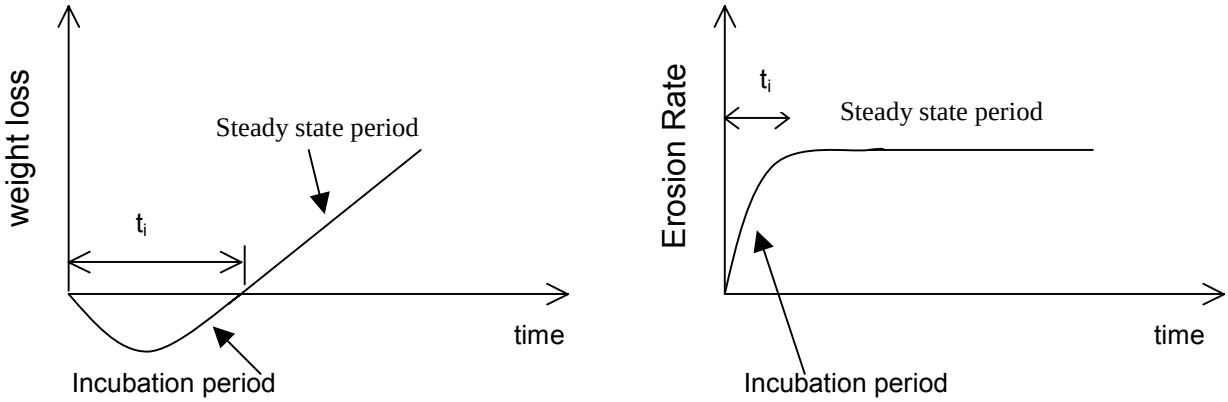

Figure 4.3: Variation of the weight of the eroded target and of the respective ER as a function of the erosion time, schematically illustrated.

4.4.6. Definition of the Erosion Direction in respect to the Fibre Orientation

Figure 4.4 presents schematically the notation of the erosion direction in case of UD composites. There is no sense to indicate the erosion direction at normal impact (90°) because the particles hit the same transverse area.

4.4.7. Specimens Preparation

Specimens were usually cut by using a Mutronic (Rieden, Germany) table disc-saw. For the case of brittle materials like CF/EP and GF/EP systems cutting was made by a diamond saw. Rectangular plates of 40x40mm^2 were usually cut for the solid particle erosion tests. These specimens were subjected to SEM observations and

Laserprofilometry. Erosion specimens were also cut in the two following shapes: 120x10 mm^2 and of 60x10 mm^2. The longer specimens were afterwards subjected to tensile tests, while the shorter ones to DMTA and ultrasonic tests.

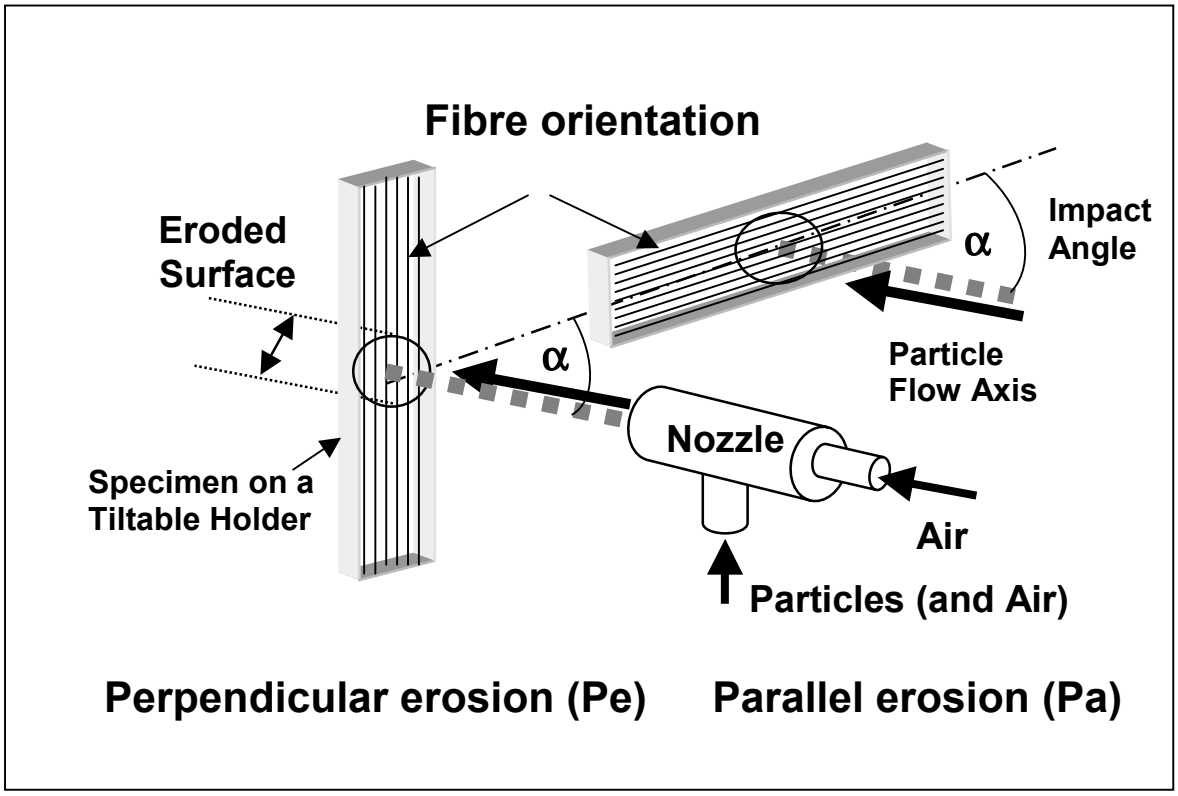

Figure 4.4: Schematic diagram of the erosion direction in UD composites

4.5. In Situ Observation of the Eroded Surfaces

4.5.1. Infrared Thermography

The infrared thermography (IT) is a technique to study the failure mode in polymers ensured by their inherently low heat conductivity. Although it is impossible to apply IT during an erosion test, thermographs were taken right after the erosion tests. As erosion involves impact, an increase in the surface temperature is expected depending on the art of the material, and on the impact angle. A Hughes infrared camera (Portland, Oregon, USA) connected to a Sony digital monitor and a videorecorder, helped to monitor the temperature variation after solid particle erosion. By correlating the IT pictures obtained from the eroded surfaces with the mass loss of the material, useful information on the fracture mode and failure mechanisms could be derived.

4.5.2. Scanning electron microscopy

The eroded surface of the specimens was studied in a scanning electron microscope (SEM; JSM 5400 of Jeol, Tokyo, Japan). Specimens were sputtered in a Balzers SCD-050 (Balzers, Liechtenstein) sputtering device for 150 sec with a Pt/Pd alloy. This resulted in the formation of a conductive layer of about 100 nm on the specimen surface making the SEM observation possible as the electrostatic charging of the surface was reduced. The use of SEM made it possible to observe what had physically occurred on eroded surfaces.

4.6. Non Destructive Testing Methods

Ultrasonic C-scanning procedure was employed to the eroded laminated composites in order to visualize the internal damages. The specimens were placed in a water tank and scanned across their surface with the help of a Panametrics 5627RPP automated ultrasonic scanning system coupled on line to a PC computer. The sensor scanning frequency was 10 MHz and scanning speed was set at 0.5 mm/s.

5. Results and Discussion

5.1. Solid Particle Erosion of Polymers

Solid particle erosion behaviour of polymers [13,17,21,44,45,51,53,55,114,115] and elastomers [20,24,25,39,47-49,54,56,67] is extensively studied and cited in literature. Possible correlation with material properties and dominating mechanisms of material removal have been discussed, but still there is a gap in the definite recommendation of beneficial characteristics for erosion resistance.

Two typical systems were selected here to represent this wide category of materials. Thermoplastic polyethylene is an engineering polymer used very often in applications that involve erosion and impact. Polyurethanes on the other hand represent extraordinarily versatile polymeric materials which can be tailored to meet highly diversified demands of applications and processing technologies such as coatings, adhesives, reaction injection moulding, fibres, foams, rubbers, thermoplastic elastomers and composites. Even within a particular group, such as polyurethane elastomers which have relatively outstanding wear properties, there exists a range of performance in which some materials behave much better than others.

5.1.1. Thermoplastic Polyethylene

Table 5.1 presents the thermal properties of the materials tested. Based on the related DSC results one can conclude, that the melting and crystallisation enthalpies agree very well with each other, and an increase in crosslinking degree is accompanied with reduced crystallinity (cf. PE1,PE2 and PE3). Note that table 5.1 also contains results derived from DSC traces taken on the eroded surfaces after testing at 15° and for two samples (PE1 and PE3) at 90°. One can recognise that the melting and crystallisation enthalpy values are either slightly higher or lower than those of the virgin samples after erosion at 15° oblique impact angle. A crystallinity increase due to heating up (annealing) of the bombarded surface is unlikely at this angle. The related change should be assigned to sample-related crystallinity inhomogeneities. The explanation behind the strong reduction of the melting and crystallisation enthalpies of the samples eroded at 90° is more clear-viz. erodent particles are embedded in the specimen surface. By this way the relative amount of the PE tested in DSC is considerably reduced.

Table 5.1: DSC results (melting and crystallisation enthalpies)
Note: virgin samples are denoted by “no”

Enthalpy [J/g]	Erosion Angle [°]	PE1	PE2	PE3	PE4
Melting	No	211.7	194.8	165.7	163.8
	15°	213.0	194.3	168.3	165.5
	90°	158.2	-	140.1	-
Crystallisation	No	214.8	194.4	165.8	164.8
	15°	212.9	188.6	168.7	165.7
	90°	158.8	-	143.5	-

The tensile characteristics read of the stress-strain curves of dumbbell specimens are tabulated in Table 5.2. In the same table the related G_c values are also given. Both slopes going either through the coordinate origin (slope2) or not (slope1) are listed. Based on the tensile data one can conclude that increasing crosslinking degree decreases the E-modulus and the stress at yielding (σ_y) but enhances the ultimate stress (σ_u) and the fracture energy.

Table 5.2: Tensile- and fracture- mechanical characteristics
Note: deformation speed *1mm/min, ** 50mm/min, ***1.5m/s

	PE1	PE2	PE3	PE4
E modulus [MPa]	1253	930	858	603
σ_y [MPa] *	31.3	27.9	28.2	19.6
σ_u [MPa]**	15	21.9	21.8	14
ε_y [%]*	11.5	15.4	14.7	16.7
ε_u [%]**	567	566	305	824
Slope1**	3.1	9.3	13	6.4
Slope2**	3.1	7.7	10.8	8.2

Figure 5.1 displays the ER as a function of the incident impact angle. One can recognise a typical ductile behaviour that usually characterise tough polymers like PE with maximum ER at low oblique impact angles (here maximum ER is found by 15°) and minimum at normal impacts. It is interesting to note that PE4 shows 2.5 times

less ER at 15° and 30° in comparison with the other PE. Recall from chapter 4 that the main difference in the base components between PE4 and PE1 is the catalyst used. However, this difference tends to be minimised as the impact angle approaches 90°. Observing the influence of the addition of crosslink agent on the ER one can say that crosslinking has no beneficial effect on the erosion resistance below 45° impact angle. Some improvement may be found beyond 60°. At normal impact (90°) the erosion resistance of the crosslinked samples is outstanding. Nevertheless it should be noted that any impact angle higher than 15° the ER of PE2 and PE3 is almost the same implying that the addition of crosslink agent beyond a specific amount (here 50%) is not valuable for the erosive resistance.

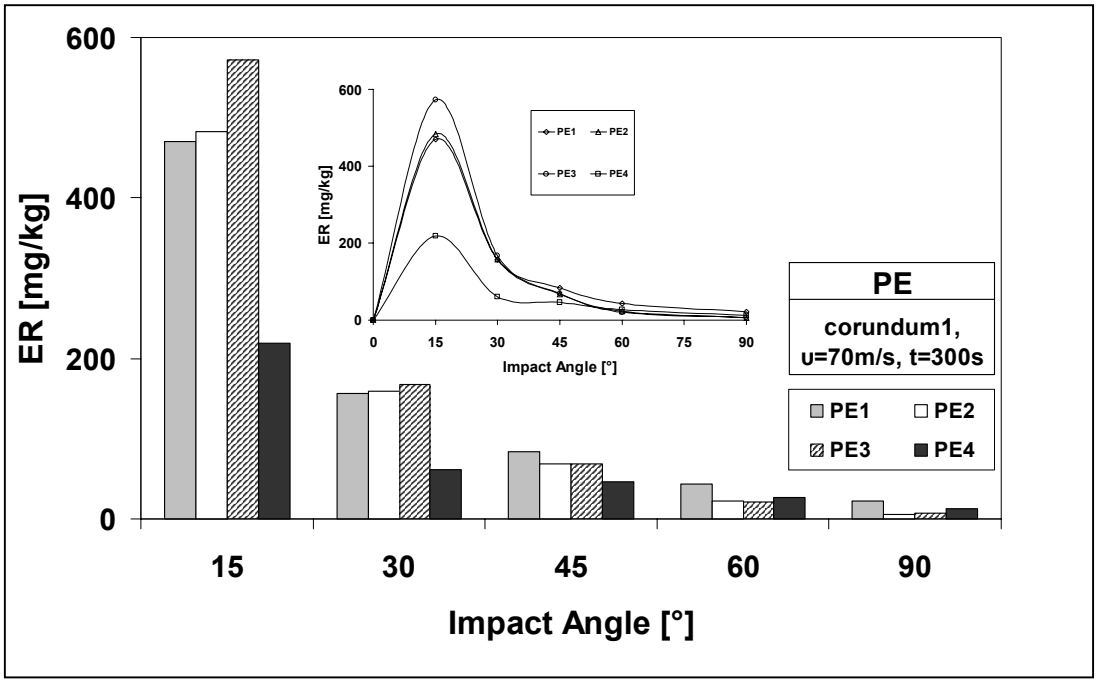

Figure 5.1: ER variation as a function of the impact angle of the PE samples

The observed ER did not correlate with the thermal, mechanical and fracture properties of the PE samples presented in Table 5.1 and 5.2 or with combination of these properties like for instance stress at yield and ultimate strain [17] confirming the complexity in these trials.

A very common question in literature deals with possible thermal effects and their role in the erosion of PE [44,45]. It is likely since each impact causes plastic

deformation and most of the impact energy is converted into heat. It is well known that solid particle erosion leads to a temperature increase of the impacted surfaces. Because PE has a low thermal conductivity, if the particles arrive fast enough, thermal energy accumulates in the surface [44]. High temperatures may soften the material and may result in a thermal stress field being superimposed upon the mechanical field of deformation. This will have important repercussions since it is acknowledged that the development and relaxation in the plastic zone of the impact site is associated with viscoelastic extrusion and fracture in polymers. These damage modes ultimately account for degradation and material loss.

Three characteristic specimens were selected (i.e. PE1, PE2 and PE4) and their eroded surfaces were observed by SEM. These observations enabled to investigate the possible thermal effects and helped us to understand the mechanisms that govern solid particle erosion at the different impact angles. Studies concentrated on the temperature rise in PE stated that the maximum temperature rise would remain insufficient for localised melting. It was estimated that thermal effects would become significant at a flux rate of ca. 180 $kgm^{-2}s^{-1}$ [45]. The flux rate even at 15° impact angle, where it shows its maximum, was definitively lower (82 $kgm^{-2}s^{-1}$) than this value and thermal effects should be not dominant. This is also confirmed from the SEM pictures of all eroded surfaces (cf. Figure 5.2).

The comparison between ductile and brittle materials according to the angle of impingement, has shown, that the ductile materials are more sensitive to abrasive particles. The maximum of the erosion lies in the area of 15° to 40° as a result of ploughing and damage accumulation processes. By contrast, brittle materials exhibit a maximum erosion rate when the impact angle is normal due to the generation and propagation of subsurface lateral cracks. Erosion rate (ER)-impact angle diagrams indicated a ductile erosion response for all PE specimens as they showed a maximum ER at 15° impact angle. Comparing the SEM pictures a to d in Figure 5.2, representing the worn surfaces after erosion at 15, 30, 45 and 90°, respectively, we can see that the maximum material removal should occur at 15 and 30° surfaces (series a and b, respectively), while the minimum loss should be observed at 90° impact (series d in Figure 5.2).

For any surface contact, various deformation mechanisms may act simultaneously for the material deformation and removal owing to the interacting surfaces. A mixed mode of material removal is dominant during solid particle erosion of the PE samples, depending on material characteristics (ductility, hardness, crystallinity etc.) and the impact angles. For example, ideal microploughing would involve just the displacement of material from the crater without any fracture (and hence no erosion). The opposite case would represent ideal microcutting. Formation of a lip and its subsequent fracture is also observed (see Figure 5.2a- sample PE4). Interlinking of lateral or radial cracks is observed at high magnifications at middle to high impact angles (cf. Figure 5.3b). The surface topography of PE1 and PE2 at 15° impact angles (a series in Figure 5.2) is very similar to that of specimens under sliding wear by a blade indenter. PE4 shows, because of its more amorphous nature, more cutting characteristics with chips formation (cf. Figure 5.3a) than PE1 and PE2.

The proportion of impacts that involve substantial material displacement (ploughing and cutting) is high at low angles. On the basis of the model of ductile polymer erosion, the materials removal take place by the formation of grooves and their snagging by subsequently impacting particles (cf. Figure 5.2b series). At oblique impact, the material removal is due to microploughing and microcutting. The microcutting and microploughing phenomena occurred at low impact angles are mainly connected with the hardness of the particles, which can penetrate into the surfaces. Plastic deformation is also observable. Under repeated impact, the extruded edges of the craters suffer severe plastic deformation. When the impacting strength exceeds the material strength, the material detaches. Under similar conditions semi-crystalline polymers show a ‘cutting’ deformation due to a tearing action on the material surface. Cutting characteristics are prominent for PE4 also at 30° impacts.

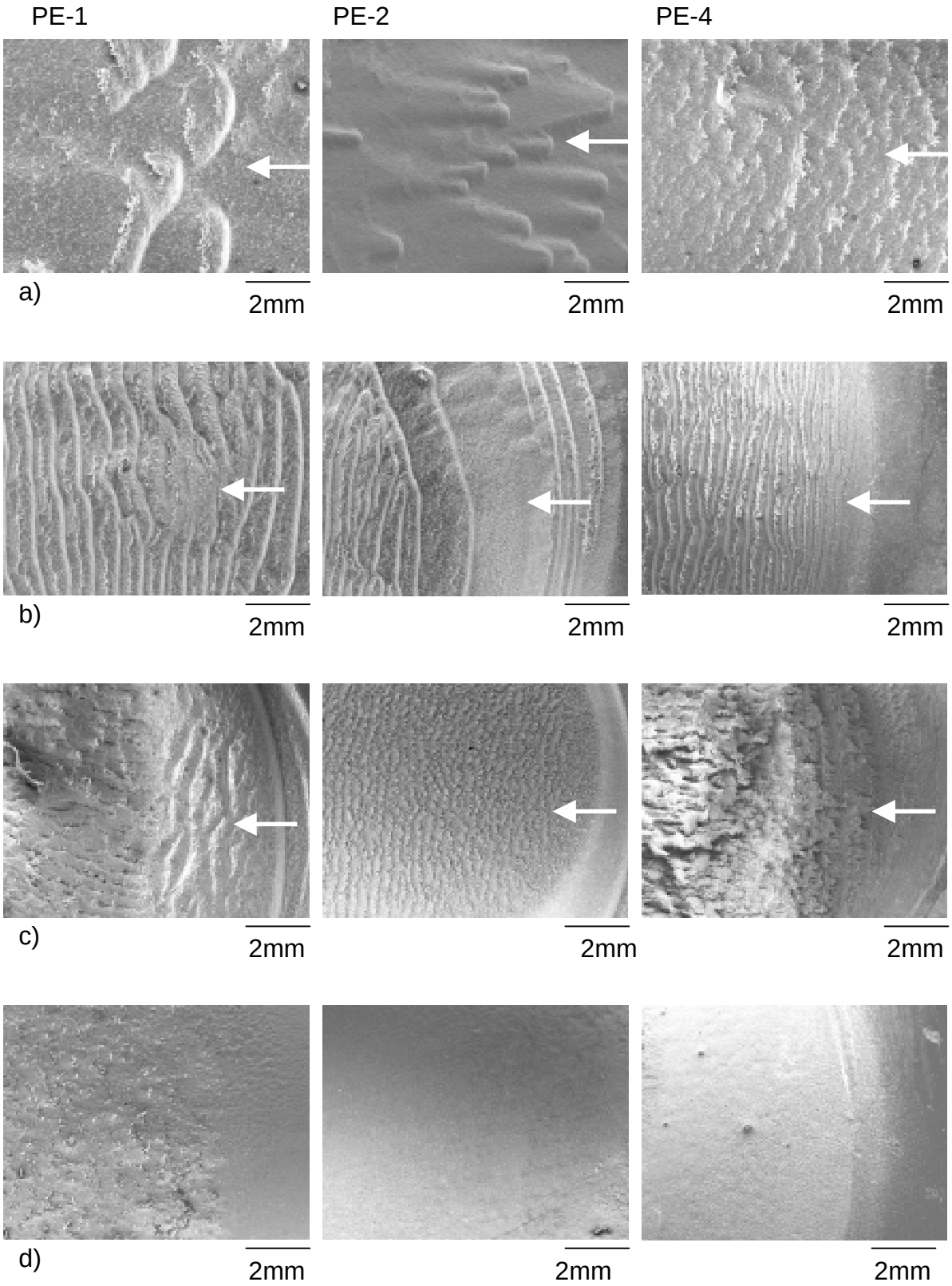

Figure 5.2: SEM of the PE eroded surfaces, at a)15, b)30, c)45 and d)90° impact angles

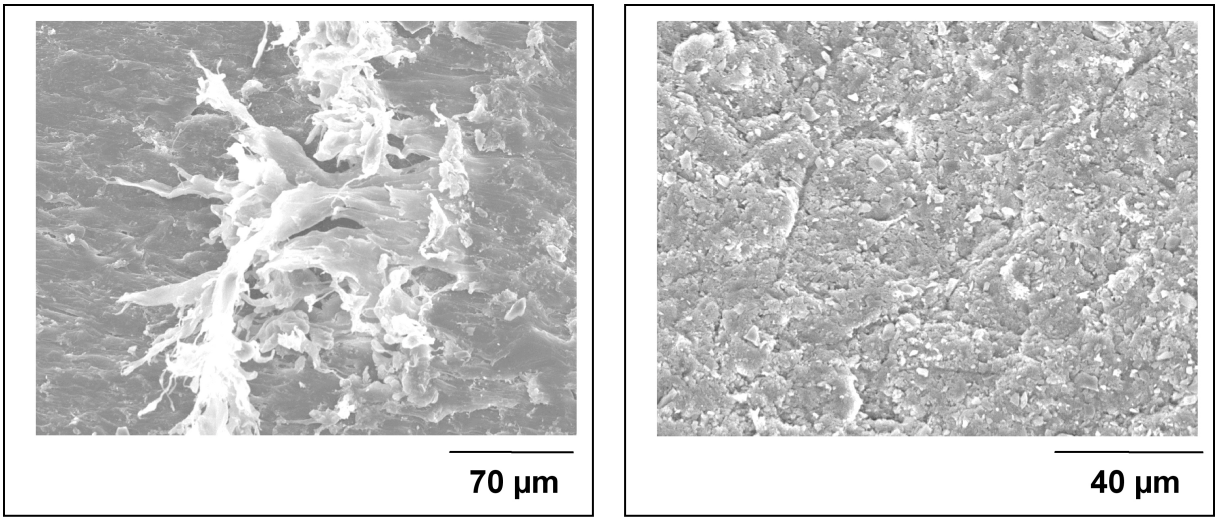

a) b)

Figure 5.3: SEM micrographs of PE4 eroded at a) 15° and b) 90° impact angles.

The surface features at low impact angles include transverse ridges. Even at 45° (Figure 5.2c, series related to PE1 and PE2) ploughing of the material can be resolved. Proceeding to 90° impact, the surface becomes smoother and only in higher magnifications networks of cracks become observable. At 90° impacts (cf. Figure 5.3b), at the beginning fine-scale cracks on the eroded surface are apparent. Continuing the erosion, a network of furrows containing fine cracks has developed. Finally, the whole surface has been broken up into a fine-scale, apparently granular structure by the repeated intersection of the surface cracks. The intersection of the cracks leads to roughening of the surface of the material.

5.1.2. Thermoplastic and Thermosetting Polyurethanes

As stated above, attempts to correlate chemical-, mechanical-, thermomechanical- and fracture mechanical- properties with wear response of polyurethanes have been presented without great success. In this paragraph a systematic study of the erosion response of six thermoplastic and twelve thermosetting commercial polyurethanes with a wide range of properties has been made. Table 5.3 presents the mechanical properties alone with the rebound resilience (RR), tear propagation resistance (τ_R) and thermal expansion coefficient (α_{TH}). These properties and some combination of them, have been proposed to relate with the erosion response of polyurethane elastomers.

Table 5.3: Characteristic properties of the polyurethane elastomers tested

	ρ	H	σ at ε=100%	σ at ε=300%	σ_u	ε_u	τ_R	RR	α_{TH}
	[g/cm^3]	[Shore A]	[MPa]	[MPa]	[MPa]	[%]	[kN/m]	[%]	[10^{-6} K^{-1}]
PU-1	1.26	95	10.6	15.8	42	692	67	61	176
PU-2	1.26	83	4.3	7.8	50	660	31	65	192
PU-3	1.26	70	2.5	4	42.3	650	15.5	52	229
PU-4	1.21	87	6.6	16	42	410	30	50	142
PU-5	1.23	86	5.6	9.5	35	550	40	52	170
PU-6	1.24	94	10	17	53	432	65	34	159
PU-7	1.24	72	6	11	52	800	-	75	174
PU-8	1.07	70	2.7	6.5	11.6	430	11.5	53	184
PU-9	1.03	80	3.5	6.7	11.7	460	19.3	50	180
PU-10	1.11	70	2.7	6	12	530	15	54	217
PU-11	1.20	55	1.8	3.6	21.2	495	-	45	211
PU-12	1.13	97	9.6	21.2	32.6	394	84.4	52	169
TPU-1	1.14	92	8.5	16	50	550	85	-	167
TPU-2	1.20	93	7	20	55	550	95	-	150
TPU-3	1.21	91	7	20	55	550	90	-	160
TPU-4	1.21	89	7.2	12.6	50	530	66	-	164
TPU-5	1.23	90	8	16	37	525	122	47	143
TPU-6	1.20	92	8	20	50	500	100	36	189

Figure 5.4 presents the ER variation of the tested materials at 15,30 (diagram a) and 90° (diagram b) impact angles. Similar to earlier observations cited in literature, maximum ER is found by 15° which is typical for elastomer materials. The ER at 30° is more than the half of that at 15° implying that the elastomers suffer more when the experimental conditions favour the abrasion. It is also apparent, that a similar behaviour in the erosion response of the polyurethanes exists at 15 and 30°, i.e. the materials with better resistance at 15° continue to resist better at 30°. This implies that the same mechanisms of material removal dominate. This is not the case, as expected, at 90°. While PU-6 for instance shows the worse response at 15° impacts, the same material shows the best resistance at 90°.

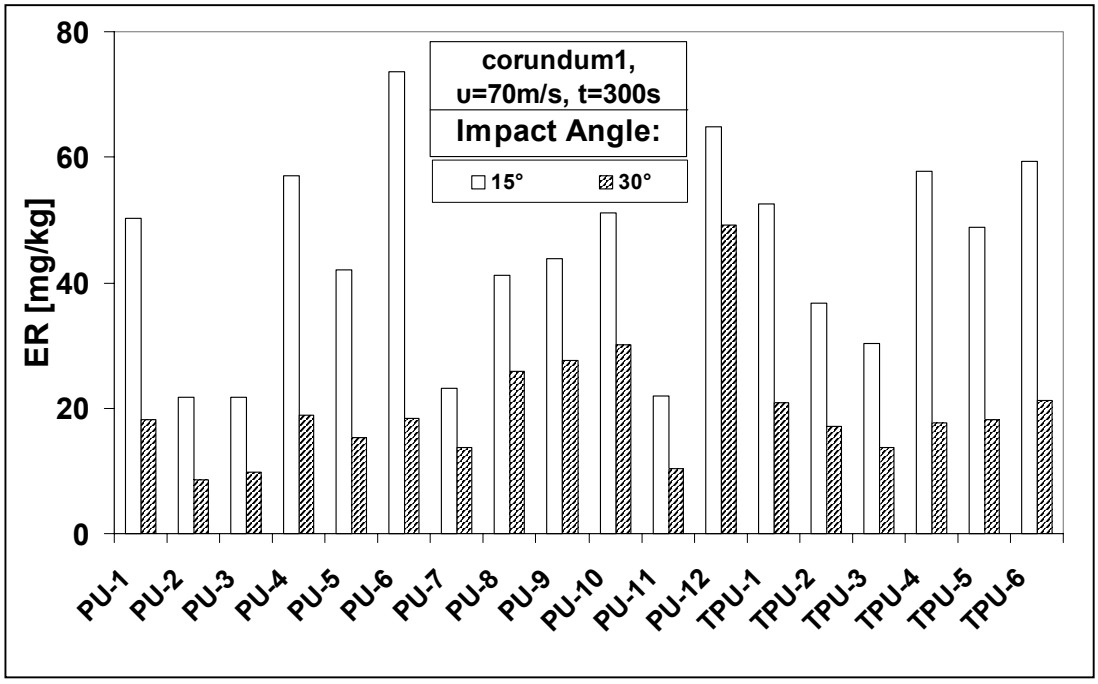

a)

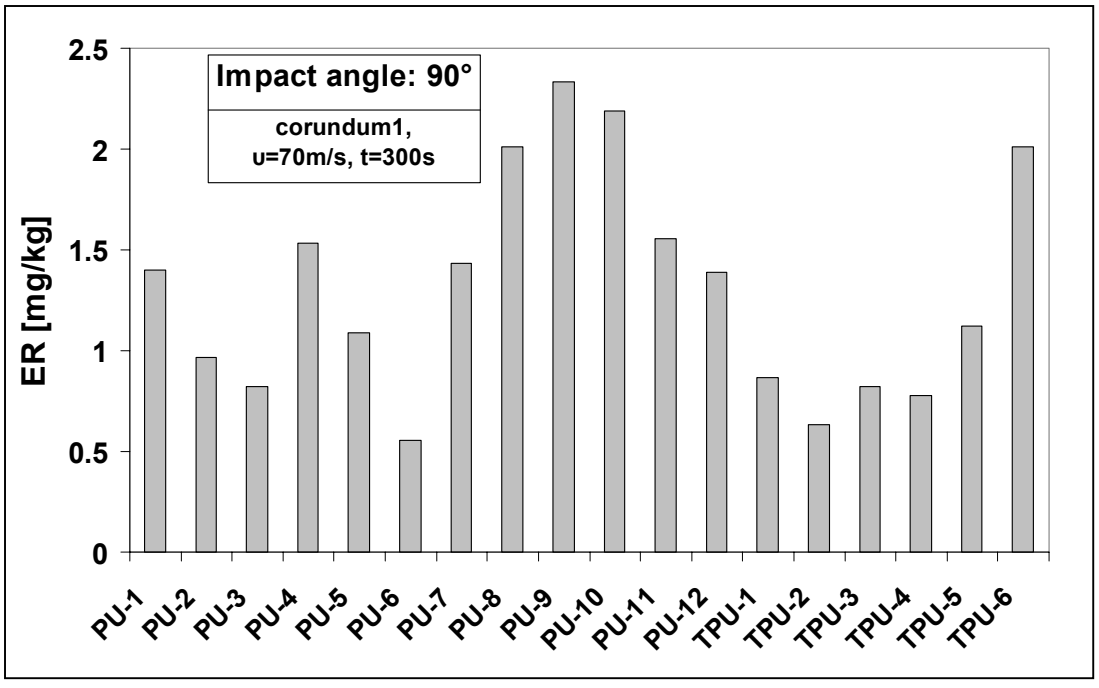

b)

Figure 5.4: ER variation of the thermoplastic and thermosetting polyurthanes at a)15, 30 and b) 90° impact angles.

In order to understand these differences, a statistical program has been applied and all possible correlations have been examined between ER and material properties listed in Table 5.3. Combination of material properties and empirical equations already mentioned in paragraph 2.3.2.1, like the quantity $(1\text{-}RR)^{1.4}$, or the combination of high yield stress and strain high yield stress have been additionally examined. Alike the results presented for the abrasive wear of polyurethane elastomers [34] a lack of correlation among polyurethane chemistry, standard mechanical properties and erosion resistance was found. An example of these results is presented in Figure 5.5, where the variation of ER is illustrated as a function of $(1\text{-}RR)^{1.4}$.

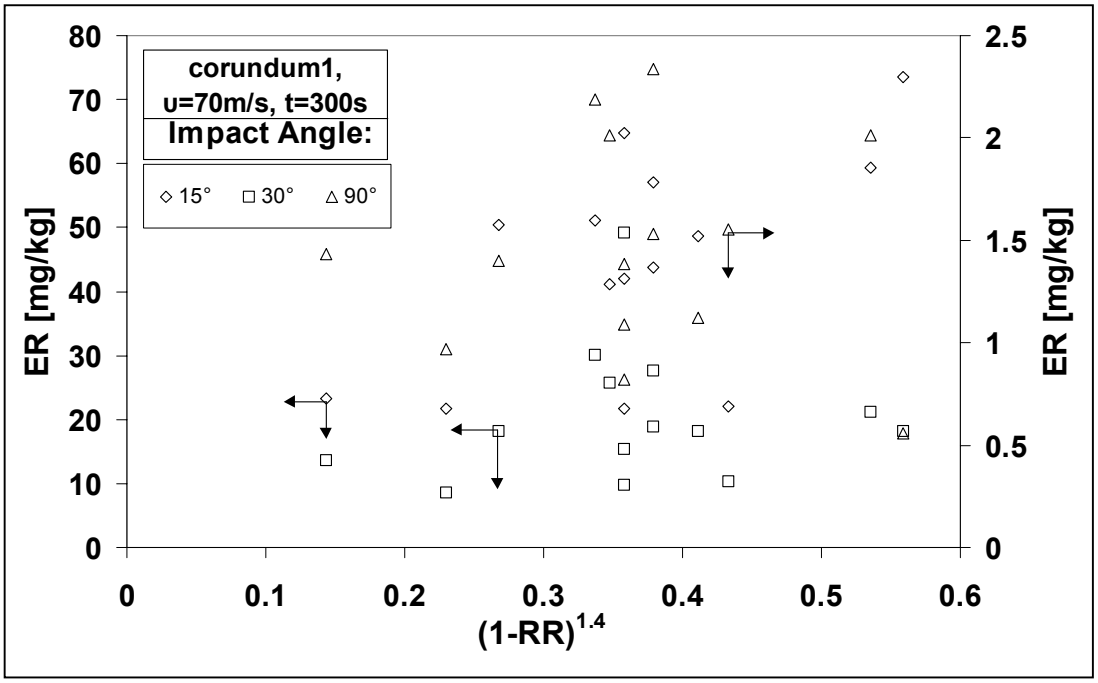

Figure 5.5: ER variation as a function of $(1\text{-}RR)^{1.4}$ for the polyurethane elastomers tested

5.2. Solid Particle Erosion of Modified Polymers

The erosive wear response of the three main categories of polymeric materials, i.e. thermosets, thermoplastics and elastomers is examined in details and reported in literature, in chapter 2 and 5.1. It was established that modification of all three categories of materials are very often used in order to tailor their properties for specific applications. These modifications may have opposite effects on various material properties and thus on the material response under different loading conditions including erosion. In the next paragraphs the influence of the commonly-used polymer modification on the erosive wear resistance will be examined and discussed.

5.2.1. Thermosetting Epoxy Resin modified with Hygrothermally Decomposed Polyurethane

Epoxy resins (EP) with and without modifiers are some of the most important thermosetting polymers widely used in different fields also as matrices in fibre-reinforced composite materials. Their brittleness and poor resistance to crack propagation is a drawback of this category of materials. The main goal of many studies was the toughening of EP in order to improve the damage tolerance of the related composites [116]. A way proposed to obtain this toughness enhancement was by elastomeric modification of the resins [117-126].

Recently it was reported that the mechanical property profile of tri- and tetrafunctional EP resins can be varied in a very broad range by modifying them with hygrothermaly decomposed polyester-urethane (HD-PUR) [98-100]. It was shown that the properties of the EP/HD-PUR systems could be set between those of crosslinked thermosets and rubbers via the HD-PUR amount. Modification of EP by HD-PUR resulted in a chemical network of lower crosslink density. The fracture -toughness and -energy of the EP/HD-PUR systems were found to vary with their crosslink density. This fact enables the investigation of the erosive behaviour as a function of the network characteristics and the fracture mechanical response of the modified EPs. It is also possible to study the solid particle erosion of a system that may show both brittle and ductile erosion behaviour depending on its composition and structural characteristics [127].

Figure 5.6 depicts the storage modulus (E') and loss factor (tanδ) spectra of the EP modified by various amounts of HD-PUR. One can notice that the T_g shifts towards lower temperatures with increasing amount of the modifier. Parallel to this change, the rubbery plateau modulus (E_R) (determined as indicated in Figure 5.6) is also reduced with increasing modifier content.

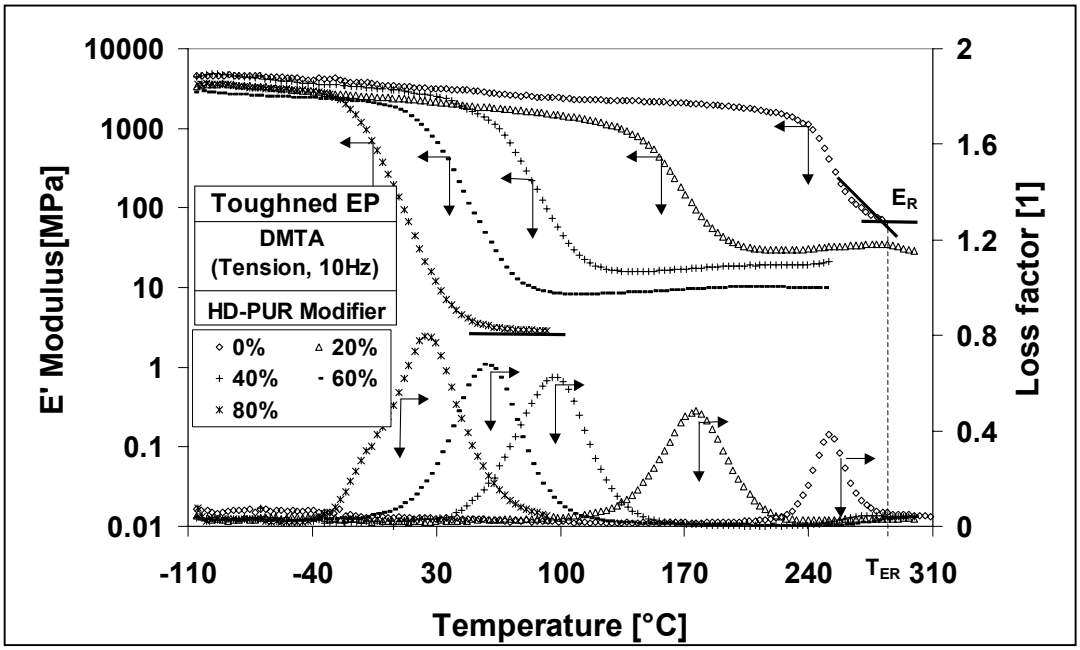

Figure 5.6: DMTA spectra of the EP/HD-PUR systems

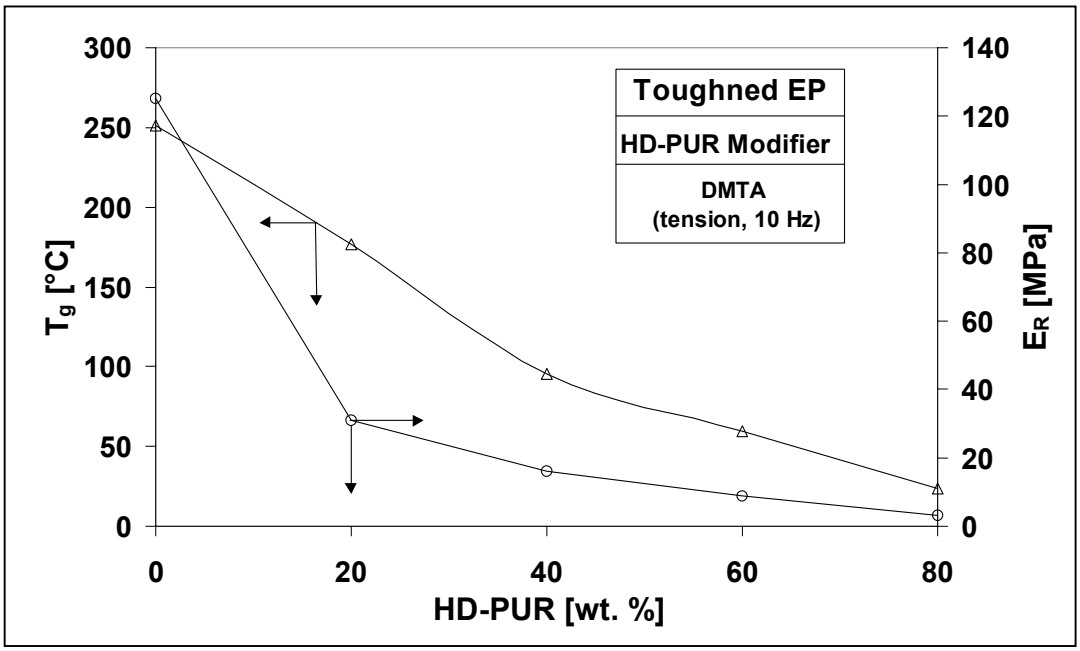

Figure 5.7: Variation of T_g and E_R as a function of the HD-PUR amount added

Figure 5.7 presents the variation of the glass transition temperature (T_g) and rubbery plateau modulus (E_R) values as a function of HD-PUR amount, as read from DMTA spectra in Figure 5.6. The reduction in both T_g and E_R implies that the HD-PUR participated in the crosslinking reaction and, thus, in the formation of the crosslinked network structure. As a consequence, HD-PUR works as an active diluent (plasticizer) in EP. This is corroborated also by the stiffness decrease of the EP compounds. All these findings are based on the fact that the hydrolytic decomposition of PUR provides a primary amine-rich rubbery compound [99,100]. HD-PUR works as an active diluent and phase separation modifier at the same time in EP resins.

In the literature, different approaches are described to show how the mean molecular mass between the crosslinks, M_c [125,126,128-131] or the cross-link density (number of chains per unit volume) v [128,132] can be determined. M_c and v values were computed by considering the rubbery plateau E_R just above the T_g, which could be well resolved for EPs with a high amount of HD-PUR (cf. Figure 5.6). For the EPs with less HD-PUR, the onset of the plateau modulus was taken (determined as indicated in Figure 5.6), as for these formulations the T_g and the thermal decomposition temperature were closely matched. According to the basic equation of rubber elasticity:

$$\mathrm{E}_R = \frac{3\rho RT}{M_c} \tag{5.1}$$

and

$$\nu = \frac{\rho \mathrm{N}_A}{M_c} \tag{5.2}$$

where ρ is the density of the EP/HD-PUR systems; R the universal gas constant (8.314 J/(molK)); N_A the Avogadro's number ($6.023*10^{23}$ mol^{-1}) and T the plateau onset temperature T_{ER} (cf. Figure 5.6).

In addition, the K_c and G_c values of the compositions were determined in accordance to ESIS protocol [103]. Table 5.4 summarises the measured and calculated data of the compositions tested here.

Table 5.4: Change in the hardness, fracture mechanical- DMTA- and cross-link-parameters as function of the amount of HD-PUR

EP/HD-PUR									
HD-PUR wt. [%]	Shore A or D	K_C [MPam$^{1/2}$]	G_C [kJ/m^2]	T_g [°C]	ρ [g/cm^3]	T_{ER} [°C]	E_R [MPa]	M_C [g/mol]	v *10^{20} [cm^{-3}]
0	85-D	0.89	0.15	251.5	1.313	282	125	141	56.1
20	85-D	0.98	0.8	176.6	1.301	210	31	505	15.5
40	80-D	1.38	1.4	95.7	1.285	135	16	817	9.5
60	68-D	0.30	2.0	59.8	1.272	93	8.7	1329	5.8
80	80-A	-	4.0	23.7	1.221	59	3.3	3064	2.4

Figure 5.8 illustrates the variation of crosslink density v as a function of the modifier content. The variation collaborates the above statement that the HD-PUR participated in the crosslink network and as the modifier content increases the crosslink density decreases; this means that the modified systems become less crosslinked.

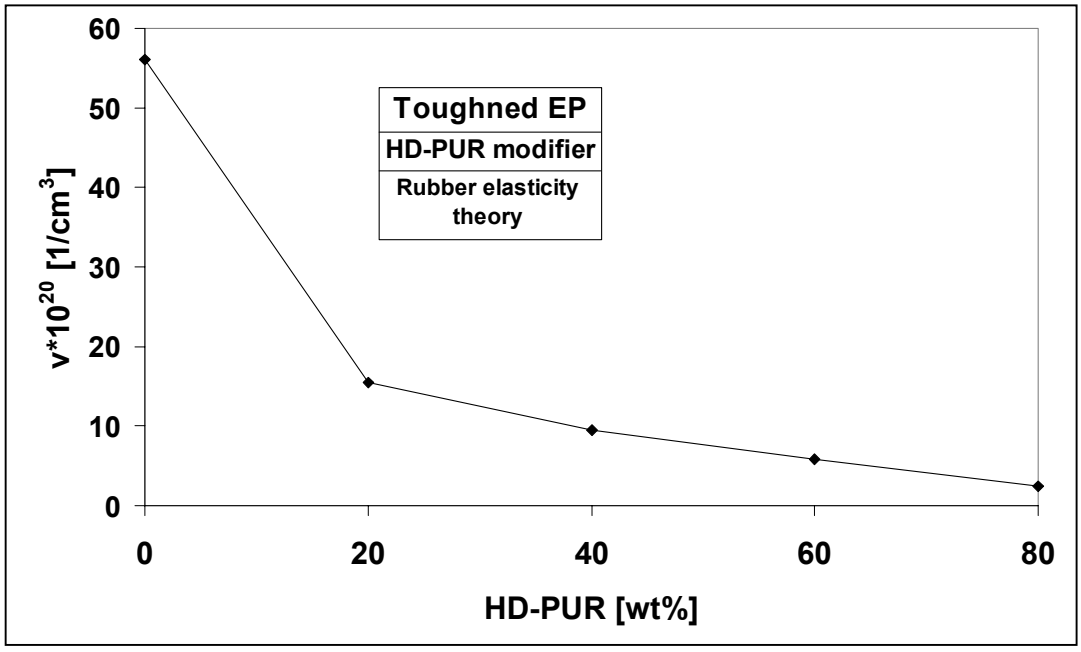

Figure 5.8: Variation of the crosslink density as a function of the HD-PUR content

The theory of rubber elasticity was often used to correlate the fracture mechanical parameters with those of the crosslinked network [98-100,126,129,130,133,134].

According to this interpretation G_c shows a linear dependence when plotted as a function of $M_c^{1/2}$. Figure 5.9 displays that the above linear relationship holds also for our HD-PUR modified EP resins.

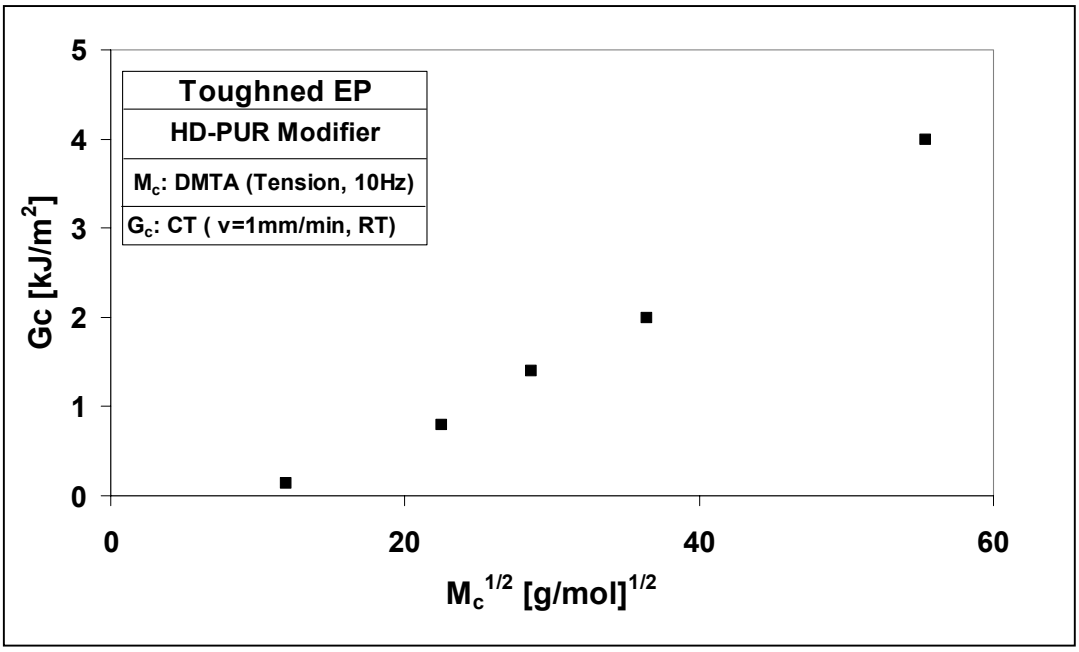

Figure 5.9: Variation of fracture energy (G_c) as a function of $M_c^{1/2}$ for the EP systems modified with HD-PUR

The modifier content leads to changes in the chemical network-, the toughness- and the fracture- characteristics of the compositions and it is expected to have a further effect on the erosion response of the EP/HD-PUR systems. Figure 5.10 illustrates the ER of the modified epoxies as a function of the modifier content and the impact angle.

The curves in Figure 5.10 show different courses upon the modifier content. The first learning is that the addition of HD-PUR results in systems with improved erosive wear resistance for a modifier content higher than 20 wt. %. This improvement is, however, strongly dependent on the impact angle. The addition of 20 wt. % modifier was not enough to modify positively the properties that influence erosion and this composition showed almost the same ER as the pure EP. The next finding is that unlike to the usual brittle response of the EP systems, the EP resin tested here showed a semi-

ductile erosion response, which can be explained via a brittle to ductile transition of the erosion response due to the experimental conditions (erodent characteristics). The impact angle related to the maximum ER shifts to 30° and the maximum ER decreases strongly, as the modifier content increases. Recall that such a shift should be associated with a change in the failure mode, viz. from brittle via ductile to a rubbery-like failure mode due to a change in the target material properties and not due to the experimental conditions (like in the case of unmodified EP systems).

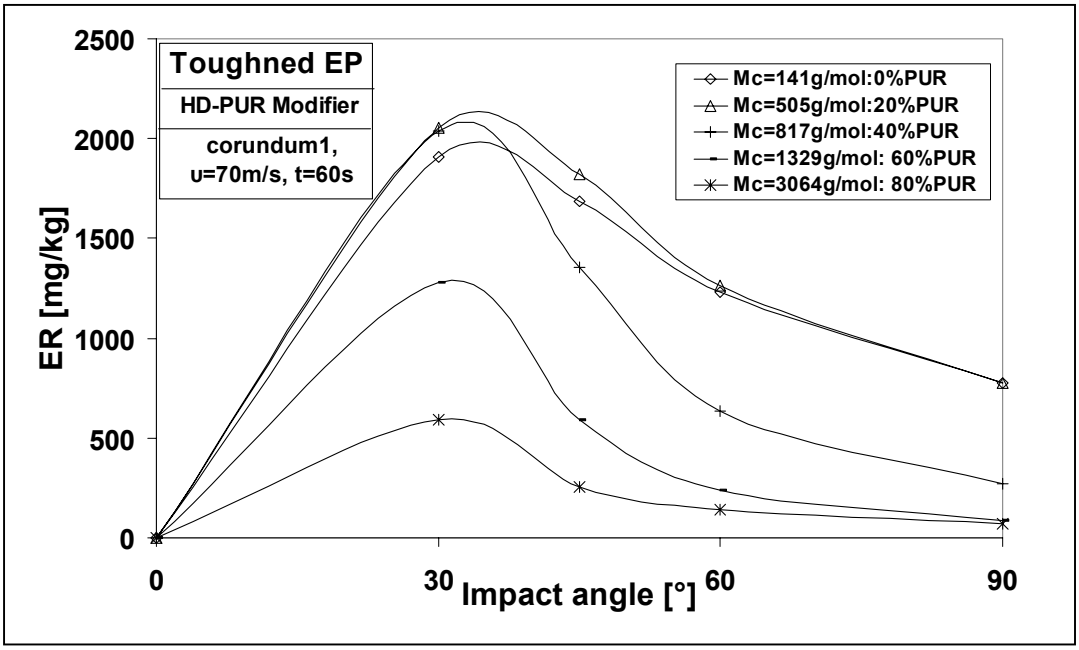

Figure 5.10: ER versus impact angle traces for the EP systems modifies with HD-PUR

As stated in chapter 2, if ER finds maximum in the range 15°-30°, the response of the eroding material is considered ductile. In contrast, if ER continuously increases with increasing impact angle and attains a maximum at 90°, the response is characterised as brittle. At this case only the normal component of the impact velocity determine the magnitude of the ER and the size of the eroding particle strongly influences the ER. Nevertheless, one should not forget the influence of the erodent characteristics on this categorisation. It is observed that brittle materials such as inorganic glass, exhibit ductile behaviour when impacted with fine particles. In the case of ductile metals it has been observed that if spherical particles are used as erodent instead of angular particles, the ER exhibits a maximum at 90° [61]. Therefore it is sometimes difficult to

distinguish if an observed transition in the ER variation stems from the experimental conditions or from the material characteristics. In order to verify the above made assumptions, the EP/HD-PUR systems were eroded with a range of erodents.

Figures 5.11 and 5.12 present the ER results of the EP/HD-PUR systems for four different erodents. In Figure 5.11 the ER varies as a function of the HD-PUR amount at constant impact angles, whereas in Figure 5.12 the same variation is illustrated this time as a function of the impact angles at constant modifier content. Both illustration types were selected for straight forward comparisons. Considering Figure 5.11 one can say that at all impact angles the maximum ER of all EP/HD-PUR systems was obtained when corundum1 was used as erodent. Generally, the harder and more angular erodents (i.e. corundum) are more erosive than the less hard and

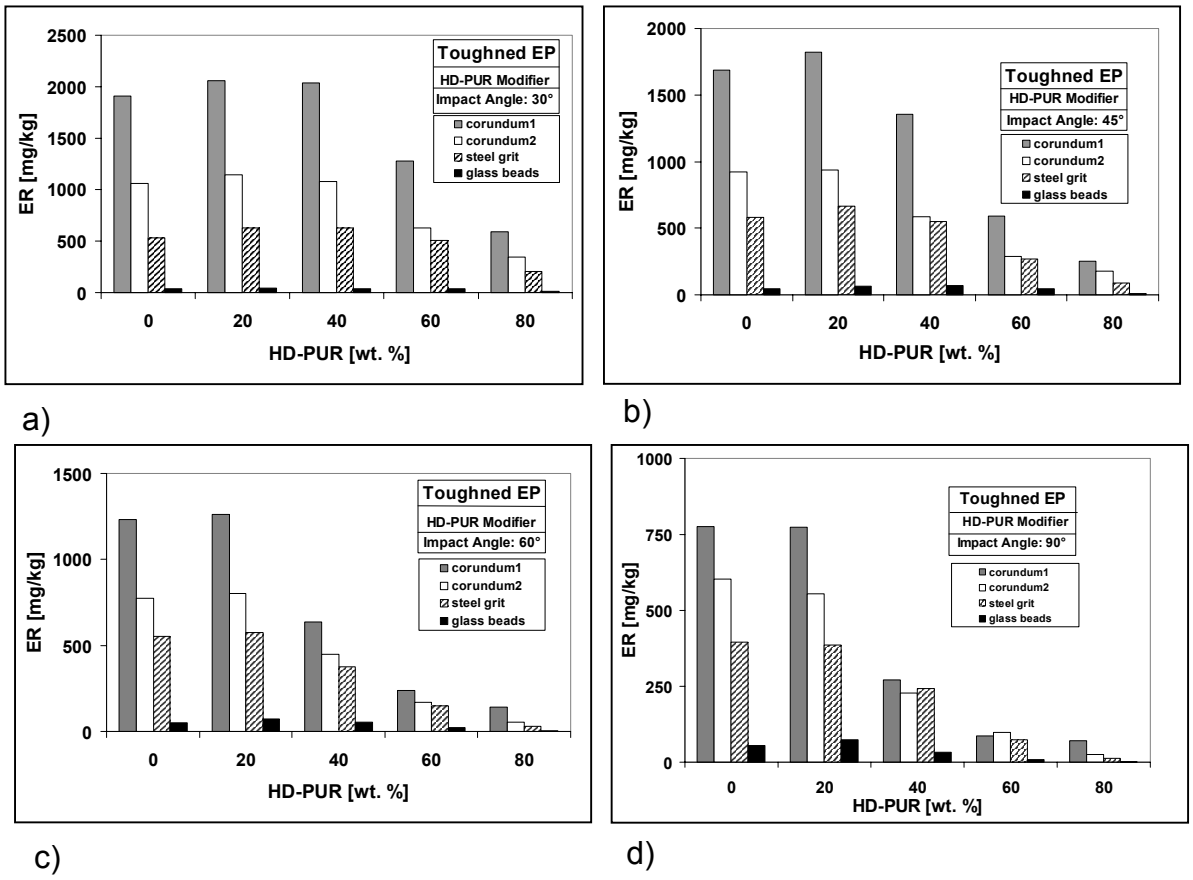

Figure 5.11: ER variation as a function of the HD-PUR wt. % content for the different erodents used, at a) 30, b) 45, c) 60 and d) 90° impact angles

less angular (i.e. glass beds) erodents. The classification of the erodents in respect to their erosive efficiency is as follows: corundum1> corundum2> steel grit > glass beads.

A shifting in the angle referred to the maximum ER of the unmodified EP is observed from 90° to 30° when sharp, angular erodents (i.e. corundum, steel grit) instead of round ones (i.e. glass beads) are used (cf. Figure 5.12a). On the other hand all types of erodents leaded to a maximum ER at 30° for the EP/HD-PUR systems with 80 wt. % modifier (cf. Figure 5.12e). Hardness and size of the erodent have a larger influence at low modifier content (up to 40 wt. %) (cf. diagrams a and b in Figure 5.12) and at low impact angles. The effect of these two parameters is lower as the modifier content and the impact angle increase. This becomes more obvious when someone observes the diagrams c and d in Figure 5.12. At 30° impact the size of the erodent seems to play an important role (look the difference between the ERs achieved by corundum1 and corundum2 respectively). The effect of erodent hardness however, is lower. Comparing the ER results of corundum2 and steel grit hardly any difference exits, especially when the impact angle approaches 90°. As

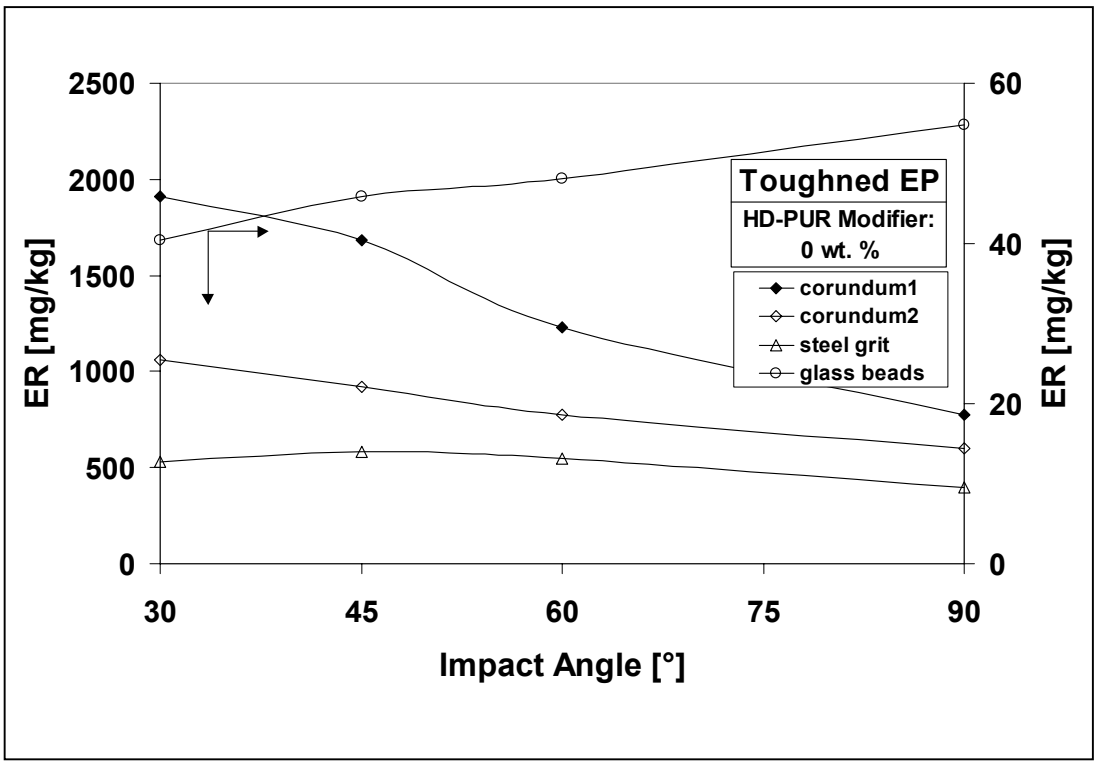

a)

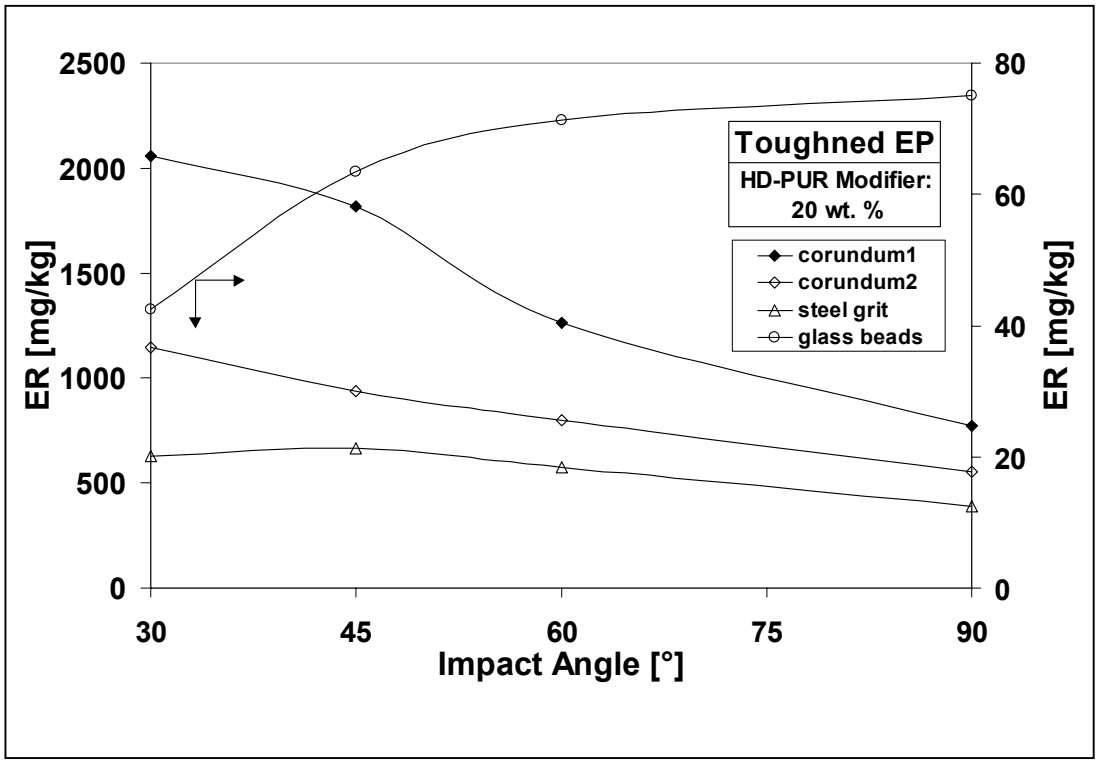
Toughned EP
HD-PUR Modifier:
20 wt. %
corundum1
corundum2
steel grit
glass beads
ER [mg/kg]
ER [mg/kg]
Impact Angle [°]
0
500
1000
1500
2000
2500
0
20
40
60
80
30
45
60
75
90

b)

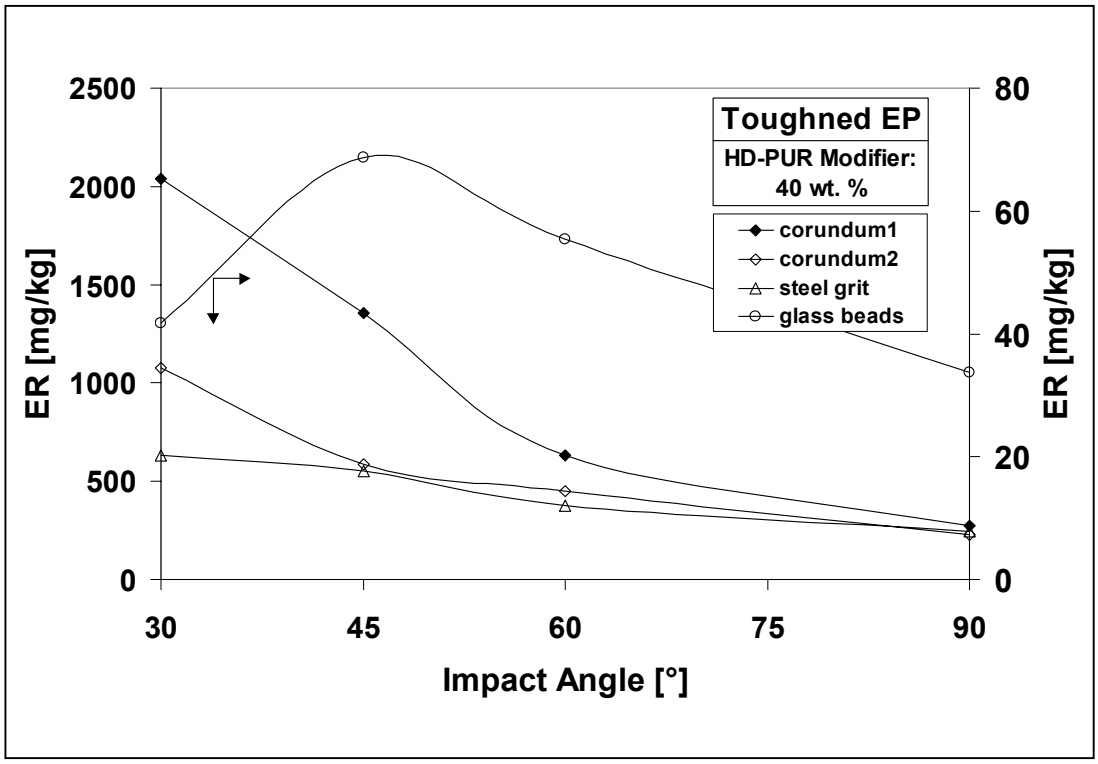
Toughned EP
HD-PUR Modifier:
40 wt. %
corundum1
corundum2
steel grit
glass beads
ER [mg/kg]
ER [mg/kg]
Impact Angle [°]
0
500
1000
1500
2000
2500
0
20
40
60
80
30
45
60
75
90

c)

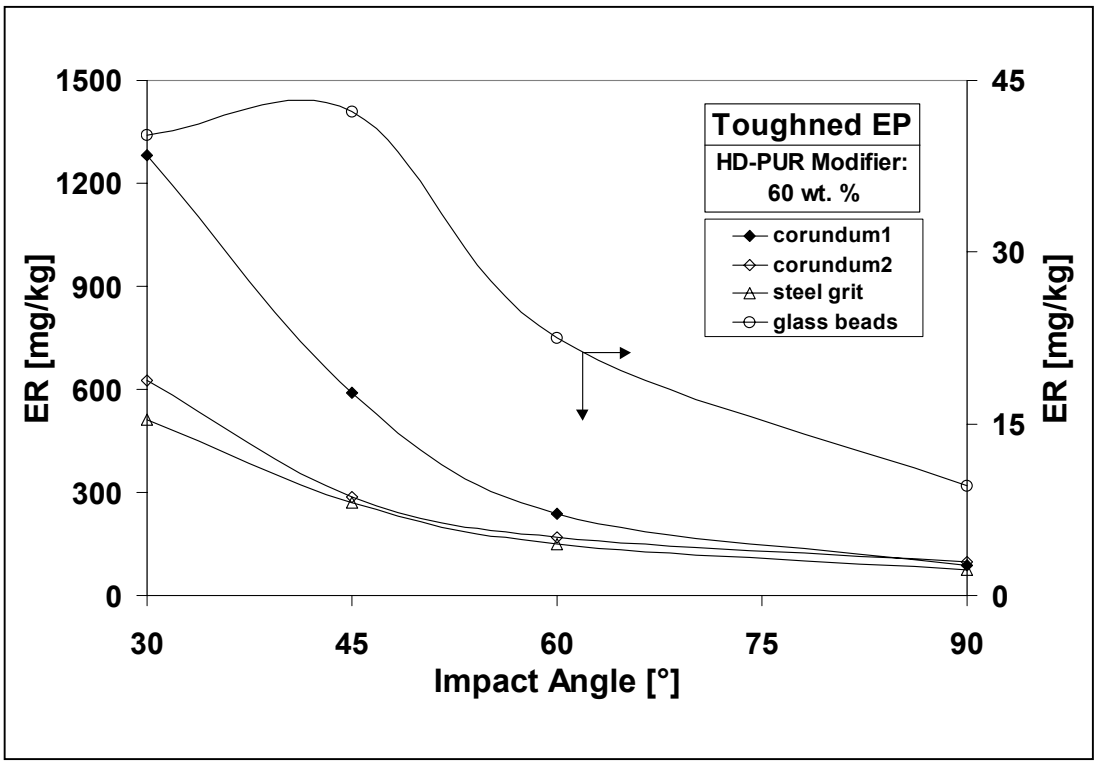

d)

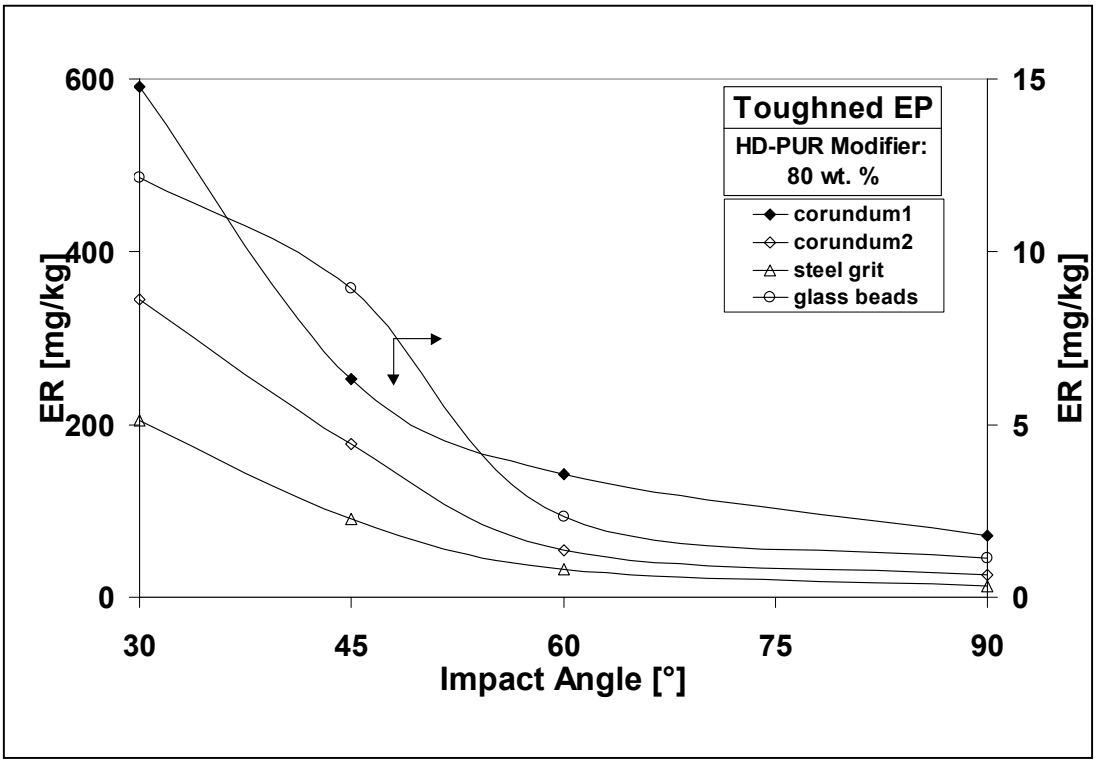

e)

Figure 5.12: ER variation as a function of impact angle for the different erodents used. Modifier content: a) 0, b)20, c) 40, d) 60 and e) 80 wt. %

impact angle comes close to 90°, the effect of the erodent size is also minimised (see Figure 5.12c,d and e).

These findings coincide with the theoretical trends reported in paragraph 2.3.1.2, i.e. that the ER is independent above a critical value of the erodent size. The critical value is also in agreement with the literature observations, in the range of 100-200 μm. Finally, the literature arguments that in the brittle mode the effect of particle hardness is more pronounced that in the ductile mode, are here also confirmed [16,17,28].

As stated in the above paragraphs, changes in the erosion response in the modified systems are expected to reflect changes in their crosslink characteristics. Figure 5.13 illustrates the direct influence of the crosslink density v on ER of the modified systems using corundum1 as erodent. The variation of the ER seems to be a step-wise function of v, the shape of which is nearly independent to the impact angle. For all impact angles, the ER-v variation starts with a plateau and is followed by a steep increase of the ER with increasing v up to a specific v value. Above this v value a

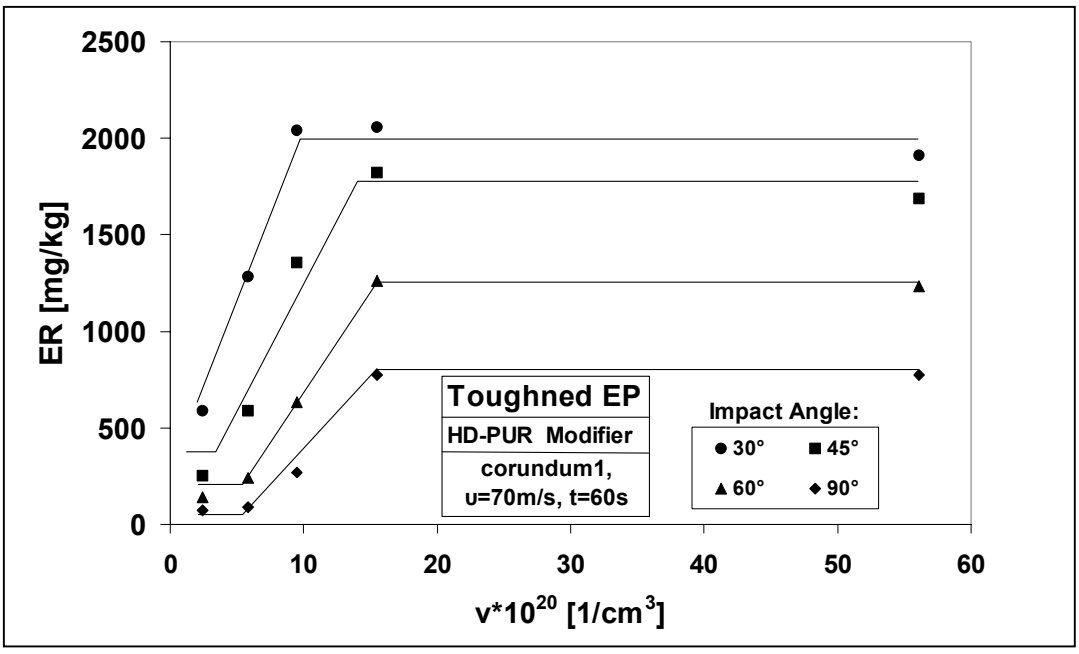

Figure 5.13: ER variation as a function of the crosslink density (v) for the EP/HD-PUR systems

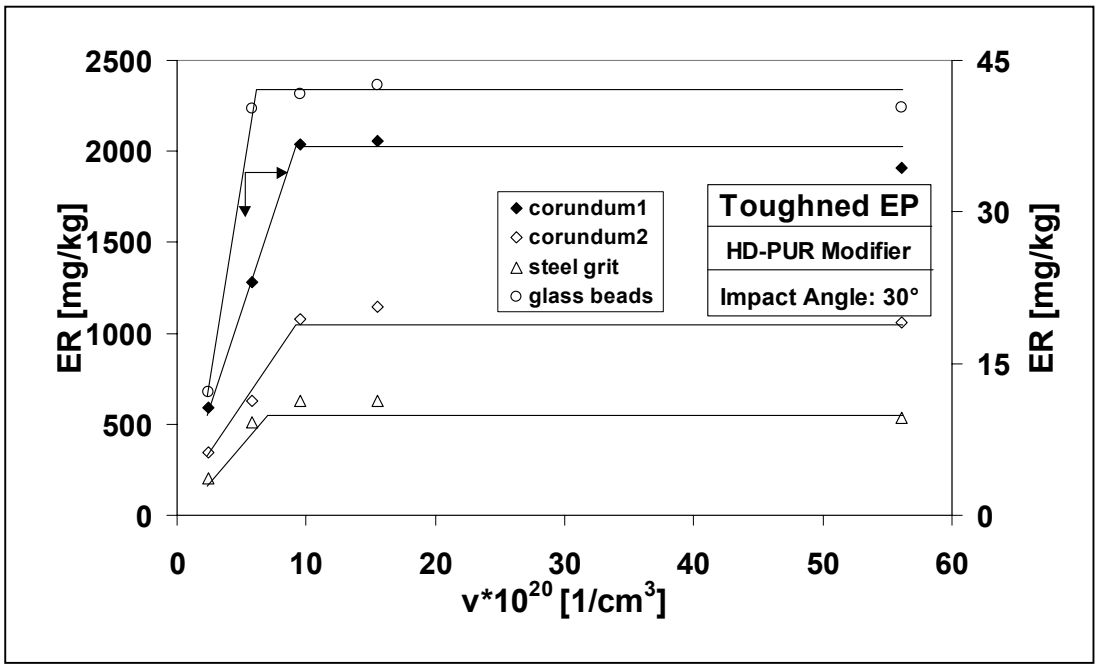

a)

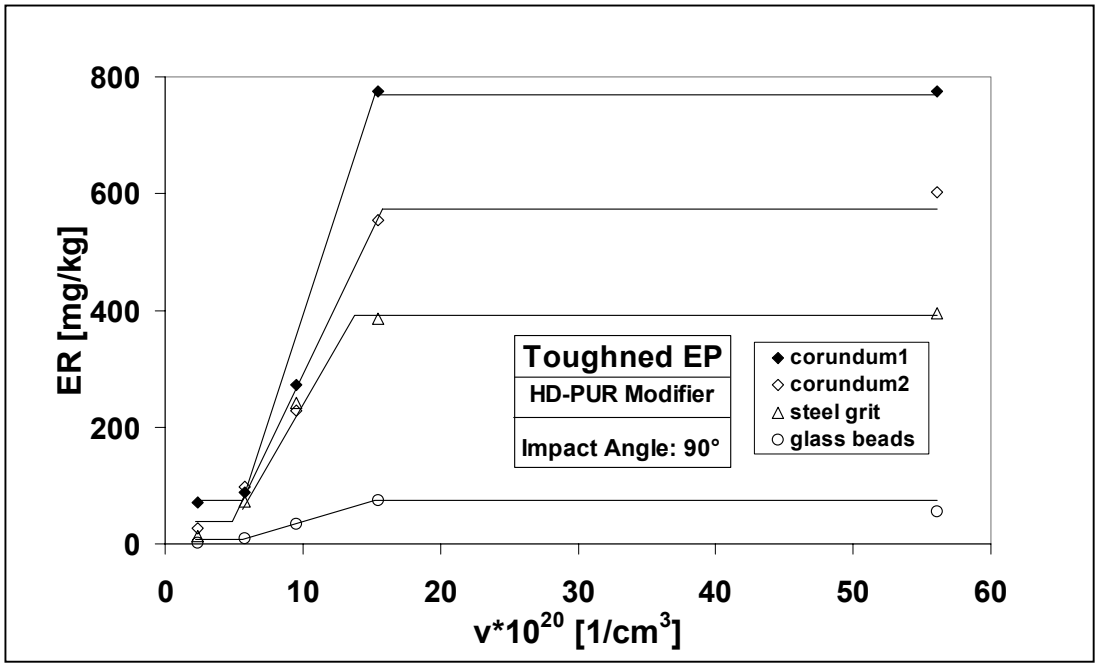

b)

Figure 5.14: ER variation as a function of crosslink density v for the different erodents used, at a) 30 and b) 90° impact angles

second plateau is observed. As the impact angle is decreasing from 90° to 30°, the first plateau becomes progressively smaller and even disappears at 30° impact (cf. Figure 5.13). The second plateau shows the opposite trend getting progressively larger as the impact angle moves towards 30°.

Observing the ER-crosslink density variation for the different erodents in Figure 5.14 at the two extreme impact angles, i.e. 30 and 90°, it is evident that the ER varies in the same way just like in diagram 5.13 independently to the art of the erodent for a specific impact angle.

The physical interpretation of the findings presented in Figures 5.13 and 5.14 is not easy, as v is a direction independent material property while ER is a direction dependent one. The existence of the two plateau indicates that for extreme values of the crosslinking density, i.e. for highly- and low- crosslinked systems, the crosslink characteristics do not influence directly the ER. The steep increase in the ER that separates the two plateau signifies that the change in the crosslink density leads to a change (i.e. transition) in the mode of erosion that has a significant influence on the erosion response.

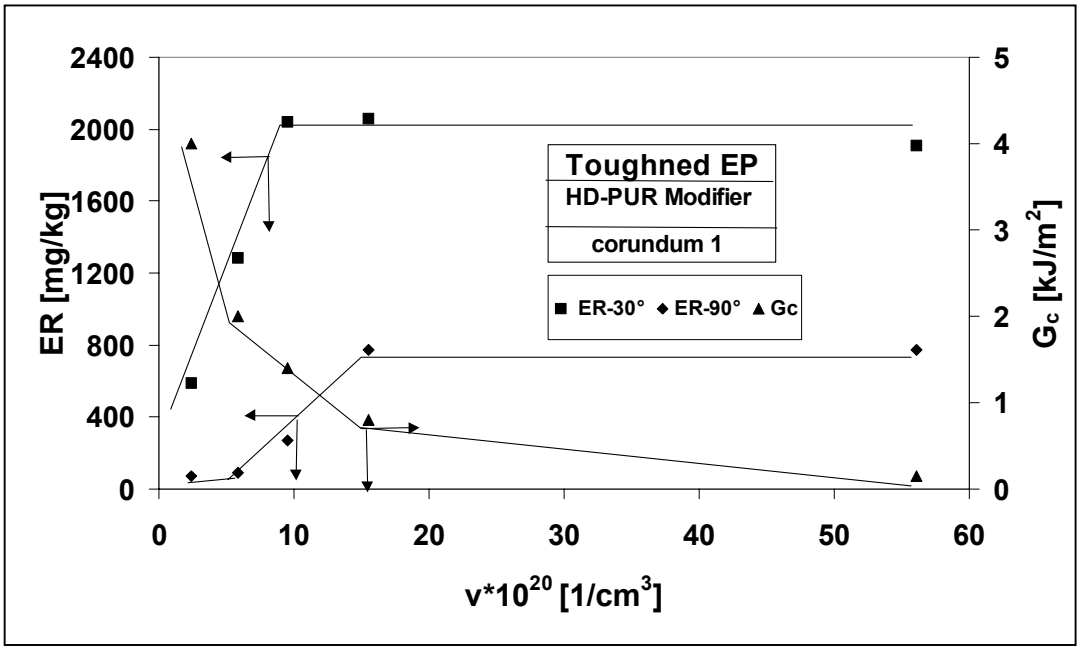

Figure 5.15: ER and fracture energy (G_c) versus crosslink density (v) for the EP/HP-PUR systems.

Recalling the influence of the crosslink density on the fracture energy of the modified systems, one can claim a further interrelation between erosion response and fracture energy. Figure 5.15 depicts the ER and fracture energy (G_c) as a function of v along with the ER at 90 and 30° impact angles. ER and G_c tend to vary adversely to each other if one observes their change as a function of the crosslink density. An increase in the ER is observed as the G_c decreases. For high crosslink density values, it is observed that G_c only slightly changes while for the same range of v the ER at 30 and 90° present the above mentioned plateau. As a consequence, the increasing resistance to erosion can be explained through the increment in G_c. The absence of the first plateau in case of 30° impacts (cf. Figure 5.15) implies further that only a slight variation in the fracture energy can have an important influence in the erosion resistance at oblique impact.

The observed dependence of the erosive wear on the impact angle for the modified EPs of various amounts of HD-PUR suggests that the erosion response changed due to the modification. At low modifier contents, characterised by high v values, brittle to semi-ductile erosion should dominate (depending on the experimental conditions). Note, that although the maximum ER of the EP and EP/HD-PUR modified with 20 wt. % systems is observed by middle impact angles, the maximum mass removal is still observed by high (close to 90°) impact angles. Characteristic SEM pictures taken on the surface of the unmodified EP samples eroded at various impact angles show a smooth surface at 30° (cf. Figure 5.16a) and a very rough one at 60° and 90° (cf. Figure 5.16b and c). A smooth surface means high, whereas a rough one low resistance to erosion in the first approximation. Figure 5.16 also suggests that the temperature of the EP during jet erosion did not reach the T_g and thus the no change in the erosion behaviour can be expected due to the temperature rise. A similar failure scenario holds for samples with less than ca. 20 wt % HD-PUR-G modifier.

By contrast, the EP with 80 wt % HD-PUR-G shows a more rough surface after particle impact at 30° (cf. Figure 5.17a) than at 60° or 90° (cf. Figures 5.17b and c). Further, Figure 5.17a evidences that rubbery-like failure occurred. The appearance of the eroded surface hints that the T_g of this composition was surpassed due to the erodent flux.

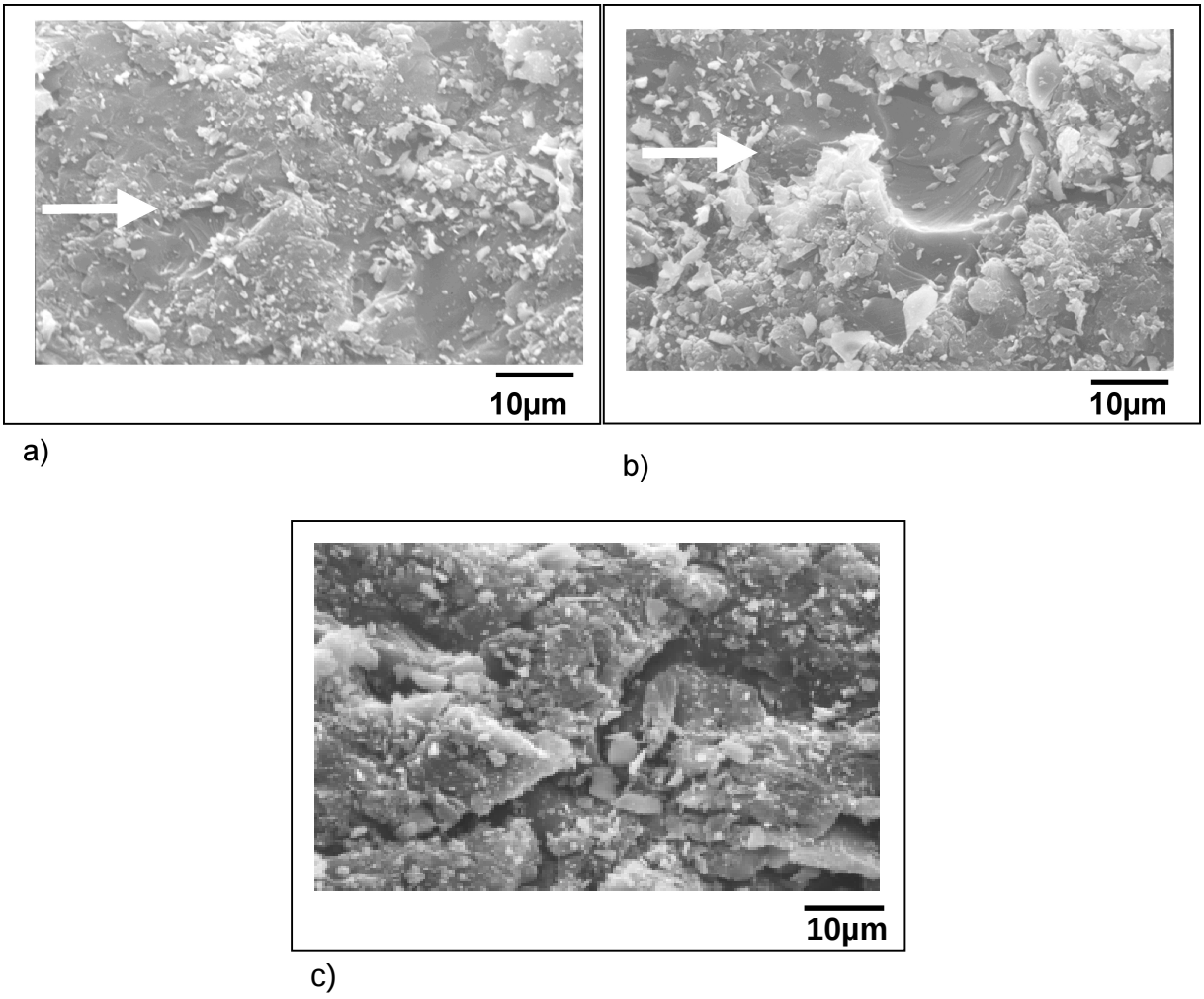

Figure 5.16: Scanning electron micrographs taken on the eroded surface of pure EP after impact at a) 30, b) 60 and c) 90° angles, respectively. Note: erosion time: 180s

The related heat softening in combination with the lower hardness (cf. Table 5.4) of the systems with high amount of modifier, explains the existence of an incubation period observed in these systems. Note that ductile and rubbery materials present a better resistance to erosion for all impact angles and they need more impact time to erode in comparison to brittle ones. During the incubation period substantial amount of impact energy is dissipated in roughening the target surface which has as consequence a smaller ER. An incubation period was observed for the case of 80 wt. % HD-PUR at 60° and 90° impact angles, where the ER was the lowest (cf. Figure 5.10).

It is already known that the impact angle is one of the important parameters in respect to the erosion behaviour. When the erosive particles hit the target at low angles, the impact force can be divided into two constituents. One is parallel (F_p) to

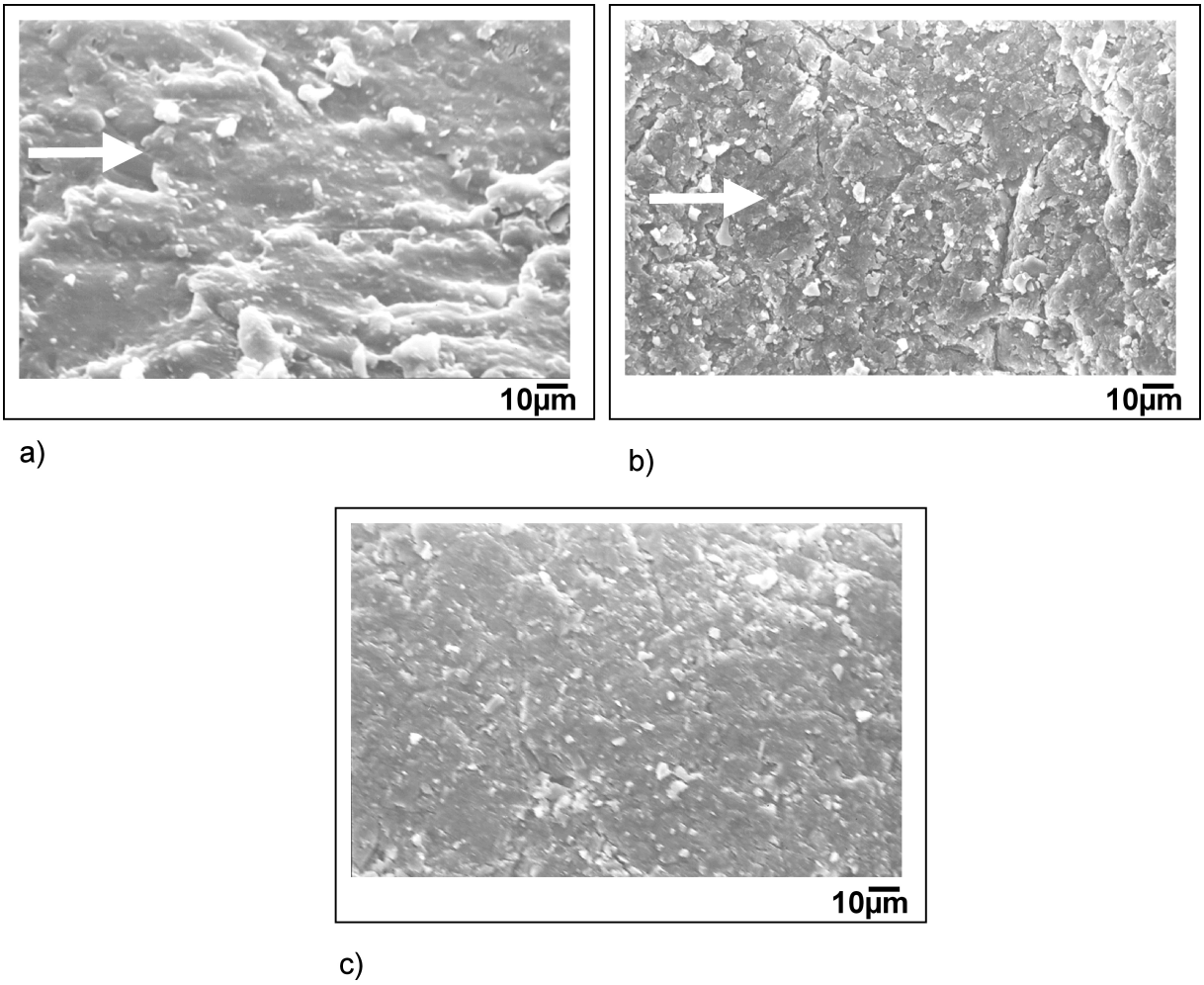

a) b) c)

Figure 5.17: Scanning electron micrographs taken on the eroded surface of EP/HD-PUR system containing 80 wt. % HD-PUR after impact at a) 30, b) 60 and c) 90° angles, respectively. Note: erosion time: 180s

the surface of the material and the other is vertical (F_v). F_p controls the abrasive and F_v is responsible for the impact phenomena. As the impact angle is shifting towards 90°, the effects of F_p become marginal. It is obvious, that in the case of normal erosion all available energy is dissipated by impact and microcracking, while at oblique angles due to the decisive role of the F_p the damage occurs by microcutting and microploughing [17,115]. This is not the case for elastomers, where in both oblique and normal impact the material removal takes place by fatigue crack propagation. At high impact angles the wear mechanism in erosion involves the

propagation of fatigue cracks under the influence of frictional stresses arising from particle impact [49]. At low angles the erosion may proceed by a catastrophic tearing process which shows many similarities to that occurring during sliding abrasion by a blade or by a smooth indentor [25]. Ploughing features characteristic for ductile type of erosion in case of thermoplastics could not be resolved. The failure in Figures 17a,b seems to support the analogy between the EP modified by high amount of HD-PUR and elastomers.

5.2.2. Polymer Blends with Thermoplastic Elastomers (PET, PBT)

Melt blending of thermoplastic polymers with various polymers and elastomers offer a good opportunity to convert them into high performance engineering plastics with desirable properties. Most efforts focus on the melt blending more with rubber and less with polymer types. Rubbers seem to be the proper toughening agent of thermoplastic polymers. Their addition results in improved toughness, provided that the rubber phase is finely dispersed in the polymer. This can only be achieved if the rubber is properly functionalised [135]. A typical method to improve the rubber performance and to stabilise the morphology of blends of thermoplastics with elastomers is dynamic curing. The selection of the elastomer type plays a crucial role by influencing the morphology and the related mechanical propertied in elastomeric blends of PET and PBT [102]. Previous works were concentrated on these effects and it was recognised that the best mechanical properties were established for those thermoplastic elastomer which contain NBR of high acrylonitrile content instead of polyolefin rubbers. It was also established that the mechanical properties of blends containing high amount of linear polyesters can be strongly improved when GMA functionalised NBR rubber are used [101].

The erosive wear behaviour of two kinds of polymer blends, i.e. PET and PBT modified with different amounts of GMA functionalised rubbers at 30, 60 and 90° impact angles is illustrated in Figures 5.18a, b and c. The comparison of these diagrams shows that both PET and PBT with and without modification exhibit typical ductile erosion response with maximum ER at 30 and minimum ER at 90° impact angles.

It is interesting to note that the unmodified PBT shows almost an double ER in comparison to that of the pure PET at 30°. At 60° both unmodified samples seem to have similar erosion response, while at 90° the opposite phenomenon of that at 30° is observed.

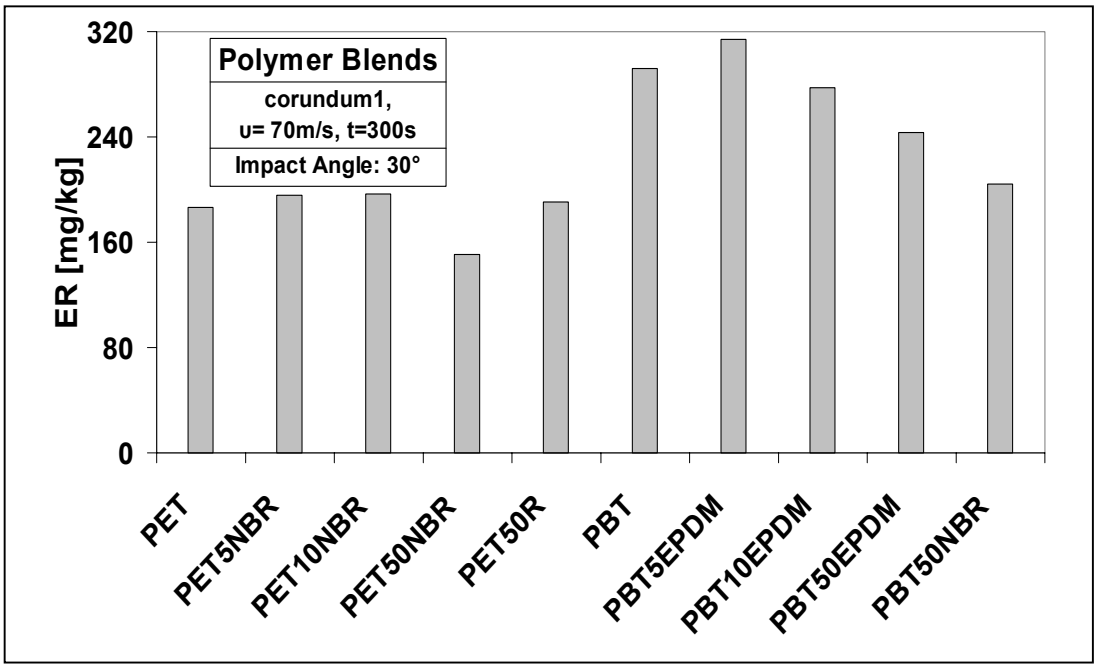

a)

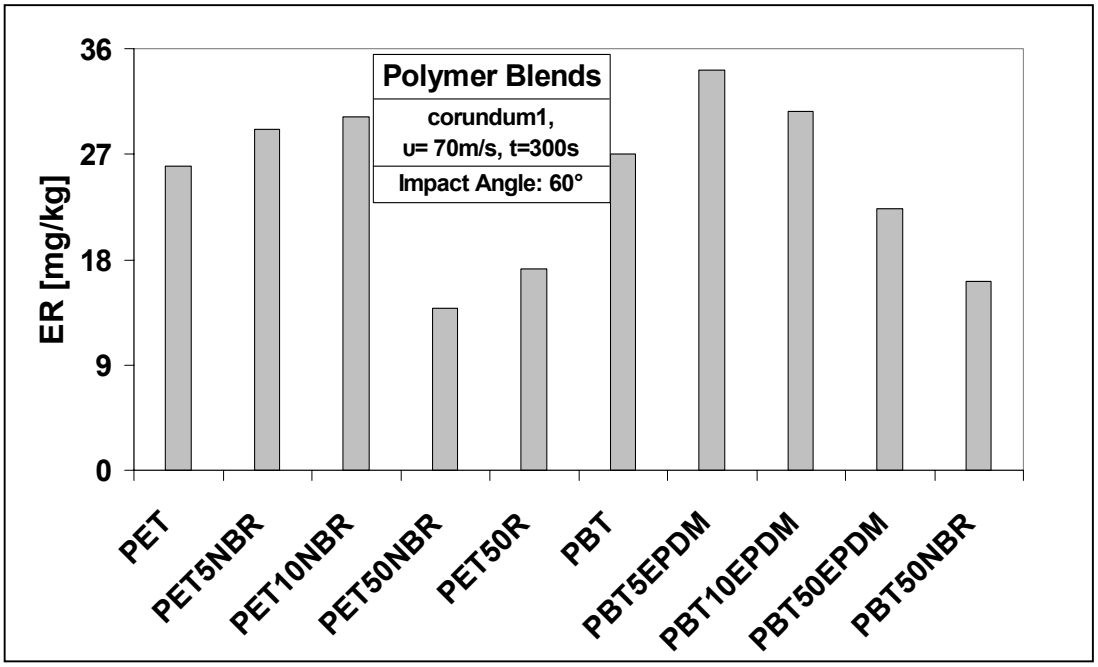

b)

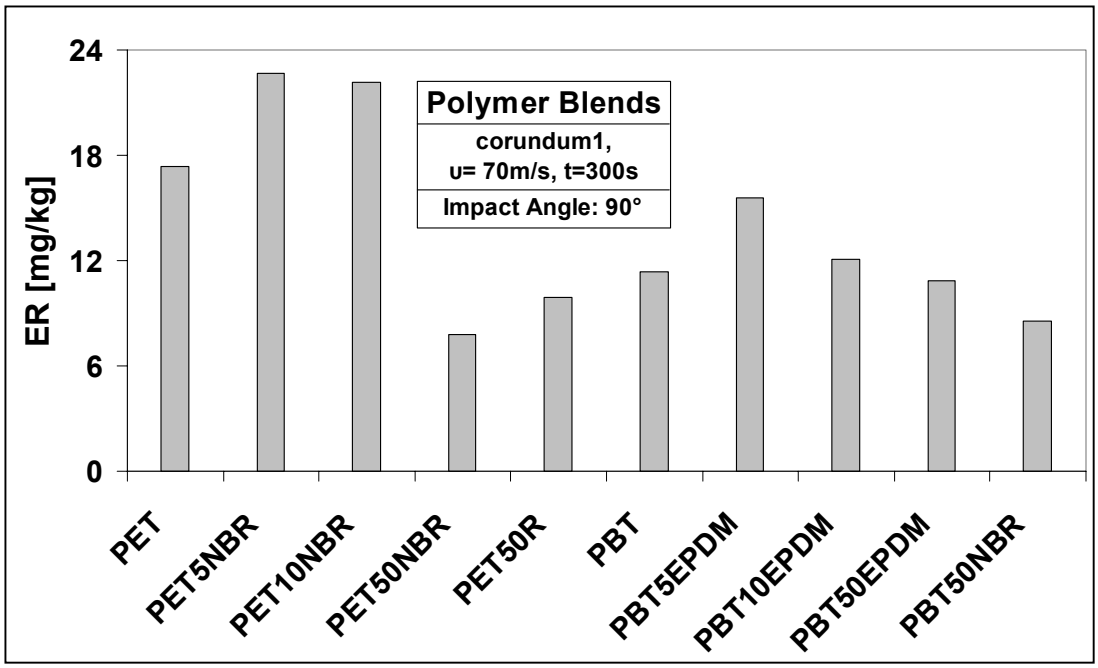

c)

Figure 5.18: Variation of ER of polymer-elastomer blends as a function of the material type and amount at a)30, b)60 and c) 90° impact angles

Considering the effect of the elastomer modification at the erosion response of the polymers and their blends at 30° impact angle, it is observed that the addition of a small amount of NBR i.e. 5 and 10 wt. % led to a small increase of the ER while even the addition of 50 wt. % of the polyolefin-type rubber did not seem to affect positively the erosion response of PET. Finally the addition of 50 wt. % NBR led to a small but clear reduction of the ER of PET. PBT was modified mainly with EPDM elastomer. For reasons of comparison it was additionally modified with 50 wt. % NBR. The rubber modification leaded to a clear reduction of the ER in all cases except the 5 wt. % modification. The NBR-modified PBT showed a better erosion resistance compered to that provided with the EPDM rubber.

It is expected that a small amount is not enough to moderate significantly and positively the polymer-blends properties in order to provide a better erosion resistance. A further possible reason behind the negative influence of the modification could be the lower compatibility of the polymer with the rubber blends when the last are adopted at small amounts. In this case the modifier acts more as

filler or second phase with poor adhesion resulting in the deterioration of the blends properties.

Similar trends in the behaviour of the modified PET, PBT are observed at 60 and 90° impact angles. The main difference observed in the erosion response of PET blends is that the modification has a more pronounced influence at 60 and 90° than at 30° impact angles. The elastomer modification of the PBT on the other hand seems to provide less benefits for the erosion response as the impact angle proceeds to 90°. Trying to understand the reasons underneath this behaviour, the concept of the 'relative toughness'(ultimate tensile strength (σ_u) multiplied by ultimate elongation (ε_u)) was adopted. The enhancement in 'relative toughness' of the polymer blends provided through the modification with rubbers is presented in Table 5.5. In this table only the un-modified and the 50 wt. % blends were considered.

Table 5.5: Ultimate stress and strain values of the unmodified and 50 wt. % modified polymer blends.

	σ_u [MPa]	ε_u [%]
PET	58.5	5.7
PET50NBR	16.7	250
PET50R	13	350
PBT	53.2	5.7
PBT50NBR	18.1	218
PBT50EPDM	19.1	296

Although not always confirmed, a general trend of increased erosion resistance with an increased strength and elongation to fracture has been observed. This trend is probably a reflection of the importance of micro-toughness in the resistance to material removal. Recall from chapter 2 that this term (according to the Ratner-Lancaster equations [65,66]) is a rough measure of the area under the stress strain curve to fracture and therefore gives an estimate of the energy to fracture. High fracture energy suggests in general a high resistance against crack initiation and propagation under very complex (fatigue and/or impact) loading conditions. It would be expected that this increase in the fracture toughness would translate into better

wear resistance in those conditions where the wear mechanism was one of fatigue crack growth.

Based on the data of Table 5.5, the trends of the ERs of the polymer blends as a function of the 'relative toughness' at 30, 60 and 90° impact angles are presented in Figure 5.19. It is very interesting to note that similar trends of the erosion response are detected, irrespectively to the impact angle. For all impact angles the ER decreases as the relative toughness increases to a specific value (i.e. 4175 [MPa*%], see Table 5.5). A further increase in the relative toughness has a negative influence in the ER indicating that a different mechanism than that of mechanical fatigue should take place (for instance tearing) and other material properties are of importance.

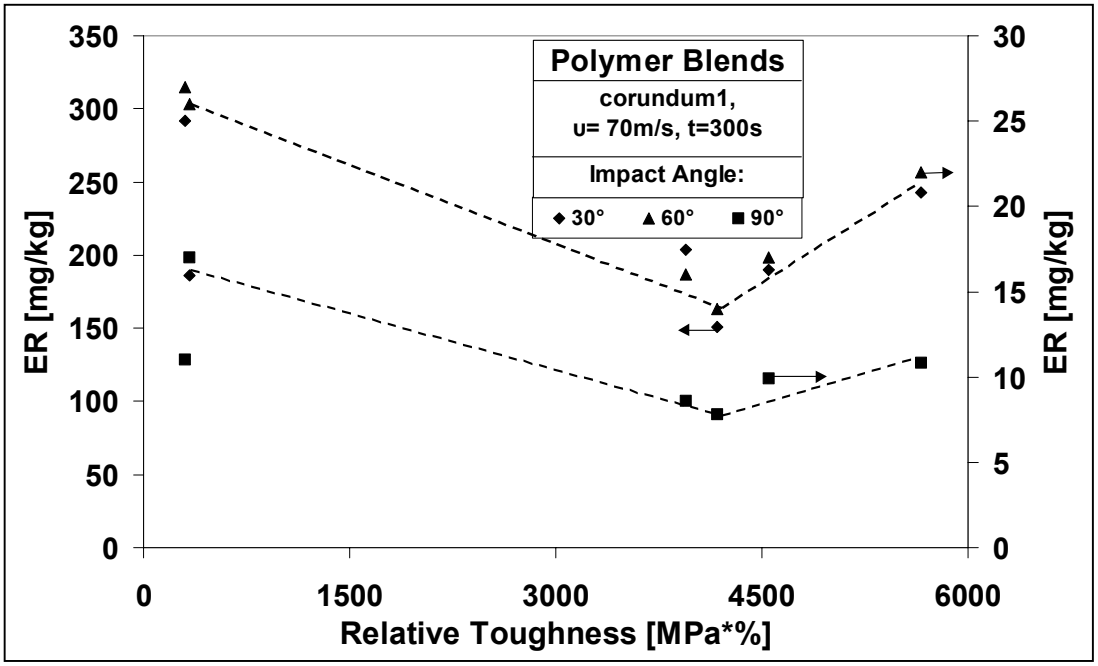

Figure 5.19: ER versus 'Relative Toughness' diagram for the modified polymer blends

5.2.3. TPU Elastomers filled with Nanoparticles

Nowadays considerable efforts are undertaken to modify polymers with nanoscale-reinforcement. One of the most promising ways to do this is the incorporation of layered silicates (bentonite-, montmorillonite-type) in the thermoplastic resins by melt compounding. The major task is to disintegrate the structural layers of the silicate

(process called exfoliation) in order to exploit the high aspect ratio of the nanoreinforecement. Nanoscale particles have been proposed as modifiers for the case of thermoplastic polyurethanes.

Properties of filled polyurethanes are dependent upon filler shape, average diameter and interfacial coupling. Frequently, filler addition is accompanied by increased strength and stiffness at the expense of substantially reduced elongation at break [136]. Nevertheless, it has been reported that for the case of nanoscale modification of polyurethane elastomers the presence of silicate layers tended to enhance not only the maximal strength of pure polyurethane, as occurred in same cases of conventional composite materials, but also the elongation at break. This is because the interfacial interaction between polyurethane and silicates contributed to the dangling chain formation in the matrix and caused a plasticising effect in polyurethane [137]. Because of the much stronger interfacial forces between the well-dispersed nanometer-sized domains, nanoscale-modification provides materials with better physical properties such as thermal, mechanical and barrier properties [137].

Table 5.6: Mechanical and thermo-mechanical properties of the nanofilled TPUs

	E-Modulus at ε=100% [MPa]	E-Modulus at ε=300% [MPa]	σ_u [MPa]	ε_u [%]	tanδ [1]	Tg [°C]
TPUa-0	3.9	6.7	17.2	953.6	0.49	-25.2
TPUa-1	5.7	7.8	14.1	953.2	0.36	-25.4
TPUa-2	4.9	6.8	12.9	975.1	0.37	-25.2
TPUb-0	16.3	20.6	33	721.9	0.16	22.8
TPUb-1	17.4	19.8	25.1	595.9	0.14	22.9
TPUb-2	17.4	19.6	26.1	625.2	0.15	22.8

Table 5.6 provides information on the mechanical properties of the pure and modified polyurethane elastomers. As can be read from this table, incorporation of nanosilicate generally improved the E-Modulus at 100 and 300% strains and affected the strain-hardening behaviour. A larger enhancement in these data was found for Southern Clay silicates. Interestingly, the nanoreinforced polyether type TPU (TPUa) showed

strain softening compared to the unfilled version. The tensile response of the polyester type (TPUb) is somewhat different from the polyether grade. The addition of nanosilicate resulted in a strain softening and in reduced elongation at break data. Nevertheless, the TPUb-2 performed better than the TPUb-1 version which is awaited to relate with the dispersion ability of the each type of silicates with the different grades of TPU (possibly marginal exfoliation).

The effect of the nanosilicate modification on the erosion response is presented in Figure 5.20. One can see a typical ductile response of modified and unmodified TPU with maximum ER at 30°. This means that the incorporation of nanosilicate did not change the mode of material removal, nevertheless it resulted in a considerable decrease of the erosion resistance at oblique impacts. The effect of the nanofilling at higher impact angles was much less pronounced.

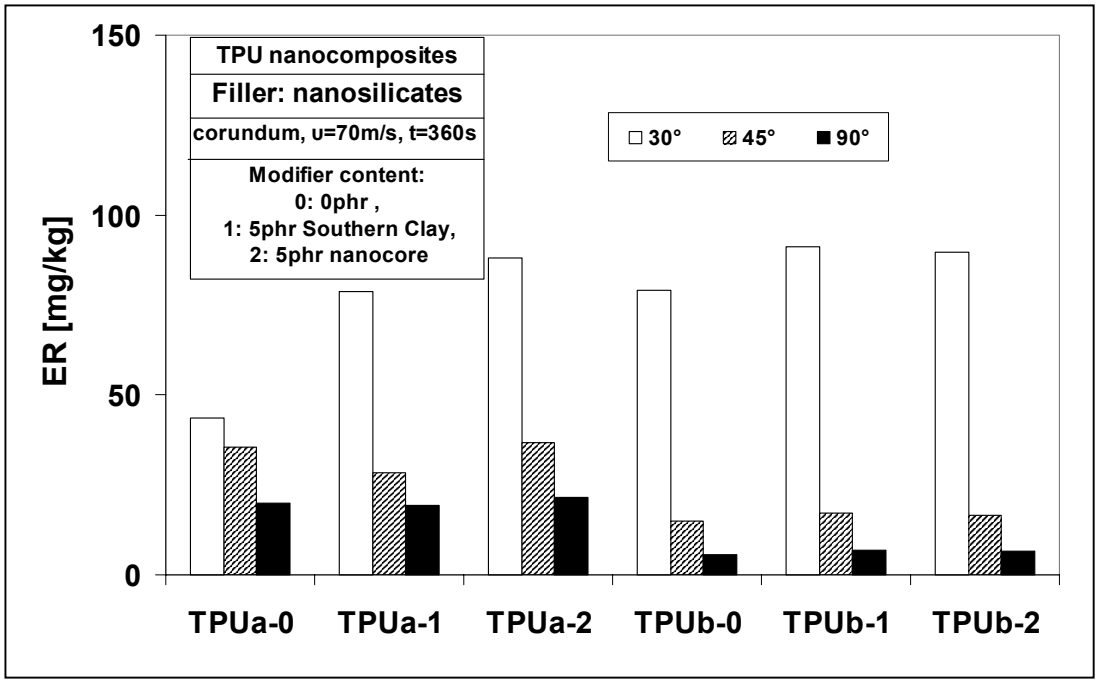

Figure 5.20: ER variation of the nanofilled TPU elastomers at 30, 45 and 90° impacts

Deterioration of the abrasive wear resistance because of the inclusion of filler has already been reported in the literature. While discussing the reason behind the filler effect, the concept of ‘Relative toughness’ was also there adopted. In that study, it

was found that the relative toughness of the virgin polymer was higher than that of the modified polymers and that was traced to the deterioration in the abrasive wear resistance. Observing Figure 5.21 one can say that the relation between ER and relative toughness is not verified in case of nanofilled polyurethanes. The deterioration can be due to the initiation and propagation of the cracks in the modified elastomers promoted by the mismatch between the matrix and the fillers.

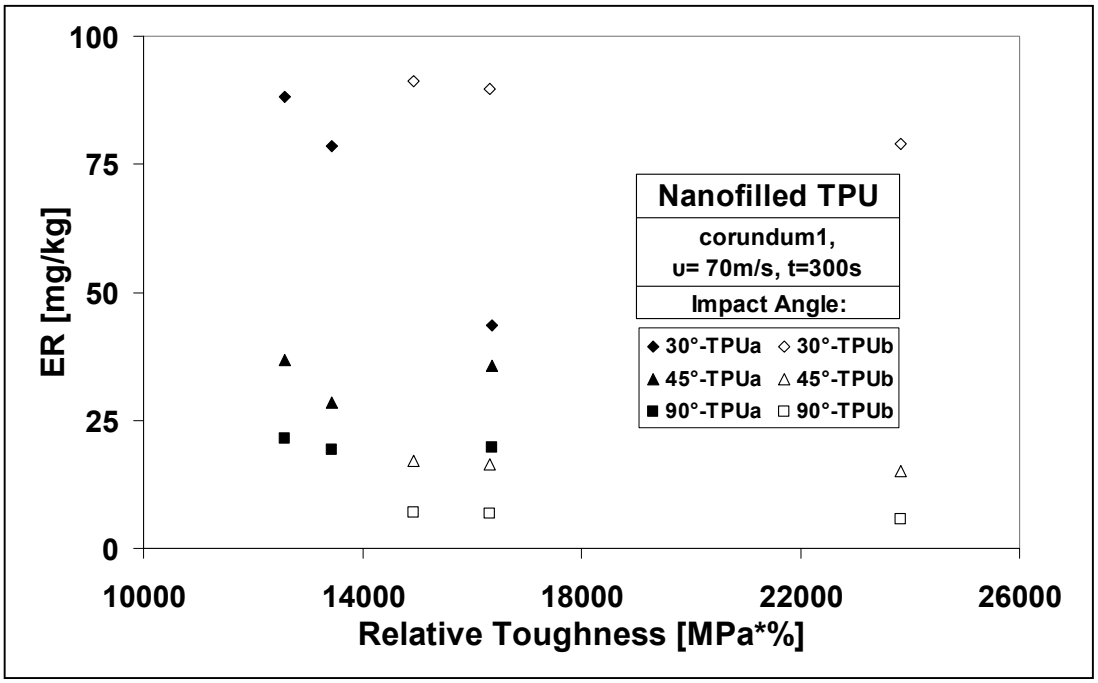

Figure 5.21: ER versus ‘Relative Toughness’ diagram for the nanofilled TPU elastomers

5.3. Solid Particle Erosion of Composites

5.3.1. Glass Fibre reinforced Polypropylene

The effect of fibre –length, -orientation and –content is of crucial interest for the erosion study, nevertheless a literature survey showed that information on these effects is limited. Different trends are observed in various studies [6,68-71,74,138] based mostly on thermosetting matrix systems. As different mechanisms of material removal seem to govern the erosion of thermoplastic matrix composites, the main target of this part of study is to elucidate these effects on the example of glass fibre/ polypropylene (GF/PP) composites [139].

Figures 5.22 and 5.23 display the influence of the impact angle, the relative fibre orientation and the fibre content on the erosion wear of UD-GF/PP. Apart of this aspect, Figure 5.24 illustrates the effect of reinforcement length in GF/PP composites with 40 wt. % fibre content. The comparison of Figures 5.22 and 5.23 indicate that a strong dependence of the erosive wear exists as a function of the relative fibre

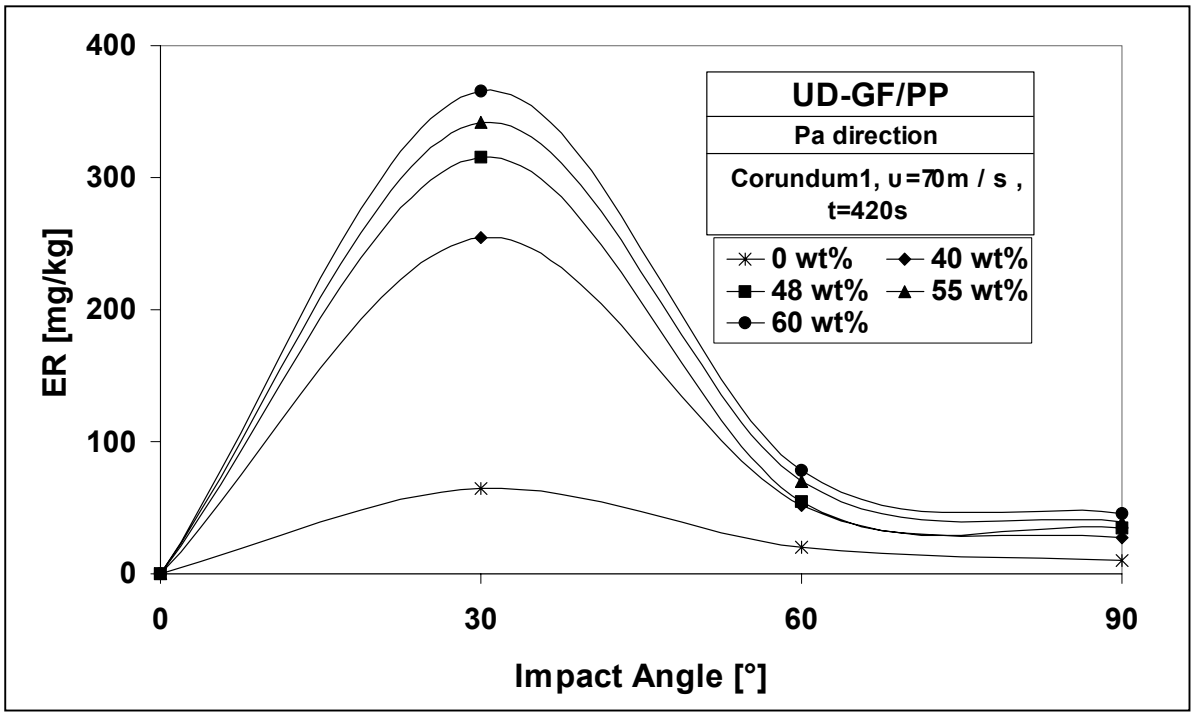

Figure 5.22: Erosion Rate (ER) as a function of impact angle and fibre content of UD-GF/PP composites containing fibres aligned parallel (Pa) to the erosion direction

orientation only at 30°-impact angle. At 60° oblique impact hardly any difference can be found between the samples impacted Pa and Pe to the fibre direction. Further, there is no sense to indicate the erosion direction at normal impact (90°) because the particles hit the same transverse area. For the UD specimens with fibres aligned Pa to the impinging direction, the erosive wear was considerably higher than that at Pe alignment to the jet. This result holds for all compositions tested and is in agreement with some past observations [66,69] however in contrast to some others [6,69,70,136].

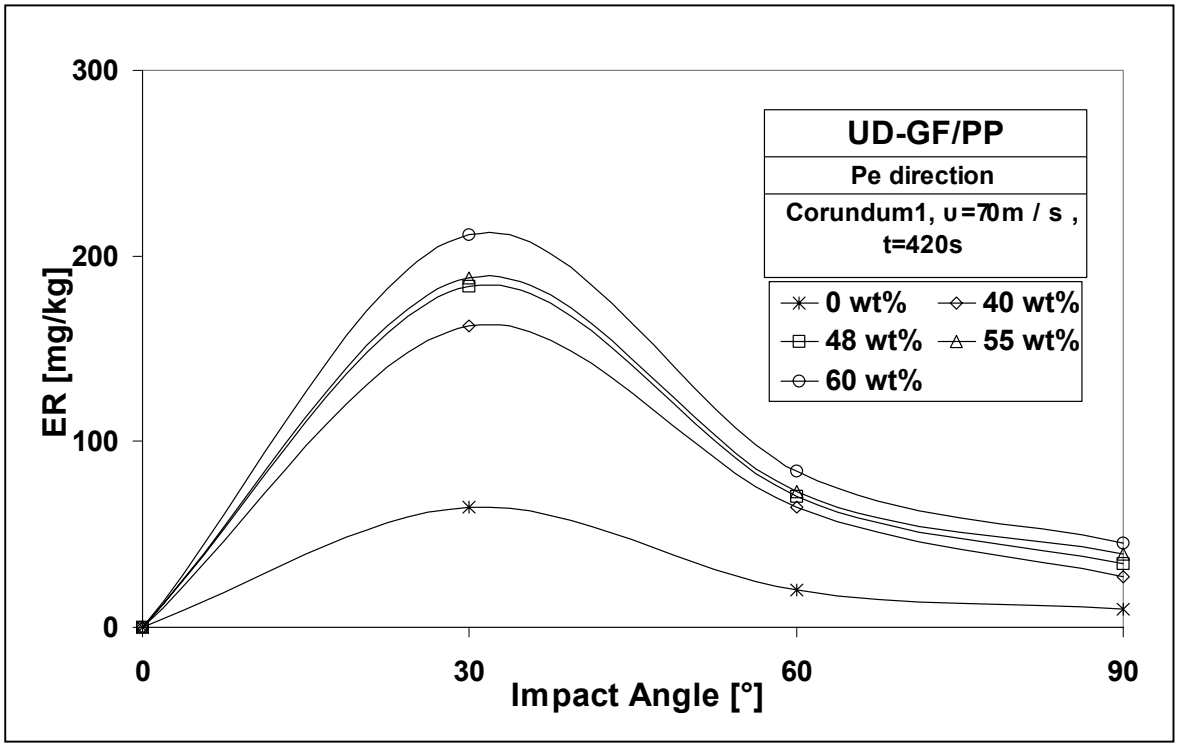

Figure 5.23: Erosion Rate (ER) as a function of impact angle and fibre content of UD-GF/PP composites containing fibres aligned perpendicular (Pe) to the erosion direction

The results in Figure 5.24 indicate that there is no difference between SGF/PP and LGF/PP. The ER values of both systems are very close to each other and the experimental scatter masks the evident difference. The erosive wear of the composites reinforced by SGF and LGF differs only slightly from that of a UD composite eroded in Pe-direction. This suggests that the mechanism of fibre removal in a composite reinforced with discontinuous, randomly oriented fibres equals with

that of an UD composite eroded in the Pe-direction. This is due to the fact that in cases of SGF- and LGF- reinforcement the probability that an erodent particle hits a fibre in Pa- direction is rather small compared to the probability that the particle impacts the fibre oblique. Accordingly when the matrix material is removed, the fibres will be fractured via microbending and removed similarly to the Pe-impact case. In Pa-impact case the fibre fracture and removal demand indentation of the erodent particle on the fibre.

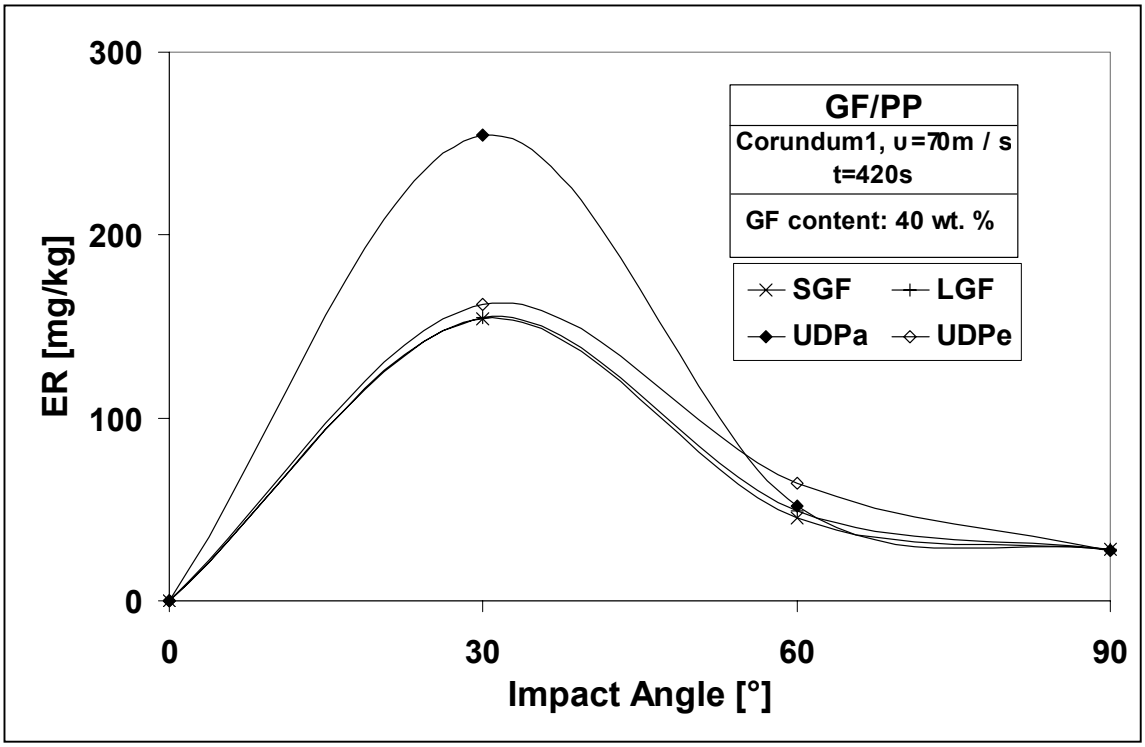

Figure 5.24: Erosion Rate (ER) as a function of fibre length and fibre orientation of GF/PP composites at 40 wt. % GF content

As observed above, the effects of the fibre length or fibre orientation on the erosive wear decrease as the impact angle moves towards 90°. This can be well explained from the fact that as the impact angle approaches 90° the exposed fibre shape does not change dramatically with a change in the fibre orientation. Furthermore, the vertical component of the impact force increases therefore the energy absorption ability becomes crucial for the erosion resistance of the composite. The ability of a composite to absorb the energy elastically depends more on its fibre content and not on the length or the orientation of the reinforcing fibres.

It is interesting to notice that almost all studies reporting on a better erosion resistance in Pa-direction refer to thermosetting matrix composites. However, a rather different mechanism governs the material removal process in a thermoplastic matrix composite. The thermoplastic matrix exhibit a ductile erosive wear (plastic deformation, ploughing, ductile tearing) instead of brittle fracture (generation and propagation of subsurface lateral cracks) in a thermosetting resin.

The SEM observations enlighten the results presented above. Figures 5.25 and 5.26 illustrate the effect of the relative fibre orientation on the erosive wear of UD-GF/PP composites. They confirm that for the case of UD-GF/PP with fibres aligned Pa to the impinging direction (Figure 5.25), the erosive wear was greater than for the Pe-direction (Figure 5.26). Under Pa- erosion, the matrix is uniformly grooved and cratered with local material removal (Figure 5.25). Between the fibres that are parallel aligned, the deformation of the matrix material is characterised by ductile flow of the material around the impact site, therefore a ploughing mechanism is encountered. The parallel component of the impact force makes the erodent particles to penetrate into the eroded surface. The ductile flow and the penetration of the erodent in the matrix are hampered by fibres aligned in Pe-direction therefore, the grooves were far less intense (Figure 5.26), and obviously less material was removed in this case.

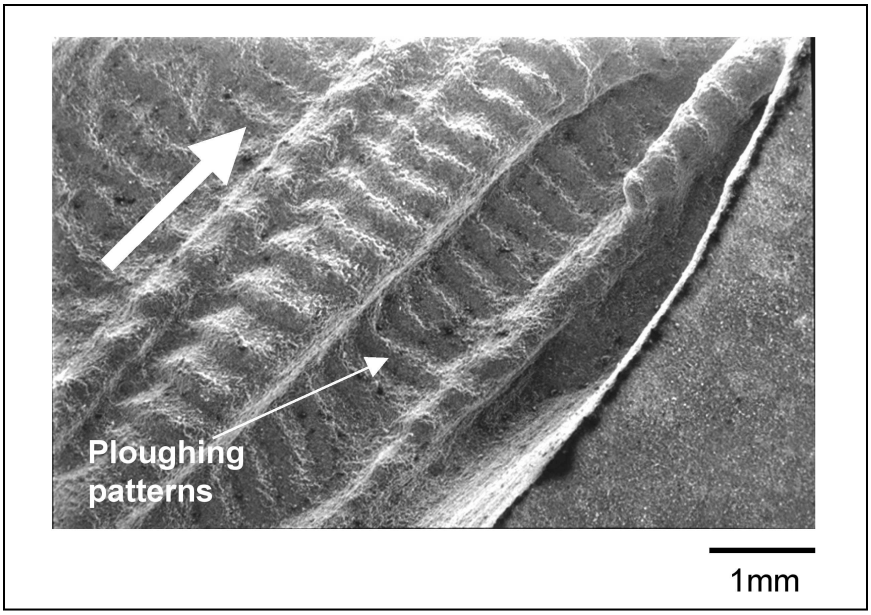

Figure 5.25: Illustration of orientation influence on surface topography of UD-GF/PP-Pa composites with 40 wt. % fibre content (erosion at 30° angle for 600s)

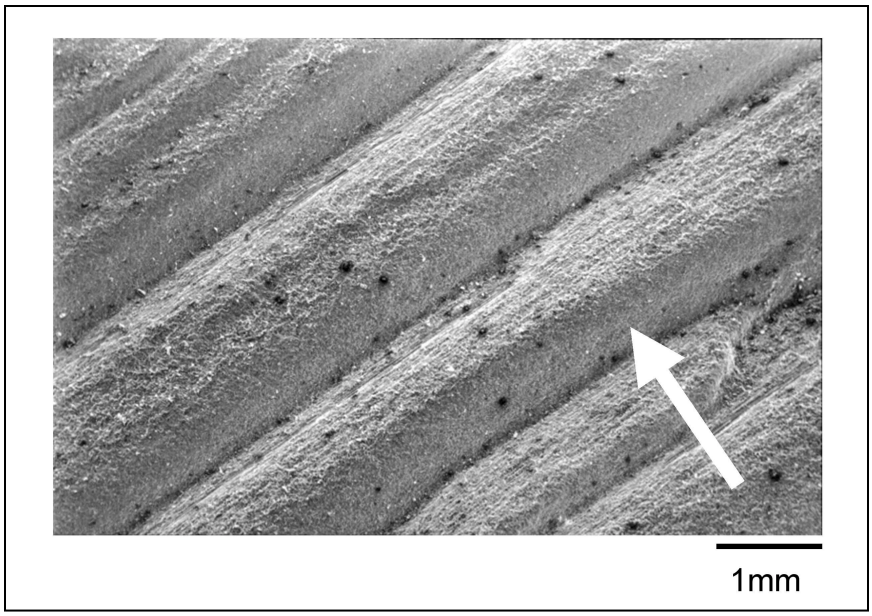

Figure 5.26: Illustration of orientation influence on surface topography of UD-GF/PP-Pe composites with 40 wt. % fibre content (erosion at 30° angle for 600s)

Analytically: In the UD composites when the matrix is removed practically nothing remains to support the exposed fibres. Although the fibre fracture is favoured in the Pe-case (due to bending) in our case it is essential to study the matrix removal since all the compositions studied have a large proportion of matrix (40 wt. % matrix correspond to 62 vol. %!). It is intuitive that the matrix can be removed more easily for Pa-direction than in Pe-direction. This is due to the fact that in Pa-direction the matrix is easily ploughed away by the erodents. On the contrary, for Pe-direction the effect of oblique impact in the matrix is restricted to an area between the fibres. This means that the matrix material is removed faster in the case of Pa- erosion and the GF is strongly exposed to the impinging erodent flux. The exposed fibres are no longer bonded to the composite and are not only removed due to erosion and fracture but also due to the lack of adhesion toward the matrix. Consequently, Pa-direction is more sensitive compared to Pe-direction.

The eroded surface of the SGF/PP composite in Figure 5.27 shows that ductile erosion occurs via plastic deformation of the matrix. No fibres are visible on the surface which is likely covered by the matrix. From this morphology, it is confirmed

that less material removal has occurred. The possible reasons behind are: a) a good proportion of fibres are oriented in the direction of the impinging particles, b) as the overall orientation is random at the surface, the other fibres will still derive support from the underlying fibres.

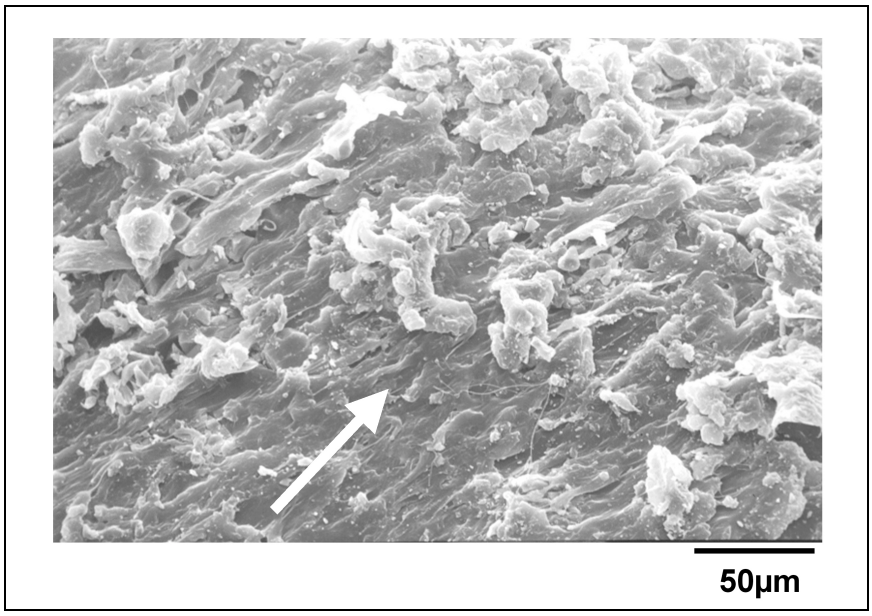

Figure 5.27: Illustration of the failure mode of SGF/PP composites with 40 wt. % fibre content (erosion at 30° angle for 600s) (Ductile mode)

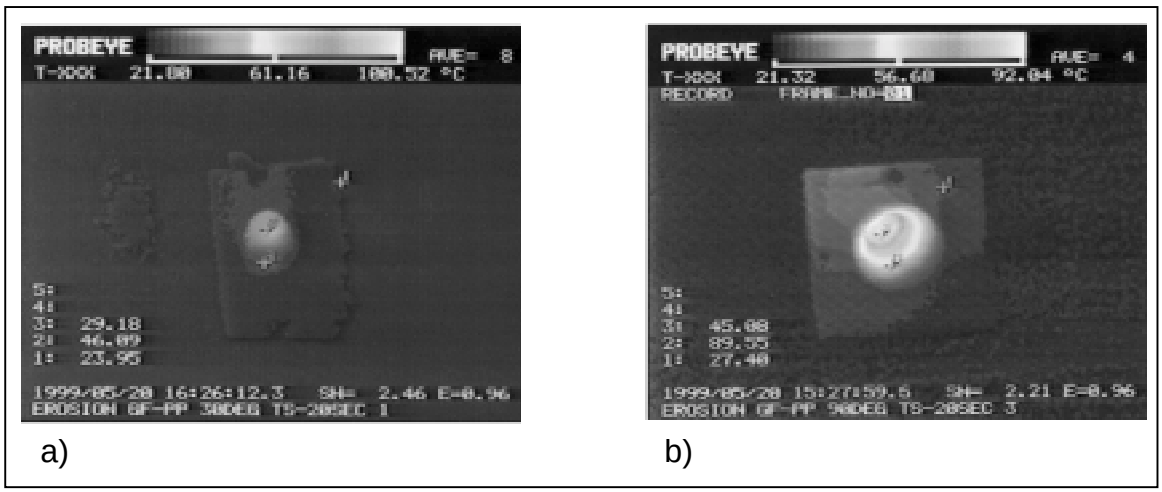

Figure 5.28: Infrared thermographic (IT) frames of GF/PP impacted at a) 30° and b) 90° impact angles, respectively

Finally, Figure 5.28 shows some IT frames, for the case of GF/PP impacted at 30° and 90° angle. The surface temperature for 30° impact was 46°C while for 90° impact, the maximum temperature was near to 90°C. This phenomenon can be explained as follows: In case of normal impact (90°), a considerable amount of impact energy is converted directly to heat which results in a temperature increase. Under oblique impact the major part of the impact energy is dissipated to detach parts from the eroded surface, which is in agreement with the observed ERs. That is the reason for a smaller temperature increase. Nevertheless, the temperature was high enough to evoke plastic deformation of the matrix that was observed by SEM.

Figure 5.29 illustrates the effect of the fibre content on the ER of the UD-GF/PP composites. The variation of the ER is presented in terms of the fibre weight fraction (w_f %). This will be useful in the application of the different rules proposed in the literature which are expressed as a function of the w_f instead of the volume fractions (v_f %).

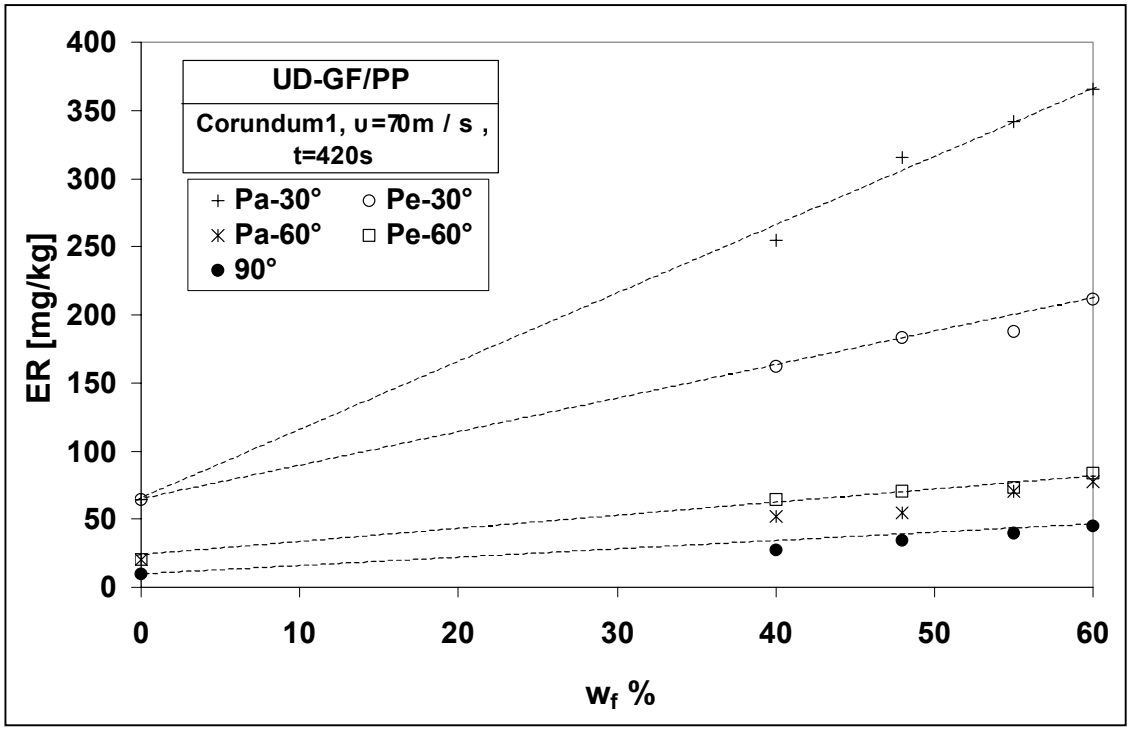

Figure 5.29: Erosion rate (ER) as a function of fibre weight fraction, impact angle and relative fibre orientation for UD-GF/PP composites

Figure 5.29 confirms the earlier observations that the relative fibre orientation plays a important role only in the case of 30° impact angle. Furthermore, the experimental values showed that independently to the impact angle, the ER increased with the addition of brittle GF. It is interesting to observe that until a fibre content of 60 wt. % the ER shows an almost linear variation with the fibre content for the three impact angles and for both erosion directions. This indicates that as long as the material removal is dominated from one of the constituents (viz. matrix) a linear variation exists between ER and w_f. However, considering the ER derived from a pure glass sample (cf. paragraph 5.4) different thoughts should be made.

Based on the results obtained from the solid particle erosion of GF/PP composites reinforced with discontinuous and continuous GF at various fibre contents, the following remarks can be made:
The wear process in thermoplastic matrix composites (GF/PP) presents a maximum ER at 30° impact angle (ductile erosion). There is a slight influence of the fibre length on the erosive wear of GF/PP composites and the role of relative fibre orientation for UD-GF/PP is evident only at 30° impact angle, where the Pa-direction exhibits the maximum ER. The fibre content seems to influence strongly the ER; the experimental results showed a linear variation of the ER with a fibre content up to 60 wt. %.

5.3.2. Glass Fibre reinforced Epoxy Resin

GF/EP systems are typical representatives of thermosetting composites. The erosive wear of such systems have received a great interest over the years. However, limited information is available on the effect of fibre/matrix adhesion on the erosion of fibre reinforced plastics [69,70,77]. Miyazaki et al. studied the effect of fibre/matrix interface strength on the erosion behaviour of unsaturated polyester (UP) and epoxy resins (EP) reinforced by treated and untreated glass (GF) [77] and carbon fibres (CF) [70], respectively. For the latter system no difference in the interfacial strength resulting from the fibre surface treatment was observed and thus its effect on the erosion rate could not be deduced. Further, the mechanisms of erosion and how inherent properties of the composites, such as interfacial shear strength, affect the erosion behaviour are less understood. This part of the work tries therefore to elucidate the effect of interfacial modification on the erosion wear of unidirectional GF

reinforced EP composites [74]. It was of interest to investigate if the relative fibre orientation influences the effect of the interface, therefore the UD-GF/EP composites were impacted in Pa- and Pe- directions. In this way the effect of the fibre orientation in a thermosetting system is additionally studied.

The τ_i value obtained from the microdroplet pull off tests was 32 MPa for the poorly (GF/EP) and 56 MPa for the well-bonded composite (GF/EP-M), respectively. This difference confirms that a suitable GF sizing may led to a significant improvement of the interfacial shear strength of the composite (improvement 75%).

Figure 5.30 displays the influence of the impact angle on the erosive wear of the UD-GF/EP systems. One can recognise that the UD-GF/EP composites undergo brittle type erosion irrespectively to the fibre orientation and interfacial modification. The maximum ER was found at 90° impact angle demonstrating the brittle erosion response of the thermosetting matrix composites.

The effect of fibre orientation on the ER can also be deduced from Figure 5.30. There is no sense to indicate the erosion direction in case of 90° impact because the particles hit the same transverse area. The UD-GF/EP composites showed a higher ER in Pe- than in Pa- direction, especially at 30° angle.

The sizing of GF had a pronounced effect on the erosive wear of UD-GF/EP. The composites with EP-compatible GF presented a much higher erosion resistance compared to the EP –incompatible sized GF containing composites, for all impact angles. The difference in the interfacial adhesion is best reflected at 90°-impact angle, where ER reaches its maximum. Accordingly the adhesion promoted by proper fibre sizing strongly improved the erosion resistance of UD-GF/EP composites. This indicates that the interface between matrix and fibre plays an important role with respect to solid particle erosion.

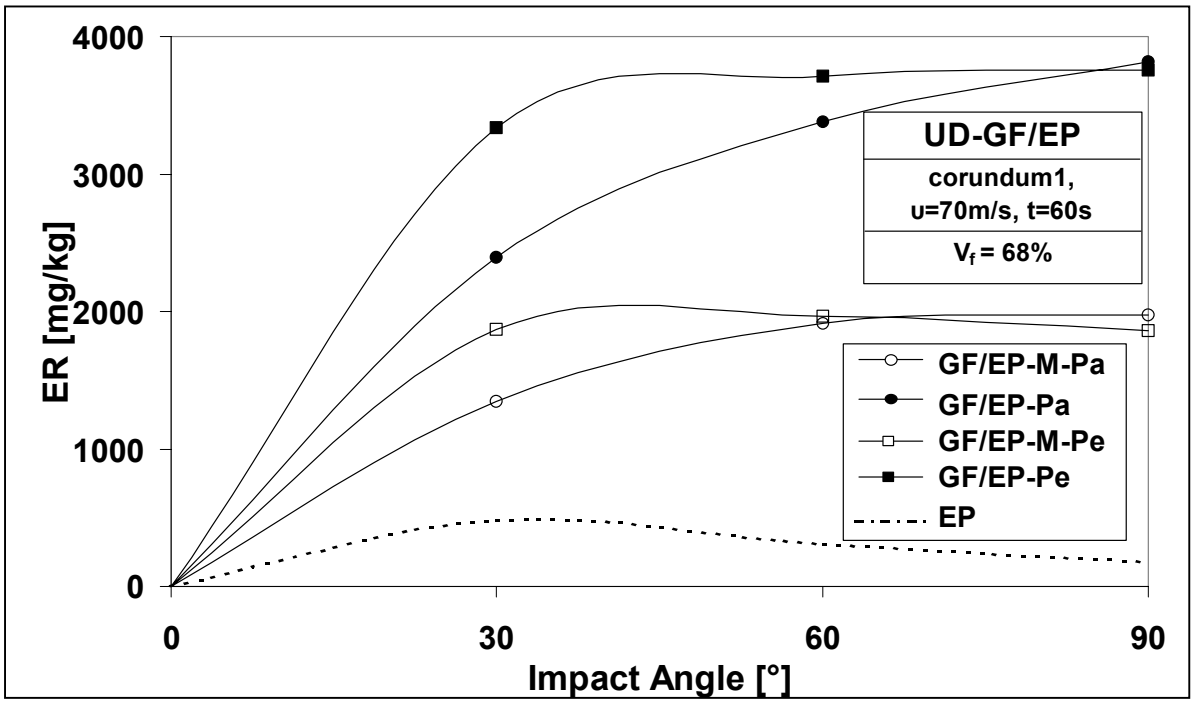

Figure 5.30: Influence of impact angle, erosion direction and interface modification on the erosive wear of EP and GF/EP-composites

The effect of relative fibre orientation on the erosion wear of UD-GF/EP is better illustrated when the SEM scans of the eroded surfaces are regarded. The failure mode in UD-GF/EP and in general in thermoset composites is a complex process involving matrix micro cracking, fibre-matrix debonding, fibre breakage and material removal [6,67,69].

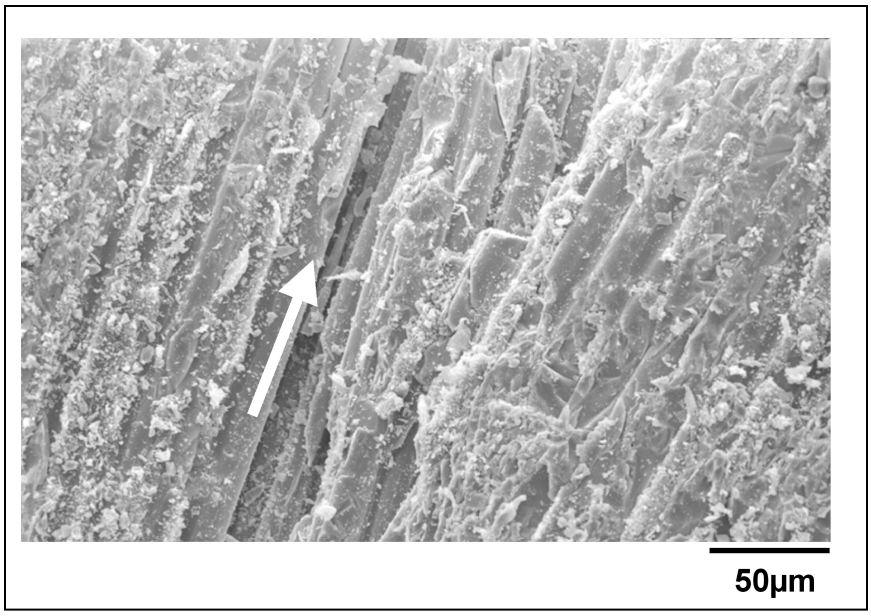

a)

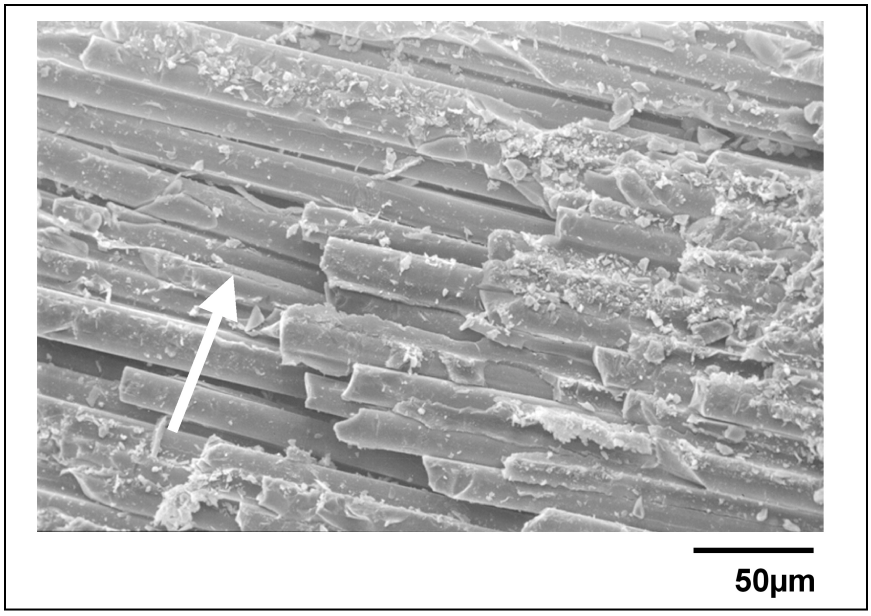

b)

Figure 5.31: SEM micrographs taken on the eroded surface of composites impacted at 30° angle for 40s Designation: a)GF/EP-Pa and b)GF/EP-Pe, respectively

The main reason for the fibre fracture is bending. In Pa-direction hardly any bending occurs in contrast to the Pe case. This becomes obvious in Figure 5.31. In Pe case broken fibres along with multiple matrix-cracking can be resolved (cf. Figure 5.31b), while in case of Pa-direction less resin is removed and there is no sign of fibre breakage (cf. Figure 5.31a). The above difference was very clear for the unmodified system, especially at an 30° impact angle (cf. Figure 5.31). There was, however, a smaller difference between the Pa and Pe directions of impact for the UD-GF/EP-M system (cf. Figure 5.30). This suggests that improved fibre/matrix adhesion is associated with a higher resistance to erosive wear even under the most severe Pe condition.

Figure 5.32 gives a scheme on the role of interface in the erosion of UD-reinforced composites. Clearly seen that under Pa impact, when the matrix material is removed, the erosive particles hit directly the fibre and thus the interface between fibre and matrix becomes less dominant. By contrast, under Pe impact the abrasive material erodes the matrix between the fibres, fractures the fibres and removes their fragments. Low interfacial shear stress between GF/EP facilitates the debonding and breakage of fibres, which are not supported by the matrix. These fibres are then

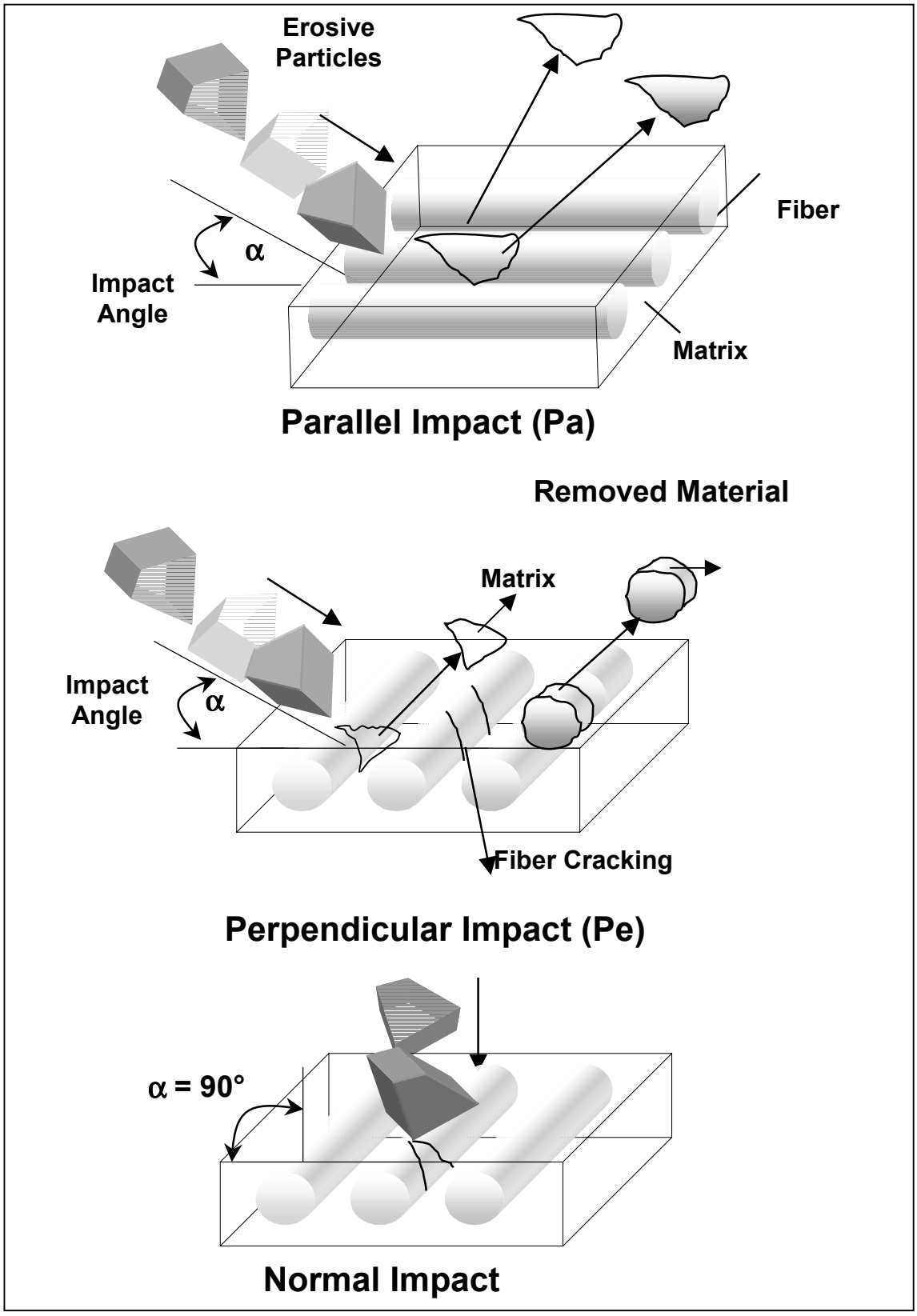

Figure 5.32: Scheme of the role of the interface on the erosion of UD fibre-reinforced composites under parallel (Pa) and perpendicular (Pe) impact conditions

removed. Good bonding between GF and EP however results in a better erosion resistance as the fibre bending due to impact is substantially reduced. As a consequence the modified systems present only a small difference between Pa and Pe impact directions during solid particle erosion.

The role of interfacial modification is further illustrated in Figure 5.33 for the case of UD-GF/EP systems eroded at 90°-impact angle. In case of unmodified system (cf. Figure 5.33b) the matrix shows multiple fracture and material removal. The exposed fibres are broken into fragments and thus can be easily removed from the worn surface. This is not the case for modified systems, where the fibre fragments are well bonded to the matrix and thus kept for longer time on the eroded surface (cf. Figure 5.33a). All these observations, based on SEM micrographs, are in line with those made in earlier studies [6,68].

The influence of interfacial modification and relative fibre orientation (parallel, Pa and perpendicular, Pe) on the solid particle erosion of UD-GF/EP composites was investigated in this paragraph. The results showed a strong dependence of the erosive wear on the jet angle. The UD-GF/EP systems presented a brittle erosion behaviour, with maximum ER at 90° impact angle. It was established that good fibre/matrix adhesion improved the resistance to erosive wear. On the other hand, the

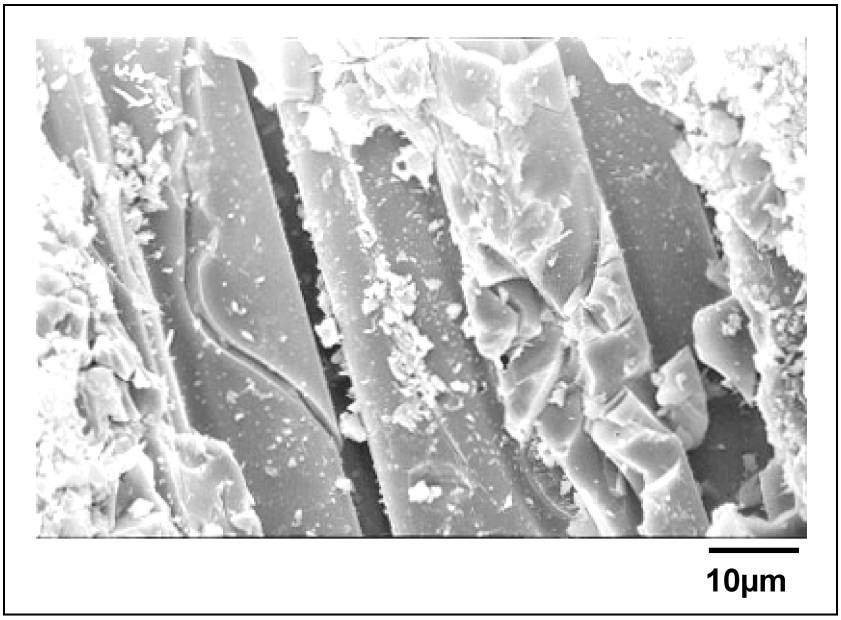

a)

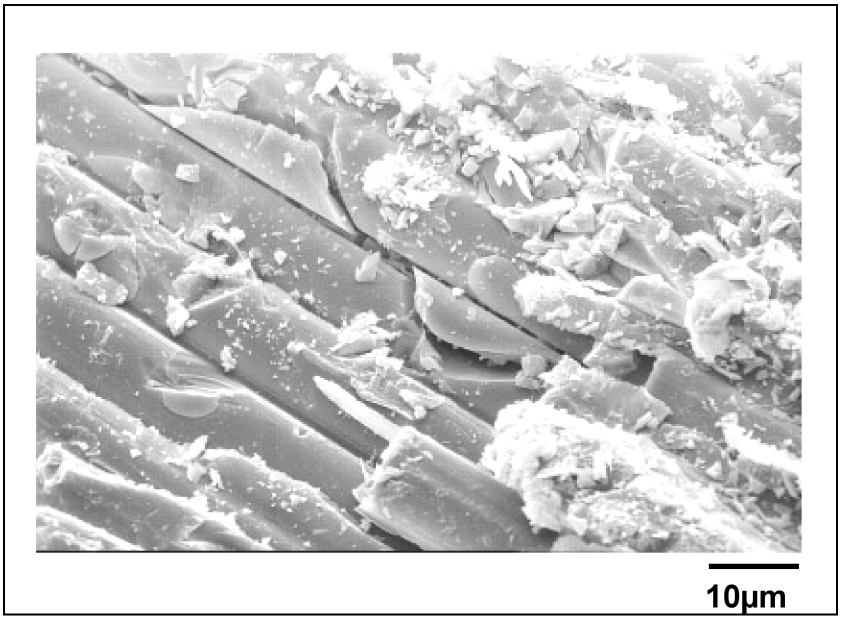

b)

Figure 5.33: SEM micrographs of UD-GF/EP composites impacted at 90° angle for 40s with good (a) and poor (b) fibre/matrix adhesion, Designation a) UD-GF/EP-M and b) UD-GF/EP

relative fibre orientation had a negligible effect except the erosion at 30° impact angle.

5.3.3. Carbon Fibre reinforced Epoxy Resin

Carbon fibre composites offer many benefits over conventional structural materials as strength and stiffness, can be tailored to meet specific design requirements by careful selection of the laminate stacking sequence. It is often reported that the damage tolerance of polymer composites is strongly improved by making use of the interlayering, interleaving concept (incorporation of a tough adhesive layer in the composites build-up) [86-91]. Interestingly no information is available on the effect of these parameters on the erosion of fibre reinforced plastics. In this part of the work the solid particle erosion characteristics of CF/EP composites will be investigated. A further aim is to elucidate how the lay-up of the laminates and the existence and position of interleaves influence their erosion wear. In the previous paragraph it was illustrated that the bonding between fibres and matrix plays a substantial role in the erosive resistance. The incorporation of interleaves in a laminate structure does not

only change the flexural response but influences also positively the bonding between the different layers. This is expected to have a further effect on the erosive resistance [140].

Figure 5.34 displays the influence of the impact time on the erosive wear of the CF/EP systems tested at 90° impact. One can observe an increase of weight loss with impact time from the beginning of the experiments. This implies that the CF/EP composites undergo brittle type erosion irrespectively to the lay-up of the laminates and existence and position of interleaves.

The effect of stacking sequence on the weight loss can also be deduced from Figure 5.34. It seems that in non-interleaved composites a readily detectable effect exists and only for the case of the GF/EP3a structure. One can claim that the 0° and 90° plies show the same erosion rate while the 45° plies show a greater resistance towards erosion. This is expected since in the case of 90° impact there is no sense to indicate the erosion direction because the particles hit the same transverse area. Accordingly the 0° and 90° plies show the same erosion response. It is already stated that the failure mode in thermoset composites involves matrix micro cracking, fibre-matrix debonding, fibre breakage and material removal. Since the main reason for the fibre fracture is bending, when the fibres are oriented in $\pm 45^{o}$ the part of the impact force that leads to material removal is smaller at 45^{o} than at 0^{o} or 90^{o} fibre orientation. The SEM observations confirm the above mentioned mechanisms.

It can also be seen that the composites with interleaves presented a much higher erosion resistance compared to that of the structures without interleaves. The difference is more pronounced in the case of CF/EP3I laminate. This hints that the position and the number of the interleaves play an important role with respect to the solid particle erosion. A first explanation for this observation is that the interleaves behave less brittle in comparison to the CF. Furthermore the existence of the interleaves resulted in a better erosion resistance as the fibre bending due to impact is substantially reduced and the fragments of the fibres are not so easily removed due to the better adhesion between the adjacent layers. A further effect, viz. “cushioning” of the impacted ply by the interleaf cannot be excluded as well.

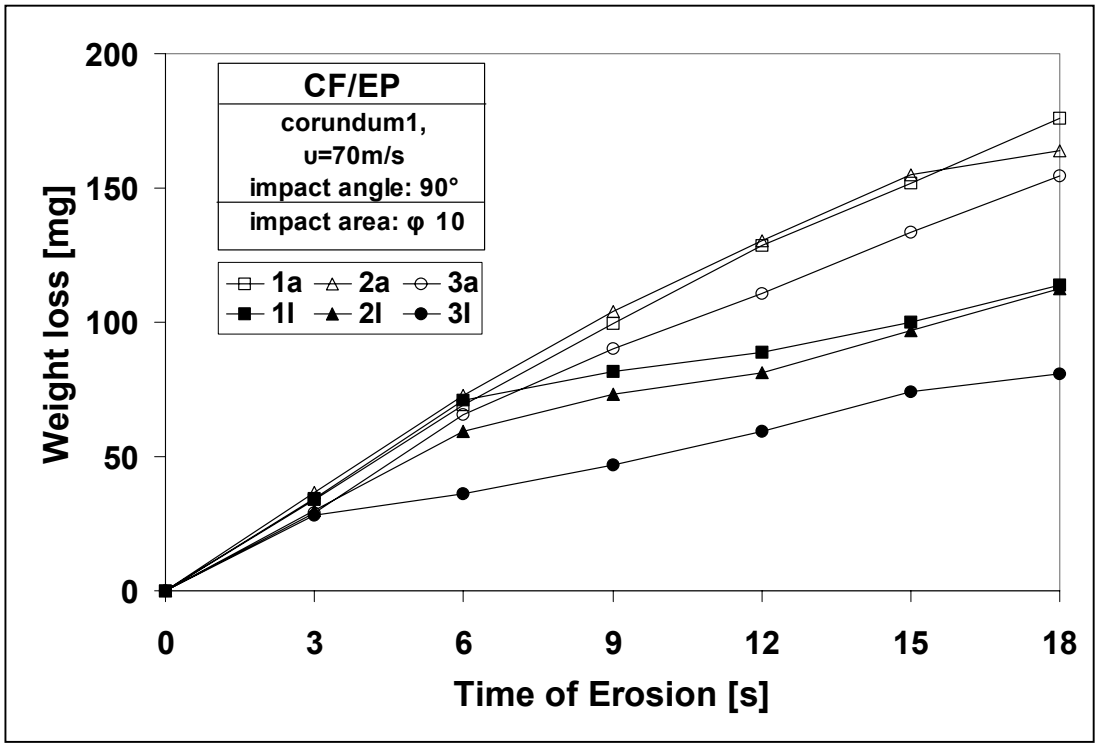

Figure 5.34: Influence of erosion time, stacking sequence, existence and position of interleaves on the erosive wear of CF/EP-composites

Based on C-scans taken from the eroded plates after 0, 6, 12 and 18s impact time it is observed that the damage in all cases of the materials tested was localised at the eroded area. There was no sight of delamination outside of the eroded area either in the plates with or without interleaves. Figure 5.35 presents representative scans of the tested specimens.

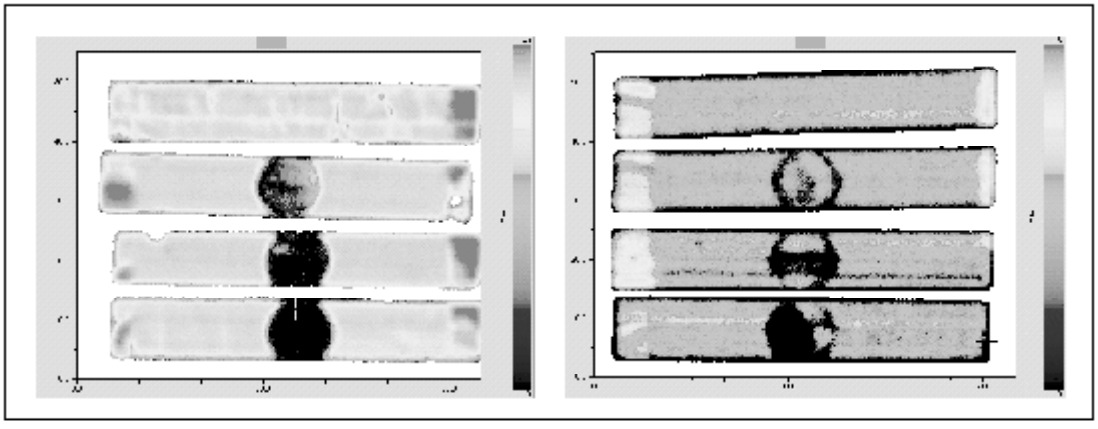

Figure 5.35: Representative ultrasonic scans of the tested composites after 0, 6, 12 and 18s erosion time: a) CF/EP1a, b) CF/EP1I

The results showed that as speculated, both stacking sequence and interleaves affect the erosion resistance of CF/EP composites. The incorporation of $\pm 45^{o}$ oriented plies as well as of interleaves leads to composites with superior erosion resistance. These conclusions are in analogy with the literature ones obtained after single impact, indicating that erosion under specific circumstances can be handled as impact fatigue.

5.4. Prediction of the ER of a composite material from the ERs of its constituents

General considerations - Presentation of the various models

The different problems and restrictions arising from the microstrusture, for the prediction of the composite ER, when the ERs of the individual constituent are known, are already pointed out and discussed in chapter 2.3.2.2. The first important factor which should be taken into account is the size of the particle impact damage. Assuming that the impact size is about 10%-20% of the erodent particle size, it can be further assumed that the impact event is smaller than the microstuctural scale so that the impact events will occur in one of the two phases, viz. PP of GF. Following this analysis the LROM (eq. 2.1) and the IROM (eq.2.2) could be applied for the case of erosive wear, respectively.

These two rules of mixture were also proposed to model the abrasive wear of UD fibre reinforced composite materials [141,142]. Unlike to the erosive wear, the applicability of these rules to the abrasive wear was limited as a steady state process was supposed to hold. To refute this limitation a new model was proposed [143], which suggests that the abrasive wear behaviour is quasi-steady state in nature. In this study, it was stated that in practice other processes such as reinforcement debonding, reinforcement fracturing and wear scarring (chip removal) beside abrasion are likely to occur in a non-steady state manner. Two mechanisms, each representing the two extremes of the quasi-state wear behaviour (maximum and minimum fibre wear resistance, respectively) were described. These rules take under consideration the modulus of elasticity E_i of the constituent phases, using further a linear and an inverse rule of mixture for the calculation of the E-modulus of the composite.

Modifying the equations for the case of erosion the following forms are obtained:

$$ER_c = v_m \frac{E_m}{E_c(L)} \frac{\rho_c}{\rho_m} ER_m + v_f \frac{E_f}{E_c(L)} \frac{\rho_c}{\rho_f} ER_f \tag{5.3}$$

with $E_c(L) = v_m E_m + v_f E_f$

$$ER_c = \frac{E_c(L)}{E_m} ER_m \tag{5.4}$$

and

$$ER_c = \frac{E_c(I)}{E_m} ER_m \tag{5.5}$$

with

$$\frac{1}{E_c(I)} = \frac{v_f}{E_f} + \frac{v_m}{E_m}$$

where ν_i the volume fraction of the respective constituent.
The equation 5.3 refers to the maximum fibre resistance assumption while 5.4 and 5.5 to the minimum fibre resistance assumption.

The linear (LROM) and inverse (IROM) rules of mixture were first evaluated for a multiphase AL-Si alloy [76]. The same rules of mixture were adopted for a glass-fibre reinforced epoxy composite [73]. A literature survey showed that information on the effects of fibre content on the erosive wear behaviour is scarce and its modelling is mostly studied for thermosetting matrix systems. As different mechanisms of material removal seem to govern the erosion of thermoplastic matrix composites, the main aim of this part of the study is to evaluate whether or not the proposed rules of mixtures can be used for glass fibre/ polypropylene (GF/PP) composites [139]. For the case of erosion at low impact angles (30°) the modified rules of mixture [143] are additionally evaluated.

Verification of the various models

Table 5.7 presents the material properties needed for the verification of the above mentioned equations. The estimation of the ER of the glass was very accurate at 30° and 60° impact angles as a straight linear behaviour was observed. Nevertheless, at 90° impact angle, the glass showed two linear variations: At the beginning of the experiment, a slope similar to that of 60° impact angle was found corresponding to an ER of 4448 mg/kg. After a specific point, saturation in the weight loss with the mass of erodent was observed, perhaps due to thermal hardening-phenomena. This led to a second, very low slope in the curve and an ER of 70 mg/kg. In the following analysis, the first slope of the curve at 90°-impact angle was taken under consideration.

Table 5.7: Material properties of GF and PP used for the evaluation of the proposed 'averaging rules of mixture'

E_f [GPa]	E_m [GPa]	ER_f [mg/kg]			ER_m [mg/kg]			ρ_f [g/cm^3]	ρ_m [g/cm^3]
		30°	60°	90°	30°	60°	90°		
76	1.2	1300	5196	4448	64	20	10	2.56	0.91

Taking into account the values in Table 5.7, the experimental data and theoretical predictions were collated. Plotting the ER vs. fibre weight content, w_f, (Figure 5.36), different trends can be observed for the three different impact angles. In the case of 30° impact the experimental values for both erosion directions lie between the LROM and the IROM. The LROM seems to be closer to the experimental data for Pa-erosion, while the IROM seems to give a better prediction for Pe-direction. The modified rules of mixture (equations 5.3, 5.4 and 5.5) proposed for the case of abrasion do not provide a better fitting to the experimental data. Although the abrasive action of the erodent at 30° impact is dominant, the impact action due to the vertical component of the force can not be any more negligible, especially when the amount of the brittle fibres in the composite is considered. The IROM seems to follow the variation of the ER with the fibre weight content in cases of 60° and 90° impact while the LROM largely overestimates the measured ER. The applicability of the LROM in some of the experimental results comes to verify the already existing remark [76], that although generally the IROM predicts better the ER of multiphase systems, when the two constituents are continuous and linear aligned along the incident erodent particle beam direction (UD-GF/PP-Pa, 30° impact), the LROM approach works well.

Consequently, the inclusion of brittle GF led to higher ERs of the GF/PP composites; the higher the fibre content, the higher was the ER. Nevertheless, the composites still failed in a ductile manner. Different approaches proposed to describe the relationship between ER and fibre content were applied. Best results were generally delivered with the inverse rule of mixture. The modified rule of mixtures proposed for abrasive wear do not seem to apply for erosive wear.

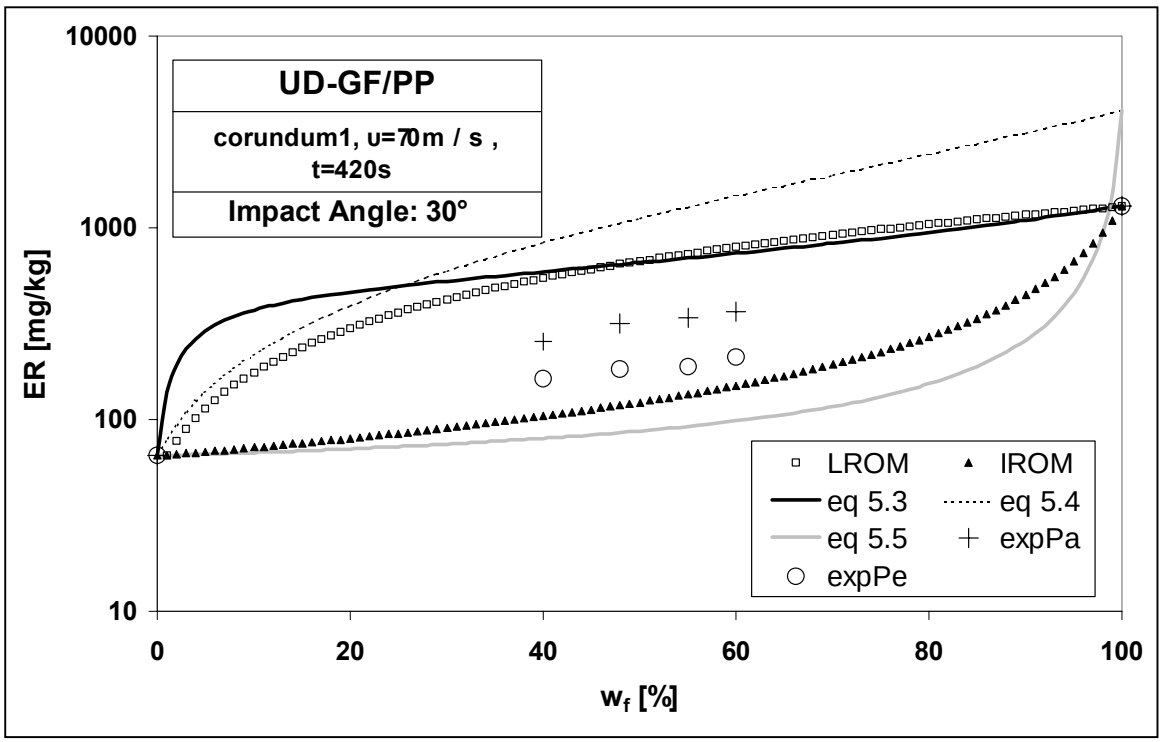
UD-GF/PP
corundum1, υ=70m / s , t=420s
Impact Angle: 30°
ER [mg/kg]
10000
1000
100
10
0
20
40
60
80
100
w_f [%]
LROM
IROM
eq 5.3
eq 5.4
eq 5.5
expPa
expPe

a)

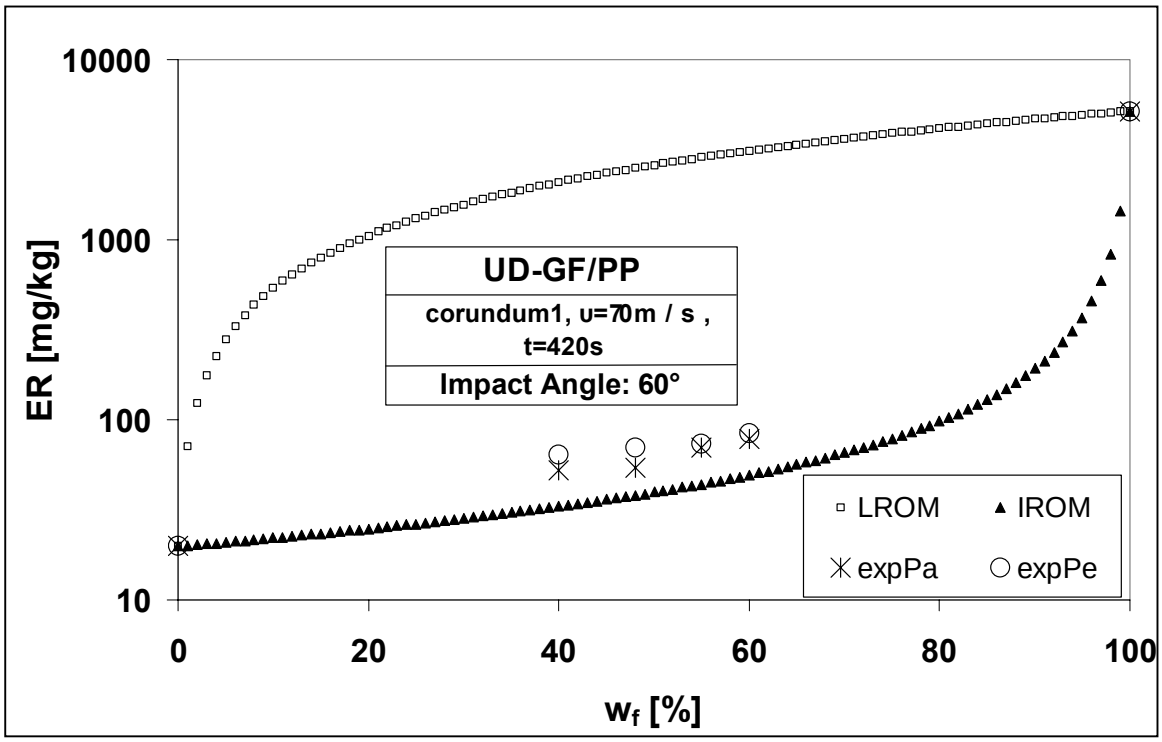
UD-GF/PP
corundum1, υ=70m / s , t=420s
Impact Angle: 60°
ER [mg/kg]
10000
1000
100
10
0
20
40
60
80
100
w_f [%]
LROM
IROM
expPa
expPe

b)

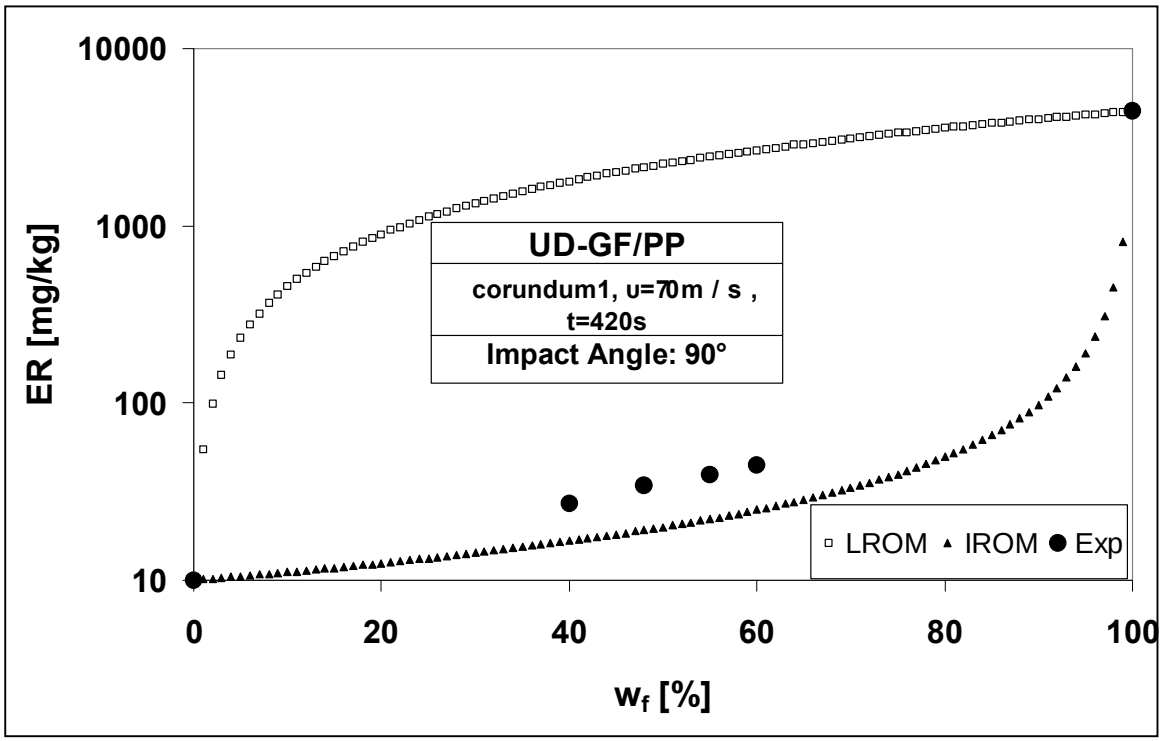

c)

Figure 5.36: Application of ‘averaging laws of mixture’ for the description of the Erosion Rate (ER) of a composite as a function of the fibre content in the case of a UD-GF/PP composite

a) 30° impact angle, b) 60° impact angle and c) 90° impact angle

5.5. Residual Strength after Solid Particle Erosion

The predictive model used in the present investigation is the result of a series of efforts started the last decade at Composite Materials Group (CMG), University of Patras and experimentally evaluated in IVW, Kaiserslautern [92-96].

The first approaches [92-97] adopted to describe the residual strength of impacted fibre reinforced (FRP) laminates presented a limitation i.e. the model's prerequisite of evaluating laminates including always $\pm 45^{o}$ oriented plies. In order to overcome this limitation, a new model was recently developed which takes into account the quasi-static response of the impacted structures.

This model was firstly presented and evaluated for the case of erosion [140]. A quick review of the model is presented in Appendix. The model takes into account the inherent material properties, the initial and post-impact tensile strength of the material and the visco-elastic response (viz. mechanical damping) of the non-impacted material.

As reported in literature, erosion results to both material removal and stiffness reduction. As a consequent, a significant degradation in strength mainly due to matrix cracking, delaminations and fibre breakage is observed. It is well established that when damage occurs in composite systems, broken fibres reduce the tensile strength whereas delaminations between layers reduce the compressive strength [84,144,145]. The damage growth in solid particle erosion occurs mainly via fibre breakage and lesser extent through delamination. Therefore the residual tensile strength after solid particle erosion may be a good indication of the damage state.

Since the ability of a polymer to withstand an impact depends on its ability to dissipate the energy of the impact, many studies look for the correlation of the impact strength and the dynamic mechanical dissipation factor [146-150]. A brief explanation is that as the strain rate is increased, the modulus becomes more linear over a longer elongation (among other things) and the sample may even break before yielding. At the strain rates of impact it is this region of the modulus of most engineering polymer composites, the exact region from which dynamic mechanical properties arise, which

is the major contributor to the impact energy dissipation process. It may now be seen why impact strength correlates with dynamic mechanical properties: they both arise from the same molecular motions [146]. The storage modulus informs us about the elastic energy storage, whereas the loss factor about the energy dissipation, or damping of a material. The dissipation ability of a material is maximised when the time scale of the deformation is the same as the internal time scale of the material. If the two time scales are substantially different, the energy dissipation is reduced. That is why the absolute tanδ value is involved in the calculation of the impact energy threshold beyond which the strength degradation starts (see Appendix).

In order to apply this semi-empirical model three test series are needed. Two tensile tests in order to determine σ_o (tensile strength of the non-impacted material) and σ_∞ (ultimate tensile strength of the impacted material) and one DMTA test to define tanδ of the non-impacted specimen.

5.5.1. Thermosetting Systems

There are many studies that report on the residual behaviour of CF/EP laminates after single impact. These materials show high energy absorption under gross failure conditions (i.e. crash-worthiness), but are prone to localised subsurface damage under impact loads. Crucial parameters for the post impact residual strength of these laminates are the stacking sequence of the laminate and the existence and position of interleaves. The effect of these parameters on solid particle erosion was illustrated in paragraph 5.2.3. This paragraph will investigate if these parameters influence also the onset of damage degradation and the residual strength after solid particle erosion [140].

DMTA spectra of the CF/EP laminates before erosion are presented in Figures 5.37a and b. Figure 5.37a shows the variation of the storage modulus (E') as a function of temperature whereas Figure 5.37b presents the loss factor variation with temperature and the shifts in the glass transition (T_g) peaks of the different laminates in respect to their lay-up as well as to the existence and position of interleaves.

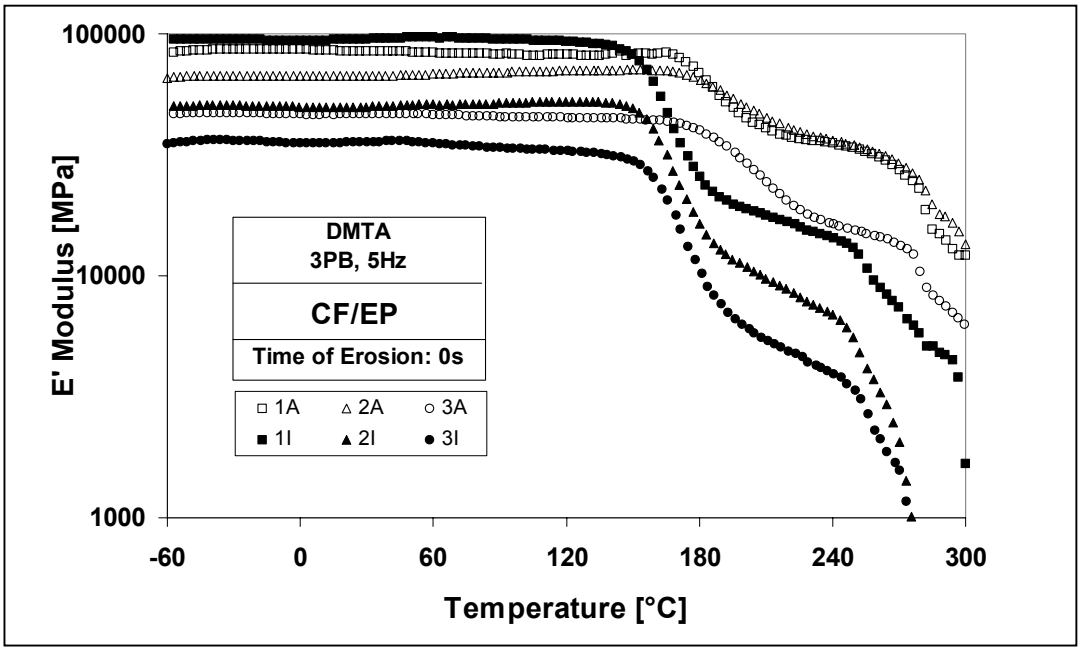

a)

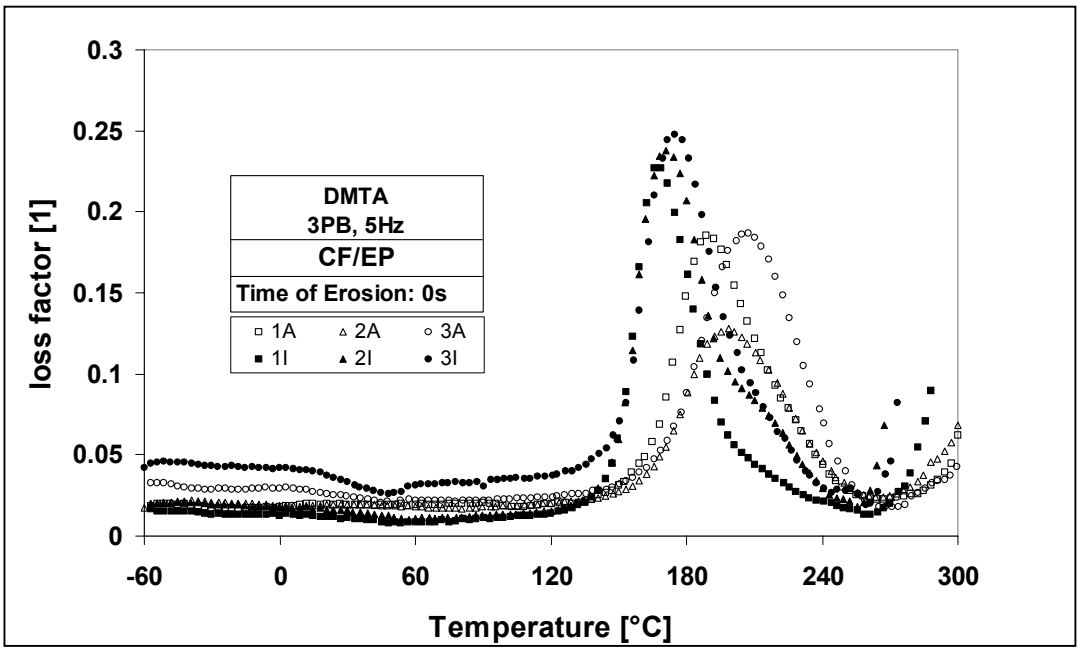

b)

Figure 5.37: DMTA spectra of the CF/EP laminates before erosion a) Storage Modulus (E'), b) loss factor (tanδ)

Table 5.8 resumes the experimental values of the tensile strength ratio (σ_r/σ_o, where σ_r= the residual tensile strength after impact) for different energies and laminates. As above mentioned, the solid particle erosion can be characterised as an impact fatigue procedure, which results in a stiffness reduction.

Table 5.8: Experimental values of the tensile strength ratio (σ_r/σ_o), for different impact energies and laminates.

	CF/EP1a	**CF/EP2a**	**CF/EP3a**	**CF/EP1l**	**CF/EP2l**	**CF/EP3l**
	σ_o=841 [MPa]	**σ_o=623 [MPa]**	**σ_o=533 [MPa]**	**σ_o=750 [MPa]**	**σ_o=550 [MPa]**	**σ_o=450 [MPa]**
U [J]	**σ_r/σ_o**	**σ_r/σ_o**	**σ_r/σ_o**	**σ_r/σ_o**	**σ_r/σ_o**	**σ_r/σ_o**
12.24	0.870	0.383	0.861	1.025	0.545	1.016
24.48	0.647	0.422	0.398	0.741	0.455	0.872
36.72	0.452	0.389	0.433	0.798	0.396	0.591
48.96	0.410	0.434	0.412	0.772	0.409	0.459
61.2	0.392	0.407	0.377	0.865	0.398	0.414
73.44	0.390	0.406	0.375	0.780	0.333	0.326

Table 5.9: Parameters used and derived by applying the proposed model to CF/EP laminates.

	σ_o [MPa]	**σ_∞ [MPa]**	**s [1]**	**m [1]**	**tanδ [1]**	**V [mm^3]**	**E_{11} [GPa]**	**U_o [J]**
CF/EP1a	841	328	0.390	0.181	0.185	1125	90	7.4
CF/EP2a	623	253	0.406	0.259	0.128	1200	59	3.3
CF/EP3a	533	200	0.375	0.259	0.187	1200	59	3.3
CF/EP1l	750	585	0.780	0.168	0.227	1275	110	20
CF/EP2l	550	200	0.364	0.257	0.238	1350	47.6	8
CF/EP3l	450	180	0.400	0.110	0.248	1500	46.5	11.8

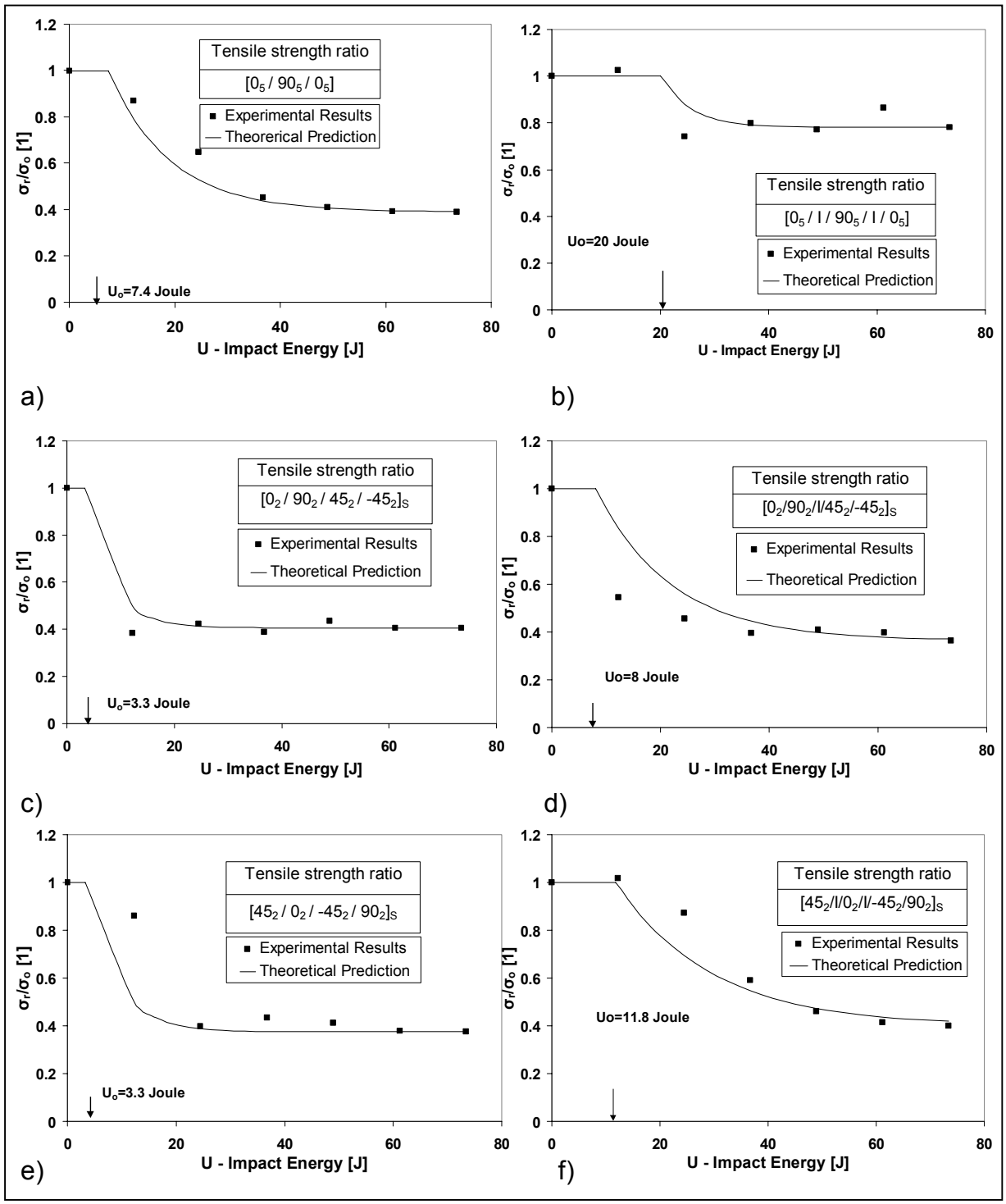

Figure 5.38: Variation of the normalised residual tensile strength, (σ_r/σ_o), versus impact energy, U and comparison to respective model predictions.

a) CF/EP1a, b) CF/EP2a, c) CF/EP3a, d) CF/EP1I, e) CF/EP2I and f) CF/EP3I

Table 5.9 presents all the characteristic of the materials used as well as their energy threshold as derived from the model. The values of σ_o, σ_∞, E_{11} and tanδ are experimentally defined. Applying equations of the proposed model, the parameters s and U_o, are calculated. For calculating m, the following elastic constants of the used CF/EP system were considered: E_1=138 GPa, E_2=8.96 GPa, G_{12}=7.1 GPa, and v_{12}=0.3. For the interleaves the respective values are E_1=3.35 GPa, E_2=3.35 GPa, G_{12}=1.29 GPa, and v_{12}=0.3.

Taking into account the U_o values as derived from eq.4 (see Appendix), a comparative study between experimental data and theoretical predictions was carried out. Plotting the tensile strength ratio σ_r/σ_o, versus impact energy, U, (Figure 5.38), it can be noted that the proposed model seems to predict well both the impact energy threshold and the tensile strength ratio for all CF/EP laminates studied.

It is interesting to note that the impact energy threshold is higher in the case of the cross-ply laminates and in the case of systems with interleaves. It is also observed that the reduction rate of the residual after impact strength in the case of the cross-ply laminates, with or without interleaves, is smaller in comparison to all other systems.

5.5.2. Thermoplastic Systems

It was stated that an increase in strain to failure of the matrix results generally in improved residual strength of the composite after impact, but this increase is limited because of the need of the composite to maintain satisfactory performance at high temperatures and in difficult environmental conditions [84]. Although thermoplastics appear to meet these two requirements, they have received little attention comparatively to thermoset composites [84]. The failure mode in thermoset matrix composites is a complex process involving matrix micro-cracking, fiber-matrix debonding, fiber breakage and material removal. Thermoplastic matrix composites behave differently. The higher matrix toughness allows substantial plastic deformation which absorbs a great deal of impact energy. The matrix is uniformly grooved due to microcutting and microploughing which results to a maximum material removal at oblique impact (30°).

As different mechanisms of materials removal govern the erosion of thermoplastic matrix composites, it was of special interest to investigate whether the model adopted in paragraph 5.5.1 for the prediction of the residual characteristics of a typical thermosetting composite (CF/EP) holds for the case of UD-GF/PP [151].

In paragraph 5.3.1 the influence of the relative fibre orientation on the erosive response was investigated for the UD-GF/PP system. It was concluded that the relative fibre orientation affects strongly the erosive wear at oblique impact (30°).

For the UD specimens with fibres aligned Pa to the impinging direction, the erosive wear was considerably higher than that at Pe alignment to the jet. No influence was observed at 60 and 90° impact angles. Therefore a comparison of the residual tensile strength of Pa and Pe erosion directions after oblique-30°- impact was a further purpose of this part of the study.

Finally, it was interesting to compare the strength degradation onset and the preserved percentage of the initial tensile strength in both ductile and brittle erosion behaviours (i.e. UD-GF/PP and CF/EP).

DMTA spectra of the UD-GF/PP before erosion are presented in Figure 5.39. This figure shows the variation of the storage modulus (E') and that of the loss factor as a function of temperature of the non-impacted material.

Figure 5.41 displays the influence of the relative fibre orientation and the impact time on the erosion wear of the UD-GF/PP system. Although the erosive response of this system is analytically described in paragraph 5.3.1, the addition of the following diagram is very useful as it allows to make direct comparisons with figure 5.40 as both diagrams are in terms of erosive time, i.e. impact-energy. The comparison of figures 5.40 and 5.41 helps us to explain the above findings. At the beginning of the erosion test the material removal is almost the same for both erosion directions (cf. Figure 5.41) therefore the onset of the strength degradation does not differ much. As the specimens are exposed further to erosion, more material is removed under Pa-impact, and therefore the Pa-direction shows larger tensile strength degradation.

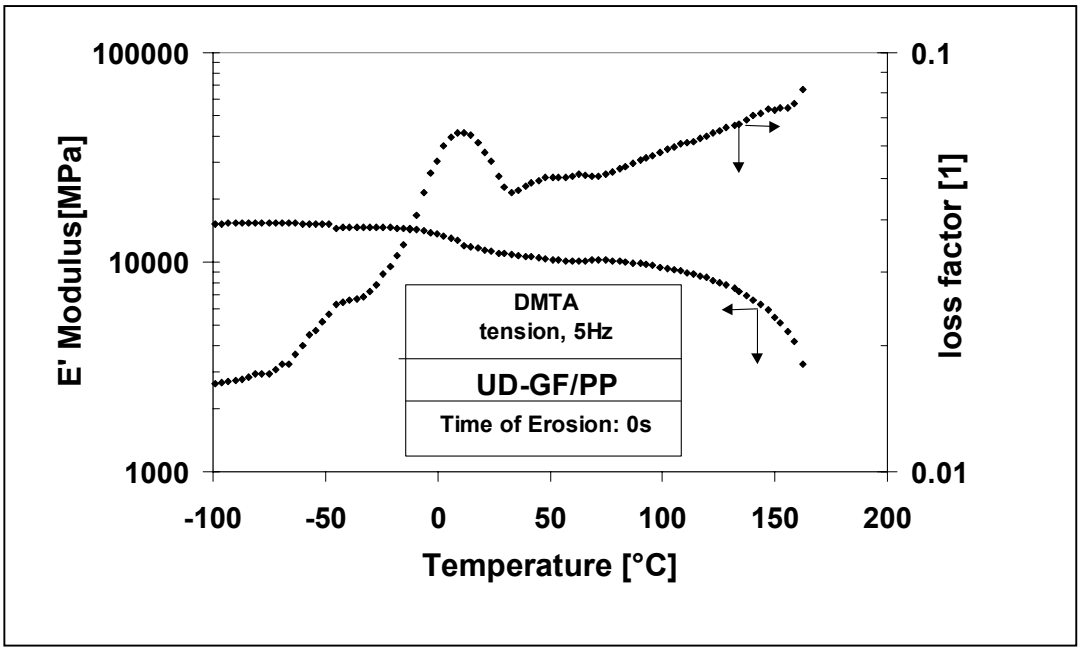

Figure 5.39: DMTA spectra of the UD-GF/PP before erosion

Table 5.10 resumes the experimental values of the tensile strength ratio σ_r/σ_o after Pa and Pe erosion for different erosion conditions (i.e. time) and thus for different impact energies.

Table 5.10: Experimental values of the tensile strength ratio (σ_r/σ_o) for different impact energies and directions.

			U [J]						
			1.02	**3.06**	**5.1**	**40.8**	**61.2**	**112.4**	**183.6**
UD-GF/PP Pa	**σ_o= 430 MPa**	**σ_r/σ_o [1]**	0.841	0.697	0.684	0.673	0.642	0.658	0.65
UD-GF/PP Pe			0.988	0.807	0.769	0.783	0.78	0.746	0.762

Table 5.11 presents all the characteristics of the UD-GF/PP (-Pa and -Pe) determined along with energy threshold (U_o) as derived from the model. The values

of σ_o, σ_∞, E_{11} and tanδ are experimentally defined, whereas the parameters s and U_o, are calculated (cf. Appendix).

Table 5.11: Parameters used and derived by applying the proposed model to UD-GF/PP composites.

	σ_o [MPa]	σ_∞ [MPa]	s [1]	m [1]	tanδ [1]	V [mm³]	E_{11} [GPa]	U_o [J]
UD-GF/PP Pa	430	280	0.65	1	0.06	1200	23.5	0.8
UD-GF/PP Pe	430	328	0.76	1	0.06	1200	23.5	1.19

Plotting the tensile strength ratio σ_r/σ_o, versus impact energy, U, (Figure 5.40), it can be noted that the proposed model holds also for the case of UD-GF/PP as it predicts well both the impact energy threshold and the tensile strength ratio in both erosion directions. The results show that there is a slight difference in the impact energy threshold for Pa and Pe impacts, but there is a clear difference in the ultimate residual strength values. The specimens eroded in Pa-direction maintained 65% of their initial tensile strength while it was 76% for those in Pe-direction.

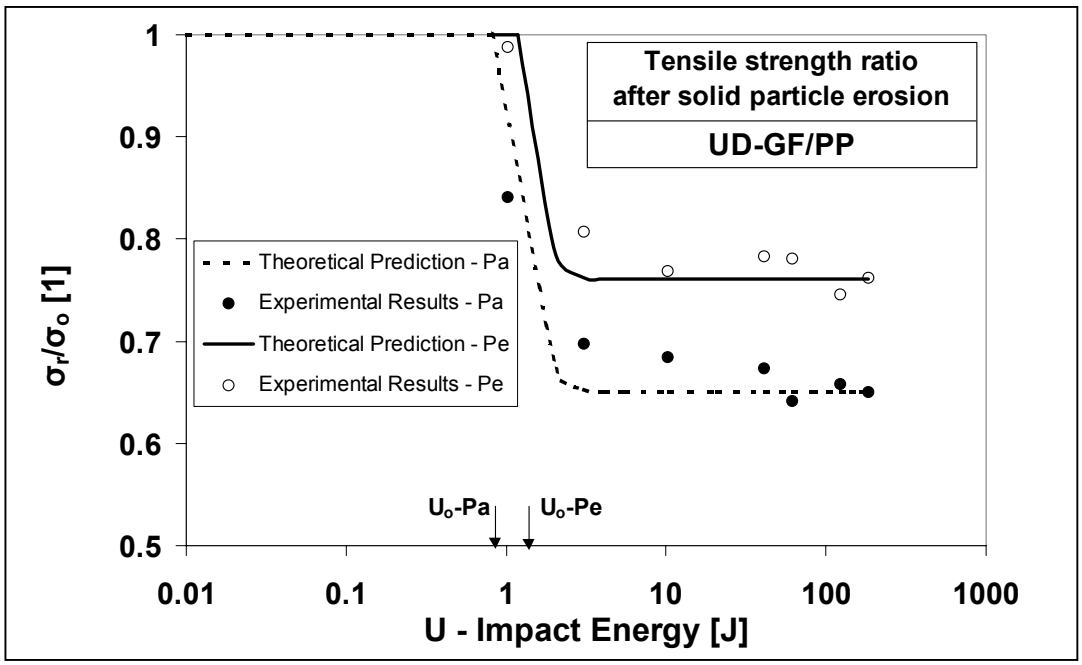

Figure 5.40: Variation of the normalised residual tensile strength, (σ_r/σ_o), versus impact energy, U and comparison to respective model predictions for UD-GF/PP impacted Pa and Pe to the erosion direction

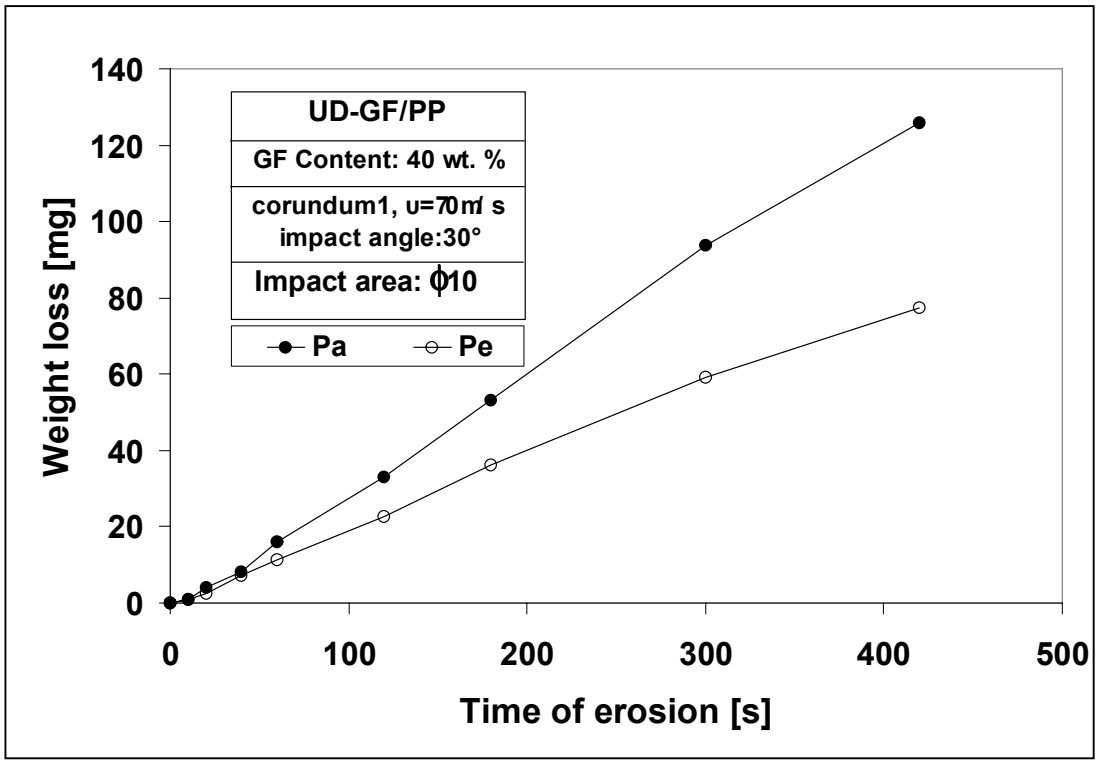

Figure 5.41: Weight loss variation as a function of impact time and fibre orientation of UD-GF/PP composites eroded at 30° impact angle

Figure 5.42 compares the onset of the strength degradation and the percentage of the tensile strength maintained after solid particle erosion for a typical thermoplastic and thermosetting system, respectively. For the first case the UD-GF/PP-Pa system was selected while for the latter a cross-ply CF/EP laminate, because these systems have shown the most severe tensile strength degradation. The thermoplastic composites presented a very quick onset of the strength degradation, and thus a very low U_o value.

Energy transferred to a material during impact can cause elastic and inelastic deformations depending on the properties of both matrix and fibre material. Strain energy has been pointed out as one of the most significant parameters to improve the properties of the composite [84]. At the same solid particle impact energy, composites of higher capacity for energy dissipation yield less fibre breakage and thus consequently a higher residual tensile strength.

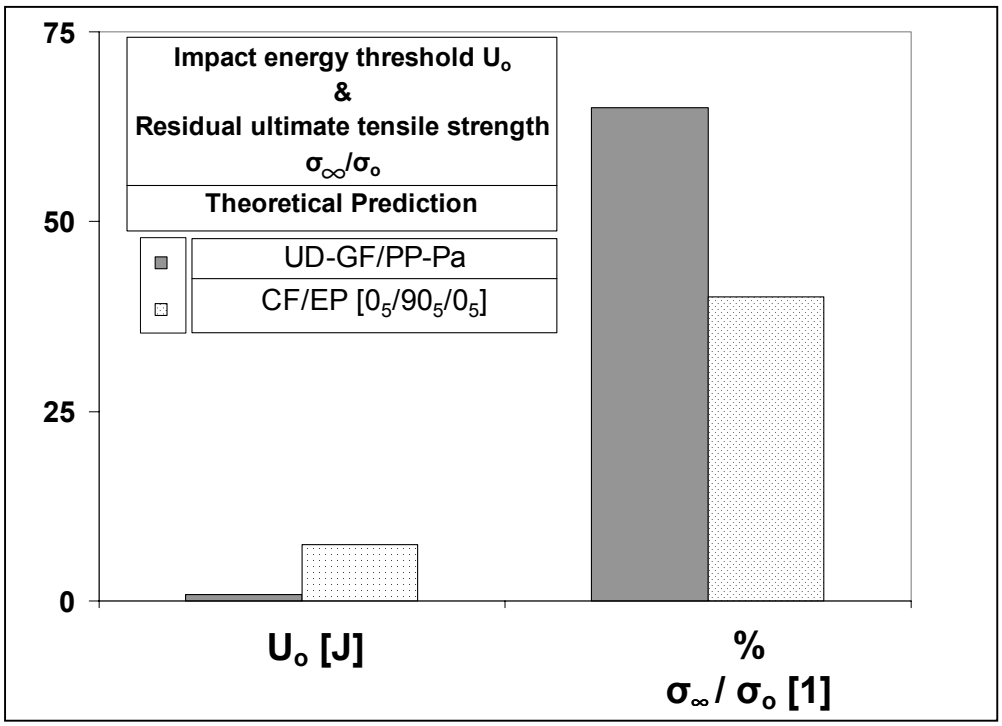

Figure 5.42: Comparison of the impact energy threshold and the normalised ultimate residual tensile strength (σ_∞/σ_o) after solid particle erosion of GF/PP and CF/EP systems

Composites composed of brittle fibre and brittle matrix, such as CF/EP, are unable to undergo gross plastic deformation and so inelastic energy absorbing processes are only involved in cracking [6,68,69]. On the contrary, for thermoplastic composites such as GF/PP, the higher matrix toughness allows substantial plastic deformation, which absorbs a great deal of the impact energy [68,69]. Better toughness due to the PP matrix and higher capacity to absorb energy due to GF resulted in a better erosion resistance of the UD-GF/PP system compared to the cross-plied CF/EP.

The above analysis showed that the model proposed for the prediction of the residual strength after solid particle erosion holds not only for CF/EP systems but also UD-GF/PP at both Pa and Pe erosion directions. The model predicts well both the impact energy threshold and the residual strength after solid particle impact. The proposed model can be used in both cases of ductile and brittle erosion behaviour although different mechanisms in the material removal seem to govern. The erosion direction

does not seem to influence the onset of the strength degradation, it influence however the ultimate residual strength. The Pa erosion direction presents both the maximum material removal and the maximum loss in the tensile strength. A comparison between a system with typical ductile erosion behaviour (UD-GF/PP) and one with typical brittle (CF/EP), shows that the ductile system is more capable on maintaining its initial tensile strength, although it presents earlier the sights of the tensile strength degradation.

6. Summary and Outlook

The present study was aimed at investigating the influence of selected material characteristics and experimental conditions on the solid particle erosion response of polymers and polymeric composites. Results and conclusions obtained during this study are summarised and presented in the next paragraphs. Suggestions on future studies are also given in the last paragraphs.

Thermoplastic Polymers, Thermoplastic and Thermosetting Elastomers

Based on the solid particle erosion response of selected polymers (i.e. polyethylene and polyurethanes), the complexity to correlate material properties and ER, as reported in literature, was further confirmed. This suggested the need of determining the exact conditions during solid particle erosion and estimating the polymer properties under this specific set of conditions, which can be a prospective work in the field of solid particle erosion.

Modified thermosetting Resins

The addition of crosslinking agent in case of PE samples indicated that crosslinking can be beneficial for solid particle erosion up to a specific value. These results were in line with those obtained on the example of modified EP resins having different crosslinking densities (v) due to the addition of HD-PUR. The variation of the ER was a step-wise function of v. It started with a plateau and was followed by a steep increase of the ER with increasing v up to a specific v value. Above this v value a second plateau was observed. The steep increase in the ER that separated the two plateau signified that the change in the crosslink density led to a change (i.e. transition) in the mode of erosion. A further interrelation between erosion response and fracture energy was found. For high crosslink density values, it was observed that G_c only slightly changes, while for the same range of v the ER presents the above mentioned plateau. As a consequence, the increasing resistance to erosion was explained through the increment in G_c.

Modified Thermosets, Thermoplastics and Elastomers

The above system, i.e. HD-PUR/EP, was also aimed to discover the effect of the toughness modification of EP resins on their erosive response. It was found that the

addition of HD-PUR resulted in systems with improved erosive wear resistance for a modifier content higher than 20 wt. %. The increase in the modifier content resulted in a change in the failure mode, viz. from brittle via ductile to a rubbery-like failure mode owing to a change in the target material properties. The cause of this change was additionally discussed in terms of the erodent characteristics. A shifting in the angle referred to the maximum ER of the unmodified EP was observed from 90° to 30° when sharp, angular erodents (i.e. corundum, steel grit) instead of round ones (i.e. glass beads) were used. The classification of the erodents in respect to their erosive efficiency was as follows: corundum1> corundum2> steel grit > glass beads. In respect to the influence of the erodent size it was found that the ER was independent on this parameter above a critical value. Up to this value, the ER increased as the erodent size increased. The critical value was in the range of 100-200 μm. The influence of the erodent hardness was more pronounced for the brittle mode than for the ductile one.

The efficiency of polymer modification in respect to the erosion resistance was further investigated through melt blending of thermoplastic polymers with elastomers and nanoparticle filled polyurethanes. It was found that a sufficient amount of elastomer can modify the relative toughness of a polymer and have a further positive influence on its erosion response. In case of nanofillers, it was found that nanoparticles can deteriorate the erosion resistance due to interfacial problems between the elastomer and the particles themselves.

Thermoplastic and Thermosetting Composites

Regarding the erosion response of fibre reinforced polymers, the following parameters were studied: matrix ductility, fibre length, orientation, fibre content, fibre/matrix adhesion, laminate stacking sequence, and finally number, position and existence of interleaves. In respect to these factors the following conclusions can be drawn:

- The erosive wear response of thermosetting matrix composites (i.e. CF/EP and GF/EP) was of brittle (showing maximum ER at normal impact), whereas the

thermoplastic GF/PP systems was of ductile type (with a maximum ER at 30° impact angle).

- In case of UD-GF/EP composites the Pe-direction relative to the fibre orientation presented the maximum ER in case of interface-unmodified systems. The impact direction had a negligible influence on the erosive wear of UD-GF/EP systems with good adhesion between matrix and fibres. In contrast the role of relative fibre orientation for UD-GF/PP was evident only at 30° impact angle, where the Pa-direction exhibited the maximum ER.

- The interface modification via GF sizing improved strongly the overall erosion resistance of the GF/EP composites. Both stacking sequence and interleaves affected the erosion resistance of CF/EP composites. The incorporation of $\pm 45^{o}$ oriented plies, as well as of interleaves, led to composites with superior erosion resistance.

- The fibre length had a slight influence on the erosive wear of GF/PP composites. The short fibre reinforced systems delivered a better erosion resistance in comparison to the UD ones.

- Finally, the fibre content influenced strongly the ER; the experimental results showed a linear variation of the ER with the fibre content up to 60 wt. % for the UD-GF/PP systems. The evaluation of the existing models and equations proposed to predict the ER of a composite system as a function of the ER of its constituents and their relative content showed that the linear rule of mixture and the inverse rule of mixture provide good bounds to the experimental ER. Recall that the inverse rule of mixture deliver generally better results. The modified rules of mixture proposed for the case of abrasion do not hold for the erosive wear.

Results after solid particle erosion of interleaved and non-interleaved CF/EP with various stacking sequences implied that the solid particle erosion can be considered as a repeated low energy impact procedure. The damage growth under erosion was likely similar to that of impact fatigue. A semi-empirical approach, initially developed

for the prediction of the residual strength after single impact, was adopted and evaluated for solid particle erosion. The model takes into account the inherent material properties, the initial and post-impact tensile strength of the material and the visco-elastic response (mechanical damping) of the non-impacted material. The model predicted well both the impact energy threshold and the residual strength after solid particle erosion (impact). Results showed that for impact energy values lower than a characteristic threshold the damage induced did not affect the residual tensile strength of the materials. It was also established that this threshold depends on the orientation of the plies, the existence of interleaves and on the energy absorption capacity of the material.

Because the material removal mechanisms that accompany erosion differ strongly in case of ductile type and brittle type of erosion, the present study verified the applicability of this model in a composite system which shows a typical ductile type of erosion (UD-GF/PP). The model predicted well both the impact energy threshold and the residual strength after solid particle impact also in case of UD-GF/PP at both Pa and Pe erosion directions. The erosion direction did not influence the onset of the strength degradation, it affected, however, the ultimate residual strength. Erosion in Pa-direction resulted in maximum material removal and maximum loss in the tensile strength.

A comparison between CF/EP and UD-GF/PP systems showed that the strength degradation onset appeared almost immediately in the latter case but the UD-GF/PP preserved a greater amount of its initial tensile strength compared to that of CF/EP systems.

Outlook

As confirmed during this study, there exists a lack of correlation between material properties and ER. At the beginning of this chapter the need of determining the exact conditions during solid particle erosion and estimating the polymer properties under these specific conditions was enlightened. More precisely it would be interesting to estimate the temperature profile and the strain rates during solid particle erosion and to try afterwards to estimate the material properties under the same conditions.

The dynamic character of solid particle erosion was obvious and a further continuation of this work could be the determination of the dynamical properties of the materials under the erosion dominating frequencies. In case of polymers and especially within the group of elastomers change in the viscoelasticity has a dramatic effect on the properties, therefore a good idea is to find out and determine especially the thermomechanical and fracture characteristics of the materials in the requested frequency range. Finally it is important to figure out those surface “properties” which are most relevant to solid particle erosion.

Because of the complexity of erosion and the interrelated properties and mechanisms the possibility of creating a data base with wear response and material properties under the same experimental conditions and of using a mathematical method or tool, like neural networks, to combine properties with erosion response would also be a promising way. All these suggestions could possible direct to a better correlation between material characteristics and ER.

In case of polymeric composites a further work could be focused on evaluating the erosion behaviour of aramid fibre reinforced composites. The erosive wear behaviour of this art of composites is not fully discussed and understood therefore a systematical study of the erosion properties, the ‘averaging rules of mixture’ and the residual properties after erosion could be of special interest.

7. Appendix

In recent research efforts it has been assumed that the applied loads are static in nature and that the composite and its constituents exhibit time-independent linear elastic behaviour. However, composite structures are often subjected to dynamic loading caused by vibration or wave propagation. In addition, many polymer composites exhibit time-dependent viscoelastic behaviour under load. Viscoelastic materials are capable of both storage and dissipation of energy under load.

Damping is simply the dissipation of energy during impact. When the contact duration is such that the structure responds quasi-statically, the nature of the dynamic character of impact can be better understood by considering linear visco-elastic models such as spring-mass models.

During impact, the kinetic energy can be converted to:

- Contact losses
- Energy dissipation during dynamic deformation i.e. damping
- Energy storage i.e. strain energy

Visco-elastic behaviour of fibre and matrix materials is not the only mechanism for the structural damping in composite materials but appears to be the dominant mechanism in undamaged polymer composites vibrating at small amplitudes. In order to understand linear visco-elastic damping better, it is important to recognise the relationship between the time scale of the applied deformation and the internal time scale of the material. The time scale for cyclic deformation is determined by the oscillation frequency, ω. In visco-elastic spring-mass models the relaxation time, λ, is a measure of the internal time scale of the material. When the frequency is the reciprocal of the relaxation time, $\omega = \frac{1}{\lambda}$, the loss modulus peaks and the storage modulus passed through a transition region.

The important point is that the dissipation of energy, whether characterised by the loss modulus or the loss factor, is maximised when the time scale of the deformation

is the same as the internal time scale of the material. If the two time scales are substantially different, the energy dissipation is reduced.

Returning back, the proposed model [140, 151, 152] is an extension of the Voigt model. It is established, that strength drops in an exponential/power law mode as the impact energy increases, so according to the new model, the degradation of the mechanical strength due to impact damage is assumed to follow an exponential decay law of the form:

$$\frac{\sigma_r}{\sigma_o} = 1 - e^{-u} \tag{1}$$

where u is a function of the impact energy as well as of the energy absorption capacity of the material expressed through tanδ. Also, σ_r and σ_o state for the residual strength after impact and the corresponding strength of the non-impacted material, respectively.

Thus, the strength degradation after low energy impact can be described by a differential equation of the type:

$$s = y + \left[\frac{1-s}{s}\right]\frac{dy}{dx} \tag{2}$$

where: $s = \frac{\sigma_\infty}{\sigma_o} =$ ultimate residual tensile strength (perforation) / tensile strength before impact

$$y = \frac{\sigma_r}{\sigma_o}$$

$$x = \frac{\Delta U}{U_o} = \frac{U - U_o}{U_o}$$

where

U = the impact energy

U_o= the impact energy threshold related to the onset of strength degradation. For impact energy values $U \le U_o$, no interior damage is induced; the impact energy causes the laminate to deform elastically. Once the impactor ceases to exert load on the plate, the latter recovers its original shape and retains its nominal strength in compression/tension.

Solving equation (2) we obtain:

$$\frac{\sigma_r}{\sigma_o} = 1-(1-s)\left[1-\exp\left(-\frac{s}{1-s}\frac{\Delta U}{U_o}\right)\right] \tag{3}$$

From physical considerations, the value of the strength degradation impact energy threshold, U_o, can be calculated by:

$$U_o = U_{elastic}\frac{\tan\delta}{\mathrm{m}(1-\mathrm{s})} = \frac{\sigma_o^2}{2\mathrm{E}_{11}}V\frac{\tan\delta}{\mathrm{m}(1-\mathrm{s})} \tag{4}$$

where:

E_{11}=is the effective longitudinal Young' s modulus of the laminate

V= the total volume of the specimen

tanδ = loss factor at the T_g of the non-impacted material.

m= is the mismatching coefficient between adjacent layers due to the difference in their fibre orientation angle [90-94] , defined as follows:

$$\mathrm{m} = \frac{\sum_{\kappa=1}^{n}\left(\overline{\mathrm{M}_\kappa}\right)_0[\mathrm{Q}_{xx,\kappa}(\mathrm{z}_\kappa{}^3 - \mathrm{z}_{\kappa\text{-}1}{}^3)]}{\sum_{\kappa=1}^{n}[\mathrm{Q}_{xx,\kappa}(\mathrm{z}_\kappa{}^3 - \mathrm{z}_{\kappa\text{-}1}{}^3)]} \tag{5}$$

Here $\left(\overline{\mathrm{M}_\kappa}\right)_0$ is the mean value for the bending stiffness mismatching coefficient of the κ-lamina, $Q_{xx,\kappa}$ is the x-direction stiffness matrix term of the κ-lamina, z_κ is the distance of the κ-lamina from the middle plane of the laminate and n is the total number of plies in the laminate. The mean value of $\left(\overline{\mathrm{M}_\kappa}\right)_0$ is defined as follows:

$$\left(\overline{\mathrm{M}_\kappa}\right)_0 = \frac{(\mathrm{M}_{\kappa\text{-}1,\kappa})_0 + (\mathrm{M}_{\kappa,\kappa+1})_0}{2} \tag{6}$$

where $\left(\overline{\mathrm{M}_\kappa}\right)_0$ refers to κ-lamina and $M_{\kappa\text{-}1,\ \kappa}$ and $M_{\kappa,\ \kappa+1}$ refer to the interfaces of the adjacent layers (κ-1), κ and κ, (κ+1).

The above-mentioned *m*-parameter depends on the laminate material system elastic properties, lay-up, stacking sequence and individual lamina thickness. For the case of UD composites, *m*=1.

8. Literature

[1] Reynolds, O.: On the action of a blast of sand in cutting hard materials. Philosophical Magazine 46 (1873), pp.337-343.

[2] Rayleigh, J.W.S.: The sand blast. Nature 93 (1912), pp.188.

[3] Finnie, I.: Some reflections on the past and future of erosion. Wear 186-187 (1995), pp.1-10.

[4] Tsiang, T.-H.: Survey of sand and rain erosion of composite materials. Journal of Composite Technology & Research 8 (1986) Nr.4, pp.154-158.

[5] Tilly, G.P.: Erosion caused by airborne particles. Wear 14 (1969), pp.63-79.

[6] Pool, K.V., Dharan, C.K.H., Finnie, I.: Erosion wear of composite materials. Wear 107 (1986), pp.1-12.

[7] Smeltzer C.E., Gulden M.E., Compton W.A.: Mechanisms of material removal by impacting dust particles. Journal of Basic Engineering 19 (1970), pp.639-654.

[8] Lüderitz K.: Erosionsbeständigkeit Kohlenstoffaserverstärkter Duroplaste. Dissertation, Institut für Werkstofftechnologie, Martin-Luther-Universität Halle-Wittenberg (1996).

[9] Maier M., von Dienst K., Ehlers C., Grellmann W., Steiner R., Leps G., Ding J., Pfefferkorn W., Kotter I., Allert E.: Faserverstärkter rotierende Bauteile, Erosions- und Schwingungsverhalten faserverstärkter rotierender Bauteile. Abschlussbericht, Forschungskuratorium Maschinenbau e.V., (1995) Heft 202, pp.1-67.

[10] Leps G., Ding J., Steiner R., Lüderitz K.: Untersuchungen zum Erosionschutz kohlenstoffaserverstärkter Duroplaste. Materialwissenschaften und Werkstofftechnik 26 (1995), pp.374-378.

[11] VDI 3822, Blatt 5.2: Schadensanalyse, Schäden durch tribologische Beansprucuhungen. In: ”VDI-Handbuch Werkstofftechnik, Konstruktion, Betriebstechnik Teil 4”. Düsseldorf: VDI-Verlag 1989.

[12] Czichos, H., Habig, K.-H.: Tribologie-Handbuch: Reibung und Verschleiß, Systemanalyse, Prüftechnik, Werkstoffe und Konstruktionselement. Wiesbaden: Friedr. Vieweg & Sohn Verlangsesellschaft GmbH 1992, pp.128-130.

[13] Veerabhadra Rao P., Buckley D.H.: Angular particle impingement studies of thermoplastic materials at normal incidence. ASLE Transactions 29 (1985) Nr.3, pp.283-298.

[14] Andrews, D.R.: An analysis of solid particle erosion mechanisms. Journal of Physics: Applied Physics 14 (1981), pp.1979-1991.

[15] Bitter, J.G.A.: A study of erosion phenomena. Wear 6 (1963), pp.169-190.

[16] Stachowiak, G.W., Batchelor, A.W.: Erosive wear (chapter 11). In " Engineering Tribology", Tribology Series 24. Amsterdam: Elsevier 1993.

[17] Friedrich, K.: Erosive wear of polymer surfaces by steel ball blasting. Journal of Materials Science 21 (1986) Nr.3, pp.3317-3332.

[18] Lancaster, J.K.: Material-specific wear mechanisms: relevance to wear modelling. Wear 141 (1990), pp.159-183.

[19] Hutchings, I.M.: Ductile-brittle transitions and wear maps for the erosion and abrasion of brittle materials. Journal of Physics. D: Applied Physics 25 (1992), pp. A212-A221.

[20] Arnold, J.C., Hutchings, I.M.: The mechanisms of erosion of unfilled elastomers by solid particle impact. Wear 138 (1990), pp.33-46.

[21] Brandstädter, A., Goretta, K.C., Routbort, J.L., Groppi, D.P., Karasek, K.R.: Solid-particle erosion of bismaleimide polymers. Wear147(1991), pp.155-164.

[22] Groß K.-J.: Erosion (Strahlverschleiß) als Folge der dynamischen Werkstoffreaktion beim Stoß. Dissertation Universität Stuttgart (1988).

[23] Marei, A.I., Izvozchikov, P.V.: Determination of the wear of rubbers in a stream of abrasive particles. In "Abrasion of Rubber". James, D. I. (ed.). London: MacLaren 1967, pp. 274-280.

[24] Arnold, J.C., Hutchings, I.M.: Flux rate effects in the erosive wear of elastomers. Journal of Materials Science 248 (1989), pp.833-839.

[25] Arnold, J.C., Hutchings, I.M.: A model for the erosive wear of rubber at oblique impact angles. Journal of Physics D: Applied Physics 25 (1992), pp.A222-A229.

[26] Roy, M., Vishvanathan, B., Sundararajan, G.: The solid particle erosion of polymer matrix composites. Wear 171 (1994), pp.149-161.

[27] Tilly, G.P., Sage, W.: The interaction of particle and material behavior in erosion processes. Wear 16 (1970), pp.447-465.

[28] Stack, M.M., Pungwiwat, N.: Slurry erosion of metallics, polymers and ceramics: particle size effects. Materials Science and Technology 15 (1999), pp.337-344.

[29] Latifi, A.M.: Solid particle erosion in composite materials. Master of Science thesis Wichita State University (1987).

[30] Shipway, P.H., Hutchings, I.M.: A method for optimizing the particle flux in erosion testing with a gas-blast apparatus. Wear 174 (1994), pp.169-175.

[31] Anand, K., Hovis, S.K., Conrad, H., Scattergood, R.O.: Flux effects in solid particle erosion. Wear 118 (1987), pp.243-257.

[32] Roy, S., Kumar, A.: Effect of blocking agents on the shock absorbing properties of the films of polyurethane adhesives. Polymer Engineering and Science 35 (1995) Nr.12, pp.1046-1052.

[33] Trofimovich, A.N., Anisimov, V.N., Kurachenkov, V.N., Strakhov, V.V., Letunovskii, M.P., Egorov, S.F.: Role of structure factor in evaluating polyurethane wear resistance. Trenie i Iznos 8 (1987) Nr.3, pp.493-499.

[34] Mardel, J.I., Hill, A.J., Chynoweth, K.R.: Wear resistance of polyurethane elastomers. Materials Forum 16 (1992), pp.155-161.

[35] Deanin, R.D., Patel, L.B.: Structure, Properties and Wear Resistance of Polyethylene. In “Advances in polymer friction and wear”. Lee, L.H. (ed). New York: Plenum 1974, pp.569-583.

[36] Rose, R.M., Cimino, W.R., Ellis, E., Crugnola, A.N.: Exploratory investigations on the structure dependence of the wear resistance of polyethylene. Wear 77 (1982), pp.89-104.

[37] Beck, R.A., Truss, R.W.: Effect of a chemical structure on the wear behaviour of polyurethane-urea elastomers. Wear 218 (1998), pp.145-152.

[38] Cho, K., Lee, D.: Effect of molecular weight between cross-links on the abrasion behavior of rubber by a blade abrader. Polymer 41 (2000), pp.133-140.

[39] Mardel, J.I., Chynoweth, K.R., Hill, A.J.: The wear of polyurethane elastomers. Materials Forum 19 (1995), pp.117-128.

[40] Kurachenkov, V.N., Kizhaev, S.A., Letunovskii, M.P., Strakhov, V.V., Anisimov, V.N., Egorov, S.F.: On the abrasive wear resistance of polyurethanes. Trenie i Iznos 11 (1990) Nr.2, pp.347-350.

[41] Mardel, J.I, Hill, A.J., Chynoweth, K.R., Smith, M.E., Johnson, C.H.J., Bastow, T.J.: An investigation of the morphology-wear performance relationships in polyetherpolyurethane thermoplastic elastomers. Wear 162-164 (1993), pp.645-648.

[42] Mardel, J.I., Chynoweth, K.R., Smith, M.E., Johnson, C.H.J., Bastow, T.J., Hill, A.J.: Mechanical behaviour and morphology of a polyetherpolyurethane. Materials Science Forum 189-190 (1995), pp.173-178.

[43] Briscoe, B.J., Evans, P.D., Pelillo, E., Sinha, S.K.: Scratching maps for polymers. Wear 200 (1996), pp.137-147.

[44] Doyle, R.A., Ball, A.: On thermomechanical effects during solid particle erosion. Wear 151 (1991), pp.87-95.

[45] Walley, S. M., Field, J. E.: The erosion and deformation of polythylene by solid-particle impact. Philosophical transactions of the Royal Society of London A. 321 (1987), pp.277-303.

[46] Oka ,Y.I., Matsumura, M., Kawabata, T.: Relationship between surface hardness and erosion damage caused by solid particle impact. Wear 162-167 (1993), pp.688-695.

[47] Hutchings, I.M., Deuchar, D.W.T., Muhr, A.H.: Erosion of unfilled elastomers by solid particle impact. Journal of Materials Science 22 (1987), pp.4071-4076.

[48] Li, J., Hutchings, I.M.: Resistance of cast polyurethane elastomers to solid particle erosion. Wear 135 (1990), pp.293-303.

[49] Arnold, J.C., Hutchings, I. M.: Erosive wear of rubber by solid particles at normal incidence. Wear 161 (1993), pp.213-221.

[50] Brandstädter, A., Goretta. K.C., Routbort. J.L., Groppi. D.P., Karasek. K.R.: Solid-particle erosion of bismaleimide polymers. Wear 147 (1991), pp.155-164.

[51] Walley, S.M., Field, J.E., Greengrass, M.: An impact and erosion study of polyetheretherketone. Wear 114 (1998), pp.59-71.

[52] Briscoe, B.: Wear of polymers: an essay on fundamental aspects. Tribology International (1981), pp. 231-243.

[53] Böhm, H., Betz, S., Ball, A.: The wear resistance of polymers. Tribology

International (1990), pp.399-406.

[54] Slikkerveer, P.J., van Dongen, M.H.A., Touwslager, F.J.: Erosion of elastomeric protective coatings. Wear 236 (1999), pp.189-198.

[55] Veerabhadra Rao, P., Buckley, D.H.: Spherical microglass particle impingement studies of thermoplastic materials at normal incidence. ASLE Transactions 27(4) (1983), pp.373-379.

[56] Arnold, J.C., Hutchings, I.M.: The erosive wear of elastomers. Journal of Natural Rubber Research 6 (1991) Nr.4, pp.241-256.

[57] Lhymn, C., Wapner, P.: Slurry erosion of polythenylene sulfide-glass fiber composites. Wear 119 (1987), pp.1-11.

[58] Ratner, S. B., Styller, E. E.: Characteristics of impact friction and wear of polymeric materials. Wear 73 (1981), pp.213-234.

[59] Meng, H.C., Ludema, K.C.: Wear models and predictive equations: their form and content. Wear 181-183 (1995), pp.443-457.

[60] Zhang, S.W., Deguo, W., Weihua, Y.: Investigation of abrasive erosion of polymers. Journal of Materials Science 30 (1995), pp.4561-4566.

[61] Sundararajan G., Roy M., Venkataraman B.: Erosion efficiency-a new parameter to characterize the dominant erosion micromechanism. Wear 140 (1990), pp.369-381.

[62] Lamy B.: Effect of brittleness index and sliding speed on the morphology of surface scratching in abrasive or erosive processes. Tribology International 1 (1984), pp.35-38.

[63] Wiederhorn S. M., Hockey B. J.: Effect of material parameters on the erosion resistance of brittle materials. Journal of Material Science 18 (1983), pp.766-780.

[64] Friedrich K.: in “Friction and Wear of Polymer Composites”. Friedrich, K.(ed.). Amsterdam: Elsevier 1986, pp. 233.

[65] Lancaster J. K.: Friction and Wear, Chapter 14. In “Polymer Science and Material Science Handbook”. Jenkins, A. D. (ed.). London: North Holland Publishing Co. 1972.

[66] Ratner S. N., Farberoua I. I., Radyukeuich O. V., Lure E. G.: Correlation between wear resistance of plastics and other mechanical properties. In “Abrasion of Rubber”. James, D. I. (ed.). London: MacLaren 1967, pp145-154.

[67] Zahavi, J., Schmitt, G.F.: Solid particle erosion of reinforced composite materials. Wear 71 (1981), pp.179-190.

[68] Tsiang,T. H.: Sand erosion of fiber composites: testing and evaluation. In “Test Methods for Design Allowables for Fibrous Composites”. Chamis, C. C. (ed.). Philadelphia: ASTM STP 1003, American Society for Testing and Materials 1989, pp. 55-74.

[69] Häger, A., Friedrich, K., Dzenis, Y., Paipetis, S.A.: Study of erosion wear of advanced polymer composites. Proceedings "ICCM-10". Street, K. (Ed.), Whistler, B. C., Canada, Cambridge: Woodhead Publishing Ltd. (1995), pp.155-162.

[70] Miyazaki, N., Hamao, T.: Effect of interfacial strength on erosion behavior of FRPs. Journal of Composite Materials 30 (1996), pp.35-50.

[71] Moos, E., Karger-Kocsis, J.: Solid particle erosion of knitted glass fabric reinforced poly(ethylene terephthalate)composites. Advanced Composite Letters 8 (1999) Nr.2, pp.59-63.

[72] Karimbaev, T.D., Nozhnitskii, Y.A., Gundarov, V.I., Rysin, L.S., Lyuttsai, V.G., Tarasov, I.A.: Fracture and wear of composite materials in interaction with a stream of abrasive particles. Mechanics of Composite Materials 2 (1980), pp.235-240.

[73] Ballout ,Y.A., Hovis, S.K., Talia, J.E.: Erosion in glass-fiber reinforced epoxy composite. Scripta Metallurgica et Materialia 24 (1990), pp.195-200.

[74] Barkoula, N.-M., Karger-Kocsis, J.: Solid particle erosion of unidirectional GF reinforced EP composites with different fiber/matrix adhesion. Journal of Reinforced Plastics & Composites, in press.

[75] Kim, D.-S., Kubouchi, M., Tsuda, K.: Effect of surface treatment of glass fiber on erosion damage of FRP. Advanced Composite Letters 6(5) (1997), pp.123-126.

[76] Hovis, S. K., Talia, J. E., Scattergod, R. O.: Erosion in multiphase systems. Wear 108 (1986), pp.139-155.

[77] Miyazaki, N., Takeda, N.: Solid particle erosion of fiber reinforced plastics.

Journal of Composite Materials 27 (1993) Nr.1, pp.21-31.

[78] Besztercey, G., Karger-Kocsis, J., Szaplonczay, P.: Solid particle erosion of electrically insulating silicon and EPDM rubber compounds. Polymer Bulletin 42 (1999), pp.717-724.

[79] Cantwell, W.J, Morton, J.: The impact resistance of composite materials. A review. Composites 22 (1991), pp.347-362.

[80] Choi, H.Y., Downs, R. J., Chang, F-K.: A new approach towards understanding damage mechanisms and mechanics of laminated composites due to low-velocity impact: Part I – experiments. Journal of Composite Materials 25 (1991), pp.992-1011.

[81] Nagai, M., Miyairi H.: The study on charpy Impact testing methods of CFRP. Advanced Composite Materials 3 (1994), pp.17-190.

[82] Tai, N. H., Yip, M. C., Lin, J. L.: Effects of low-energy impact on the fatigue behavior of carbon/epoxy composites. Composites Science and Technology 58 (1998), pp.1-8.

[83] Hitchen, S. A., Kemp, R. M.: The effect of stacking sequence on impact damage in a carbon fiber/epoxy composite. Composites 26 (1995) Nr.3, pp.207-214.

[84] Abrate, S.: Impact on laminated composites: Recent advances. Applied Mechanics Reviews 47 (1994) Nr.11, pp.517-544.

[85] Strait, L. H., Karasek, M. L., Amateau, M. F.: Effects of stacking sequence on the impact resistance of carbon fiber reinforced thermoplastic toughened epoxy laminates. Journal of Composite Materials 26 (1992) Nr.12, pp.1725-1739.

[86] Sela, N., Ishai, O.: Interlaminar fracture toughness and toughening of laminated composite materials. A review. Composites 20 (1989), pp.423-435.

[87] Sela, N., Ishai, O., Banks-Sills, L.: The effect of adhesive thickness on interlaminar fracture toughness of interleaved CFRP specimens. Composites 20 (1989), pp.257-264.

[88] Lu, W. H., Liao, F. S., Su, A. C., Kao, P .W., Hsu, T. J.: Effect of interleaving on the impact response of a unidirectional carbon/epoxy composite. Composites 26 (1995) Nr.3, pp.215-222.

[89] Yuan, Q., Karger-Kocsis, J.: Effects of interleaving on the impact and impact fatigue responses of cross-ply carbon fiber/epoxy laminates. Polymers & Polymer Composites 3 (1995) Nr.3, pp.171-179.

[90] Yuan, Q., Friedrich, K., Karger-Kocsis, J.: Low-energy charpy impact of interleaved CF/EP laminates, Part I. Effects of interleaving on stiffness degradation. Applied Composite Materials 2 (1995), pp.119-133.

[91] Yuan, Q., Karger-Kocsis, J.: On the efficiency of interleaves in carbon fiber/epoxy composite laminates by the fractal approach. Journal of Materials Science Letters 15 (1996), pp.842-845.

[92] Papanicolaou, G. C., Stavropoulos, C.D.: New approach for residual compressive strength prediction of impacted CFRP laminates. Composites 26 (1995) Nr.7, pp.517-523.

[93] Stavropoulos, C. D., Papanicolaou, G. C.: Effect of thickness on the compressive performance of balistically impacted CFRP laminates. Journal of Materials Science 32 (1997), pp.931-936.

[94] Papanicolaou, G. C., Stavropoulos, C. D., Mouzakis, D. E., Karger-Kocsis, J.: Residual tensile strength modelling of polymer-polymer microlayer composites after low energy impact. Plastics Rubber and Composites, Processing and Applications 26 (1997) Nr.9, pp.412-417.

[95] Papanicolaou, G. C., Blanas, A. M., Pournaras, A. V., Stavropoulos, C. D.: Impact damage and residual strength of FRP composites. In Key Engineering Materials, “Impact Response and Dynamic Failure of Composites and Laminate Materials, Part 1: Impact Damage and Ballistic Impact”. Kim, J. K., Yu, T. X. (ed.). Switzerland: Trans Tech Publications 141-143 1998, pp.127-148.

[96] Stavropoulos, C. D., Papanicolaou, G. C., Karger-Kocsis, J., Mouzakis, D. E.: Effect of $\pm 45^{o}$ layers on the residual compressive strength of impacted glass fibre/ polyester laminates. In “Seventh International Conference on Fibre Reinforced Composites Conference Proceedings FRC”. Gibson, A. G. (ed.). Cambridge, UK: Publishing Ltd. 1998, pp. 327-337.

[97] Papanicolaou, G. C., Pournaras, A. V., Mouzakis, D. E., Karger-Kocsis, J., Bofilios, D. A.: Probabilistic approach for residual compressive strength of CFRP laminates after low velocity impact. In “Progress in Durability Analysis of Composite Systems”. Reifsnider, K. L., Dillard, D. A., Cardon, A. H., (ed.). Rotterdam: Balkema 1998, pp. 325-330.

[98] Gremmels, J.: Partieller hygrothermischer Abbau von Polyester-Polyurethan und dessen Anwendung-ein Beitrag zur Entwicklung eines neues

Recyclingverfahrens. Bd. 12, Kaiserslautern: IVW 2001. Zugl. Diss. Universität Kaiserslautern (2000).

[99] Karger-Kocsis, J., Gremmels, J.: Use of hygrothermal decomposed polyester-urethane waste for the impact modification of epoxy resins. Journal of Applied Polymer Science 78 (2000), pp.1139-1151.

[100] Karger-Kocsis, J., Gremmels, J.: Toughening of epoxy resins by partially decomposed polyurethane waste. SPE-ANTEC 46 (2000), pp.840-844.

[101] Papke, N.: Neue thermoplastische Elastomere mit co-kontinuierlicher Phasenstruktur auf Basis von Polyester/ Elastomer Blends unter Verwendung gezielt chemisch funktionalisierter Elastomere. Bd. 13, Kaiserslautern: IVW 2000. Zugl. Diss. Universität Kaiserslautern (2000).

[102] Papke, N., Karger-Kocsis, J.: Thermoplastic elastomers based on compatibilised poly(ethylene terephthalate) blends: Effect of rubber type and dynamic curing. Polymer 42 (2001), pp.1109-1120.

[103] ESIS 28: Fracture Mechanics Testing Methods for Polymers, Adhesives and Composites. Moore, D. R., Pavan, A., Williams, J. G., (ed.). Oxford: Elsevier Science 2001.

[104] Hoecker, F., Karger-Kocsis, J.: On the effects of processing conditions and interphase of modification on the fiber/matrix load transfer in single fiber polypropylene composites. Journal of Adhesion 52 (1995), pp.81-100.

[105] DIN 53 505: Härteprüfung nach Shore A und D (1987).

[106] N. N.: Kunststoffe, Bestimmung dynamisch-mechanischer Eigenschaften. DIN EN ISO 6721-1-7, December 1996.

[107] DIN-Taschenbuch 18: Kunststoffe 1, Prüfnormen über mechanische, thermische und elekrische Eigenschaften. Berlin: Beuth-Verlag, 1980.

[108] ASTM G76 83: Standard practice for conducting erosion tests by solid particle impingement using gas jets. USA: ASTM PA (Reapproved 1989).

[109] DIN 50 332: Strahlverschleiß-Prüfung 1989.

[110] Ruff, A. W., Ives, L. K.: Measurement of solid particle velocity in erosive wear. Wear 35 (1975), pp.195-199.

[111] Häger, A. M., Walter, R., Friedrich, K., Dzenis Y.: Jet erosion testing of composite materials by a modified instrumented sand blasting cabin. In ”Composites Testing and Standarization ECCM-CTS 2”. P. J. Hogg, K. Schulte,

H. Wittich (eds.). Cambridge, U.K.: Woodhead Publishing Ltd 1994, pp. 419-427.

[112] Kosel, T. H., Anand, K.: An optoelectronic erodent particle velocimeter. In “Corrosion and Particle Erosion at High Temperatures”, Srinivasan, V. Vedula, K (ed.). The Minerals, Metals and Materials Society 1989, pp.349-368.

[113] Shipway, P. H., Hutchings, I.: Influence of nozzle roughness conditions in a gas-blast erosion rig. Wear 162-164 (1993), pp. 148-158.

[114] Thai, C. M., Tsuda, K., Hojo, H.: Erosion behavior of polystyrene. Journal of Testing and Evaluation 9 (1981) Nr.6, pp. 359-365.

[115] Wang, Y. Q., Huang, L. P., Liu, W. L., Li, J.: The blast erosion behaviour of ultrahigh molecular weight polyethylene. Wear 218 (1998), pp.128-133.

[116] Hunston, D. L., Moulton, R. J., Johnston, N. J., Bascom, W. D.: Matrix resin effects in composite delamination: Mode I fracture aspects. In “Toughened Composites”. Johnston, N. J. (ed.). Philadelphia, USA: American Society of Testing Materials 1987, pp.74-94.

[117] Siebert, A. R.: Morphology and dynamic mechanical behaviour of rubber-toughened epoxy resins. In “Rubber-Modified Thermoset Resins”, Washington, DC: Advanced Chemical Society 1984, pp.179-191.

[118] Garg, A. C., Mai, Y.-W.: Failure mechanisms in toughened epoxy resins-A review. Composite Science Technology 31 (1988), pp.179-223.

[119] Yee, A. F., Pearson, R. A.: Fractography and failure mechanisms of rubber modified epoxide resins. In “Fractography and Failure Mechanisms of Polymers and Composites”. Roulin-Moloney, A.C. (ed.). London: Elsevier Applied Science 1989, pp. 291-350.

[120] Bascom, W. D., Hunston, D. L.: Fracture of elastomer-modified epoxy polymers. A review. In “Rubber-Toughened Plastics; Advanced Chemical Series 222” Riew, C. K. (ed.), Washington DC: American Chemical Society 1989, pp.135-172.

[121] Kinloch, A. J.: Relationship between the microstructure and fracture behavior of rubber-toughened thermosetting of polymers. In “Rubber-Toughened Plastics; Advanced Chemical Series 222” Riew, C. K. (ed.). Washington DC: American Chemical Society 1989, pp. 67-91.

[122] Sue, H.-J.: Study of rubber-modified brittle epoxy systems. Part I. Fracture toughness measurements using the double-notch four-point-bend method. Polymer Engineering Science 31 (1991), pp.270-274.

[123] Sue, H.-J.: Study of rubber-modified brittle epoxy systems. Part II. Toughening mechanisms under mode-I fracture. Polymer Engineering Science 31 (1991), pp.275-288.

[124] Yee, A. F, Pearson R. A.: Toughening mechanisms in elastomer-modified epoxies. Part I. Mechanical studies. Journal of Materials Science 21 (1986), pp. 2462-2474.

[125] Hwang, J.-F., Manson, J. A., Hetzberg, R. W., Miller, G. A., Sperling, L. H.: Structure property relationships in rubber-toughened epoxies. Polymer Engineering Science 29 (1989), pp.1466-1476.

[126] Karger-Kocsis, J., Friedrich K.: Microstructure-related fracture toughness and fatigue crack growth behavior in toughened, anhydrate-cured epoxy resins. Composite Science and Technology 48 (1993), pp.263-272.

[127] Barkoula, N.-M., Gremmels, J., Karger-Kocsis, J.: Dependence of solid particle erosion on the cross-link density in an epoxy resin modified by hygrothermally decomposted polyurethane. Wear 247 (2001), pp.100-108.

[128] Levita, G., De Petris, S., Marchetti, A., Lazzeri, A.: Crosslink density and fracture toughness of epoxy resins. Journal of Materials Science 26 (1991), pp.2348-2352.

[129] Pearson, R. A., Yee, A. F.: Toughening mechanisms in elastomer-modified epoxies. Part III. The effect of cross-link density. Journal of Materials Science 24 (1989), pp.2571-2580.

[130] Urbaczewski-Espuche, E., Galy, J., Gerard, J.-F., Pascault, J.-P., Sautereau, H.: Influence of chain flexibility and crosslink density on mechanical propertied of epoxy/amine networks. Polymer Engineering Science 31 (1991), pp. 1572-1580.

[131] Murakami, S., Watanabe, O., Inoue, H., Ochi, M., Shiraishi, T., Shimbo, M.: Fracture behavior of toughened epoxy resins cured with N,N'-dimethylethylenediamine. Polymer 33 (1992), pp.572-576.

[132] Glad, M. D., Kramer, E. J.: Microdeformation and network structure in epoxies. Journal of Materials Science 26 (1991), pp. 2273-2286.

[133] Iijima, T., Yoshioka, N., Tomoi, M.: Effect of cross-link density on modification of epoxy resins with reactive acrylic elastomers. European Polymer Journal 28 (1992), pp.573-581.

[134] Shaw, M.C., Young, E.: Rubber Elasticity and Fracture. Journal of Engineering Materials and Technology 110 (1988), pp.258-265.

[135] Mouzakis, D. E., Papke, N., Wu, J. S., Karger-Kocsis, J.: Fracture toughness assessment of poly(ethylene terephthalate) blends with glycidyl methacrylate modified polyolefin elastomer using essential work of fracture method. Journal of Applied Polymer Science 79 (2001), pp.842-852.

[136] Zilg, C., Thomann, E., Mülhaupt, R., Finter J.: Polyurethane nanocomposites containing laminated anisotropic nanoplarticles derived from organophilic layered silicates. Advanced Materials 11 (1999) Nr.1, pp.49-52.

[137] Tien, Y. I., Wie, K.H.: Hydrogen bonding and mechanical properties in segmented montmorillonite /polyurethane nanocomposites of different hard segment ratios. Polymer 42 (2001), pp.3213-3221. (362)

[138] Mathias, P.J., Wu, W., Goretta, K.C., Routbort, J.L., Groppi, D.P.K., Karasek, K.R.: Solid particle erosion of a graphite-fiber-reinforced bismaleimide polymer composite. Wear 135 (1989), pp.161-169.

[139] Barkoula, N.-M., Karger-Kocsis, J.: Effects of fibre content and relative fibre orientation on the solid particle erosion of GF/PP composites. Wear 252 (2002), pp.80-87.

[140] Barkoula, N.-M., Papanicolaou, G. C., Karger-Kocsis, J.: Prediction of the residual strengths of carbon-fibre/epoxy composite laminates with and without interleaves after solid-particle erosion. Composites Science and Technology Technology 62(1) (2002), pp. 121-130.

[141] Khruschov, M. M.: Principles of abrasive wear. Wear 28 (1974), pp.69-88.

[142] Zum Gahr, K.-H.: Microstructure and wear of materials. Amsterdam: Elsevier Tribology Series 10, 1987.

[143] Yen, B.K., Dharan, C.K.H.: A model for the abrasive wear of fiber-reinforced polymer composites. Wear 195 (1996), pp.123-127.

[144] Dorey, G.: Impact and Crashworthiness of Composite Structures. In “Structural Impact and Crashworthiness “. Davies, G. A. O. (ed.). London: Elsevier Applied Science 1984, pp.152-192.

[145] Bishop, M. S., Dorey, G.: The effect of damage on the tensile and compressive performance of carbon fibre laminates. AGARD CP. No.355. London: Controller HMSO 1983, pp.10.1-10.10.

[146] Sacher E.: Secondary structural motions in polycarbonate. II. Identification of the motions and their relation to impact strength. Journal of Macromolecular Science, Physics B 11 (1975) Nr.3, pp. 403-410.

[147] Wada, Y., Kasahara, T.: Relation between impact strength and dynamic mechanical properties of plastics. Journal of Applied Polymer Science 11 (1967), pp. 1661-1665.

[148] Wolstenholme W. E.: Characterizing impact behavior of thermoplastics. Journal of Applied Polymer Science VI (1962) Nr.21, pp.332-337.

[149] Vincent, P. I.: Impact strength and mechanical losses in thermoplastics. Polymer 15 (1974), pp. 111-116.

[150] Sacher E.: A relation between toughness and dynamic mechanical properties of polymer films. Journal of Applied Polymer Science 18 (1975), pp. 1421-1425.

[151] Barkoula, N.-M., Karger-Kocsis, J., Papanicolaou, G. C.: Prediction of the residual tensile strength after solid particle erosion of UD-GF/PP composites and comparison with CF/EP composites. Journal of Composite Materials (in press).

[152] Papanicolaou, G. C., Samoilis, G., Giannis, S., Barkoula, N.-M., Karger-Kocsis, J.: A model for the accurate prediction of the residual strength after damage due to impact and erosion of FRP's". In 14th US National Congress of Applied Mechanics special volume in honour of Professor Daniel I.M.: "Recent Advances in Experimental Mechanics" (June 23-28, 2002, Virginia Tech.). Kluwer Academic Publishers (to be published).

9. List of Publications

1. Barkoula, N. M., and Karger-Kocsis, J.: Sandstrahl-Erosion von Polymeren und Polymer-Verbundwerkstoffen. IVW-Kolloquium 2000, IVW-Schriftreihe Band 4, 11.-12. Oktober 2000, pp.189-193.
2. Barkoula, N. M., Gremmels, J., Karger-Kocsis, J.: Dependence of solid particle erosion on the cross-linked density in an epoxy resin modified by hygrothermally decomposed polyurethane. Wear 247 (2001), pp.100-108.
3. Moos, E., Barkoula, N. M., Karger-Kocsis, J.: Strahlerosionsverhalten von Polymeren und Polymeren Verbundwerkstoffen. Kunststoffe 4 (2001), pp. 113-115.
4. Barkoula, N. M., Karger-Kocsis, J.: Solid particle erosion of unidirectional GF reinforced EP composites with different Fiber/Matrix adhesion. Journal of Reinforced Plastics and Composites (in press).
5. Barkoula, N. M., Papanicolaou, G. C., Karger-Kocsis, J.: Prediction of the residual tensile strength after solid particle erosion of CF/EP composite laminates with and without interleaves. Composites Science and Technology 62(1) (2002), pp. 121-130.
6. Barkoula, N. M., Karger-Kocsis J.: Effects of fibre content and relative fibre orientation on the solid particle erosion of GF/PP composites. Wear 252 (2002), pp.80-87.
7. Barkoula, N. M., Karger-Kocsis, J., Papanicolaou, G. C.: Prediction of the residual tensile strength after solid particle erosion of UD-GF/PP composites. Journal of Composite Materials (in press).
8. Papanicolaou, G. C., Samoilis, G., Giannis, S., Barkoula, N.-M., Karger-Kocsis, J.: A model for the accurate prediction of the residual strength after damage due to impact and erosion of FRP's". In 14th US National Congress of Applied Mechanics special volume in honour of Professor Daniel I.M.: "Recent Advances in Experimental Mechanics" (June 23-28, 2002, Virginia Tech.). Kluwer Academic Publishers (to be published).